QUALITATIVE AND QUANTITATIVE ANALYSIS ON SOME CHARACTERISTICS OF CIRCULAR SECTOR MICROSTRIP ANTENNAS

A THESIS SUBMITTED IN PARTIAL FULFILLMENT OF THE REQUIREMENTS FOR THE DEGREE OF DOCTOR OF PHILOSOPHY

SUDIP KUMAR GHOSH

PH.D. REGN NO: MZU/Ph.D./1179 of 23.04.2018
MZU REGN NO: 1702110

DEPARTMENT OF ELECTRONICS & COMMUNICATION ENGINEERING
SCHOOL OF ENGINEERING AND TECHNOLOGY
SEPTEMBER 2021

QUALITATIVE AND QUANTITATIVE ANALYSIS ON SOME CHARACTERISTICS OF CIRCULAR SECTOR MICROSTRIP ANTENNAS

BY

SUDIP KUMAR GHOSH

Department of Electronics & Communication Engineering

Name of Supervisor : Prof. Sudipta Chattopadhyay

Name of Joint Supervisor : Prof. L. Lolit Kumar Singh

Submitted

In partial fulfillment of the requirement of the Degree of Doctor of Philosophy in Electronics and Communication Engineering of Mizoram University, Aizawl

Department of Electronics and Communication Engineering
School of Engineering and Technology
MIZORAM UNIVERSITY
(*A Central University*)
Tanhril**,** Aizawl - 796 004, Mizoram

CERTIFICATE

This is to certify that the thesis entitled "**Qualitative and Quantitative Analysis on Some Characteristics of Circular Sector Microstrip Antennas"** submitted to Mizoram University for the award of the degree of **Doctor of Philosophy Electronics and Communication Engineering** by **Sudip Kumar Ghosh**, Ph.D Registration No. **MZU/Ph.D/1179** of **23.04.2018**, is Ph.D scholar in the Department of Electronics and Communication Engineering, under our guidance and supervision and has not been previously submitted for the award of any degree in any Indian or foreign University. He has fulfilled all criteria prescribed by the UGC (Minimum Standard and Procedure governing Ph.D. Regulations). He has fulfilled the mandatory publication (Publication enclosed) and completed Ph.D. course work. It is also certified that the scholar has been admitted in the Department through an entrance test, followed by an interview as per UGC Regulation of 2016.

Date: February, 2022   (Prof. Sudipta Chattopadhyay)
Place : Aizawl   Supervisor

                                                             (Prof. L. Lolit Kumar Singh)
                                                                    Joint Supervisor

MIZORAM UNIVERSITY
Aizawl -796 004

(February 2022)

DECLARATION

I, Sudip kumar Ghosh, hereby declare that the subject matter of this thesis entitled "**Qualitative and Quantitative Analysis on Some Characteristics of Circular Sector Microstrip Antennas**" is the record of work done by me, that contents of this thesis did not form basis of the award of any previous degree to me or to do the best of my knowledge to anybody else, and that the thesis has not been submitted by me for any research degree in any other University/Institute.

This is being submitted to the Mizoram University for the degree of Doctor of Philosophy in **Electronics and Communication Engineering.**

Date: (Sudip Kumar Ghosh)
                                                                              Candidate

                                                                              (Prof. Sudipta Chattopadhyay)
                                                                              Supervisor

(Prof. N. P. Maity)   (Prof. L. Lolit Kumar Singh)
Head of the Department   **Joint Supervisor**

knowledge and strength that had lead me successfully to the end of this research work.

<div align="right">**SUDIP KUMAR GHOSH**</div>

Table of Contents

List of Figures

List of Tables

List of Abbreviations

MA	-	Microstrip Antenna
CAD	-	Computer Aided Design
CMA	-	Circular Microstrip Antenna
RMA	-	Rectangular Microstrip Antenna
RF	-	Radio Frequency
CSMA	-	Circular Sector Microstrip Antenna
PTFE	-	Poly Tetra Fluro Ethylene
CP	-	Co-polar Radiation
XP	-	Cross-polar Radiation
CCMA	-	Conventional Circular Microstrip Antenna
XPD	-	Cross-polarization discrimination
DPS	-	Defected Patch Surface
DGS	-	Defected Ground Structures
HFSS	-	High-Frequency Structure Simulator
dB	-	Decibel
dBi	-	Decibels Relative to Isotropic
S_{11}	-	Reflection Co-efficient
f_r	-	Resonance Frequency
J_m	-	Bessel functions of order m
J'_m	-	Derivative of Bessel function of order m
χ'_{mn}	-	n^{th} zero of derivative of Bessel function of order m.
k	-	Propagation vector
k_z	-	Propagation constant along the z direction.
q_1	-	Fringing factor
C_{dyn}	-	Dynamic capacitance
$C_{e,dyn}$	-	Dynamic fringing capacitance
φ_0	-	Sector angle
	-	Radial dimensionfrom the apex of the patch to the
ρ		edge of patch

m	-	Number of circumferential variation
n	-	Number of radialvariation
$\bar{J}$	-	Excitation of feed-probe current density
$\bar{E}$	-	Induced electric field
$P_{excited}$	-	Effective power
ρ_f	-	Radial feed location
ΔG	-	Change in gain

CHAPTER

1

Introduction

1.1   Introduction

In the present era, and future inclination of development of wireless communication has become popular and prolific than ever before with advancement of civilization. With the technological advancement of various wireless communication technologies such as 5G, LTE, WiFi, Li-Fi,RFID, 6LoWPAN etc. have greatly boosted the potential capabilities of internet of things (IoT) and made it more user friendly than ever. So, the research on wireless communication technology attracts the new researchers to develop these emerging technologies with integration of microstrip antenna (MA) due its plentiful advantages like light weight, low profile, small size and ease in implementation on curved surface. The concept of microstrip antenna was begun in 1953 by Deschamps [1]. The basic structure of a microstrip antenna (MA) is parallel plate conductor which composed of a very thin conducting material strip (patch) printed on ground plane & dielectric (substrate) in between. The shaped of Patch conductor can have any geometrical shape; it is made of copper or gold etc. The conventional geometry of a widely used microstrip antennas in form of circular patch has been depicted in Fig. 1.1. The value of relative dielectric constant (ε_r) of the substrate is generally taken as low in the span of 2 to 10 i.e. Polytetrafluoroethylene (PTFE ε_r = 2.33), flame retardant (FR4 ε_r = 4) materials etc.

Two decades later Howell [2] demonstrated theoretical and practical design method in perspective of dipole antenna. Thereafter Munson [3] implemented a

microstrip as an Omni-directional antenna for application of aircraft / airborne system.

(a)

(b)
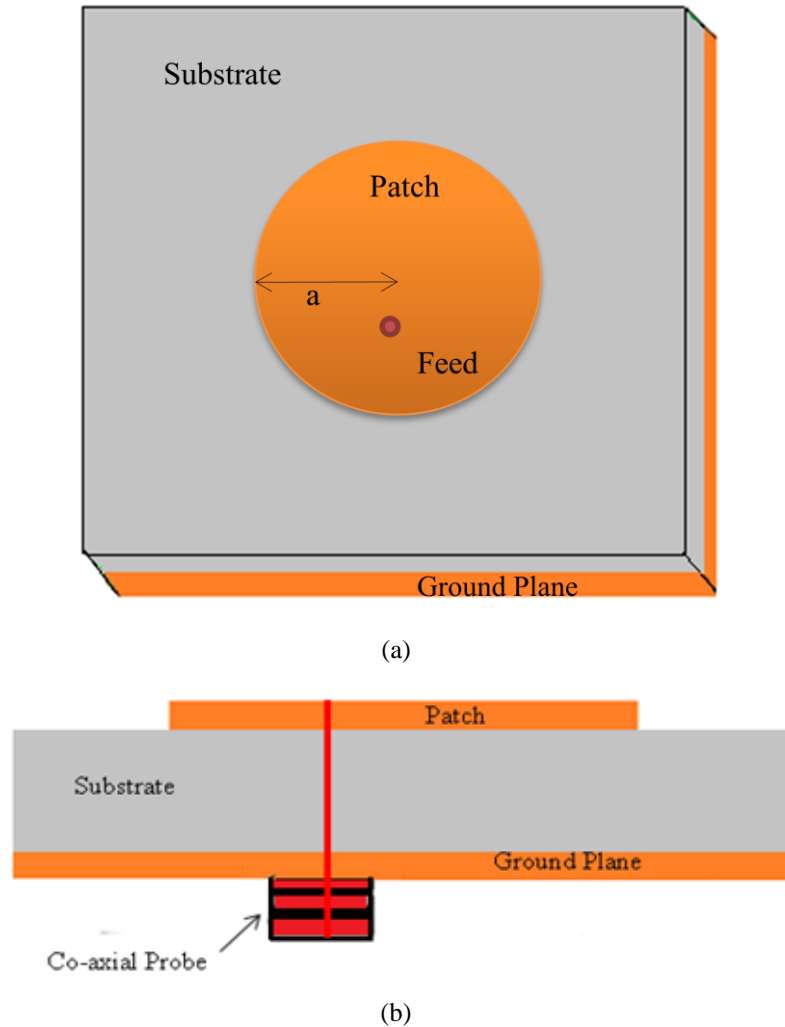
Fig. 1.1 Basic structure of circular microstrip antenna (a) Top view (b) Side view.

Advantages and Limitations of MA

The microtrip patch antenna has numerous advantages like ease to printed on the circuit board, accure less patch area, low profile, not bulky in size , in view of this flexibility it can be placed to any curve surface and any shape of structure can be achived through molding it. Plenty number of MA can be manufactured due to less expensive andeffortless fabrication. This microstrip antenna are also serve to modern wireless communication system as it is easily compatable to the technology related to the microwave monolithic integrated circuit (MMIC) and opto electronic integrated circuit (OEIC). It is equally applicable to the linear, circular polarisation

and also support any kind of frequency opration like dual , triple frequencyetc. Large area can be coverd with in limited space by making array configaration. It is easily mounted on the stiff suface due to robustness.The microtrip patch antenna has some limitations besides many advantages discuss below.

Compare to the conventional antenna, it has following disadvantages like inbuilt low bandwidth and low gain limited to 2-5 dBi only. Improvement of bandwidth is restricted to 1-5% after given an extra effort. The efficiency of the conventional MA is not promising and to achive good polarisation purity , excess effort need to pay. Power handling capability is also low. Extra amount of radiation comes from feed and junction which enhances additional complexity.

Following limitations can be overcome by using thicker substrates, etching slots in patch surface, addition to parasitic patches on the top of the patch area or introducing aperture coupled stacked patch antennas.

The theoretical analysis and practical verification of different geometry MA gets attracted to the research community that came into sight in between [4]-[14]. The wonderful literature on microstrip antenna was first published [15] in 1980 as a hand book which covers multiple aspects on MAs of different geometry. Followed by [15] James, Hall and Wood [16] brought a new edition on design aspect of microstrip antenna in 1981. The fundamental Antenna theory and multiple design issues of microstrip antenna were well covered by Balanis [17] in 1997. Different kind of design and analysis including broad banding and new feed mechanism has been reported in [18] by R. Garg et.al. In the following section 1.2 the basic feeding mechanism of MA has been described. Some elaborate method of feeding mechanism has been reported in [19]-[28].

This chapter deals with the different fedding techniques of MA in section 1.2, The radiation charecteristics of MAs have been discussed in section 1.3, Choice of patch geomatry has been deccribed in section 1.4. Finally, the preface of the dissertation has been described briefly in section 1.5.

1.2   Different Fedding Techniques

When MA get excited by applying any certain voltage signal to the patch. It starts radiating and maximum radiation come out from its edge and goes in the broadside

direction and no radiation (ideally) in the end fire direction. To get efficient radiation, the MA can be generally fed by direct (contact) or indirect (non-contact) way. Co-axial fed, microstripline fed, proximity coupled fed and aperture coupled fed is most popular out of contact or non-contact method.

1.2.1 Co-axial Feed Technique

In this technique, the probe conducting material is connected through the dielectric to the radiating patch. This is very widely used technique, where probe can be placed at anywhere of the patch to match 50 Ω impedance. This is easy to fabricate and match impedances.

(a)

(b)
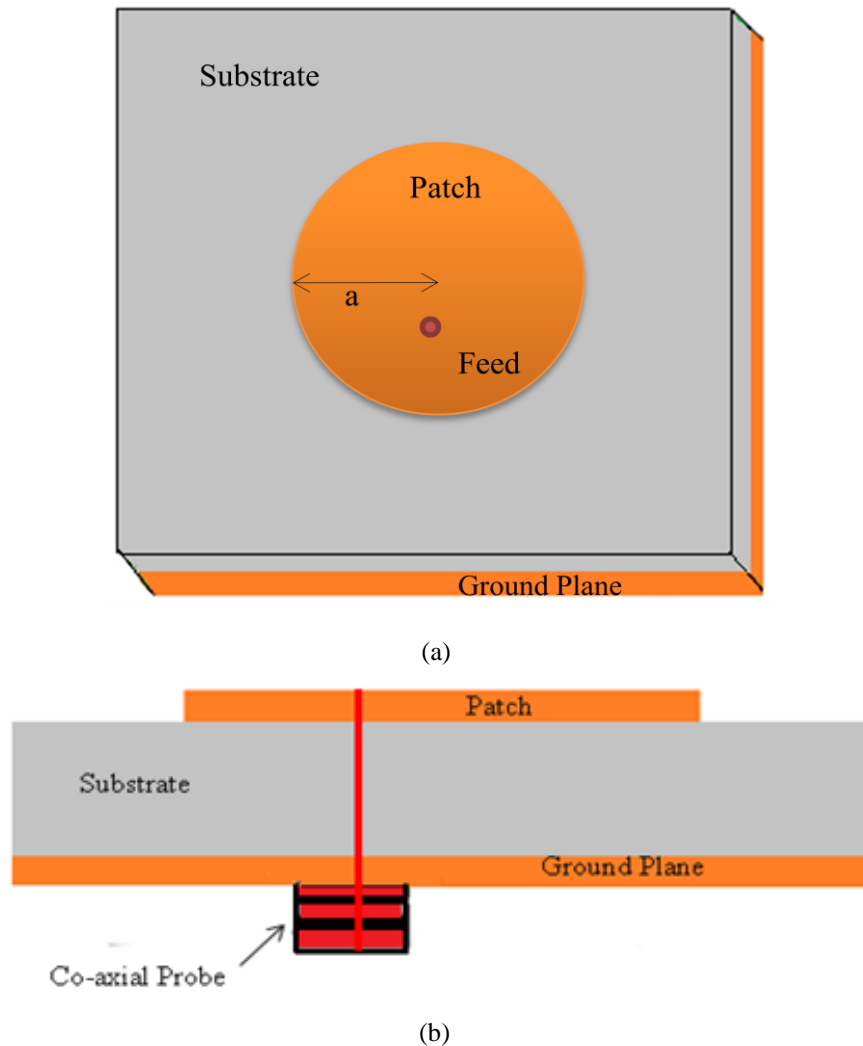
Fig. 1.2 Co-axial feed circular microstrip antenna (a) top view (b) side view

This technique suffers in narrow bandwidth around 2-3% and high cross

4

polarization radiation due to asymmetries in feed position and feed induced spurious radiations. Also, coaxial feed introduces large inductance in case of thick substrates. In the Fig. 1.2 co-axial probe fed microstrip antenna in top view and side view has been shown. Where '*a*' is the radius of circular patch.

1.2.2   Microstripline Feed Technique

In this method, a strip of conducting material is joined directly to the edge of the patch as shown in Fig. 1.3. It is one of the common feeding techniques. To achieve better impedance matching, the controlling of inset cut position movement to the patch is desire only. It is easy to fabricate, simple to model and analyze. However, the feedlines increase spurious radiations from antenna. With increase in substrate thickness, surface waves are increased in antenna. Also, such feed line contributes in exciting higher order modes in antenna and enhancing cross polar radiation from antenna. Further, it has low bandwidth around 2-3%.
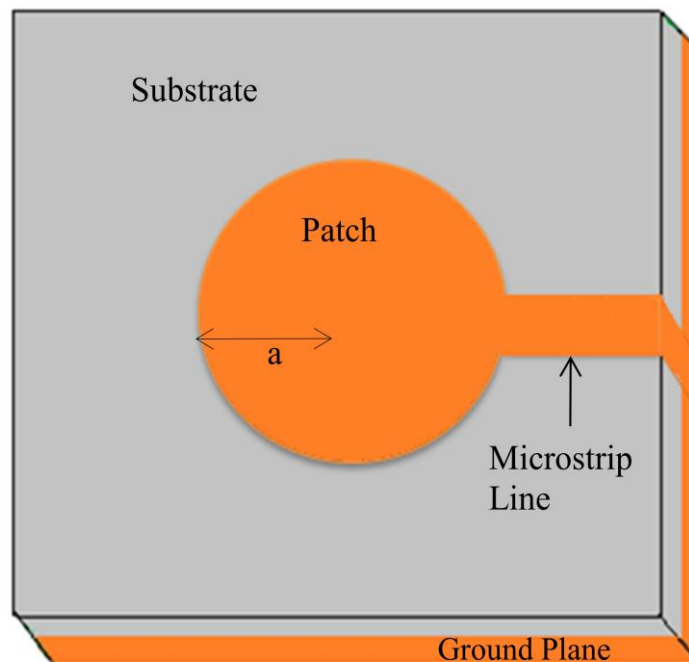
Fig. 1.3 Microstripline feed circular printable antenna.

1.2.3   Proximity Couple Feed Techniques

There are two dielectric material substrate 1 (ε_{r1}) and substrate 2 (ε_{r2}). Patch is mounted on the 2nd dielectric , the feedline is placed in between the two dielctric.

The ground plane is placed below 1st dielectric material. In this type of method, microstrip line conducting material does not connected directly to the patch.That's why this feeding technique is known as electromagnetic coupling which is shown in Fig. 1.4. The advantage of having this type of feeding technique is that provides large bandwidth around 13% and eliminates unwanted spurious radiation. Fabrication is quite difficult due to which this technique becomes expensive.
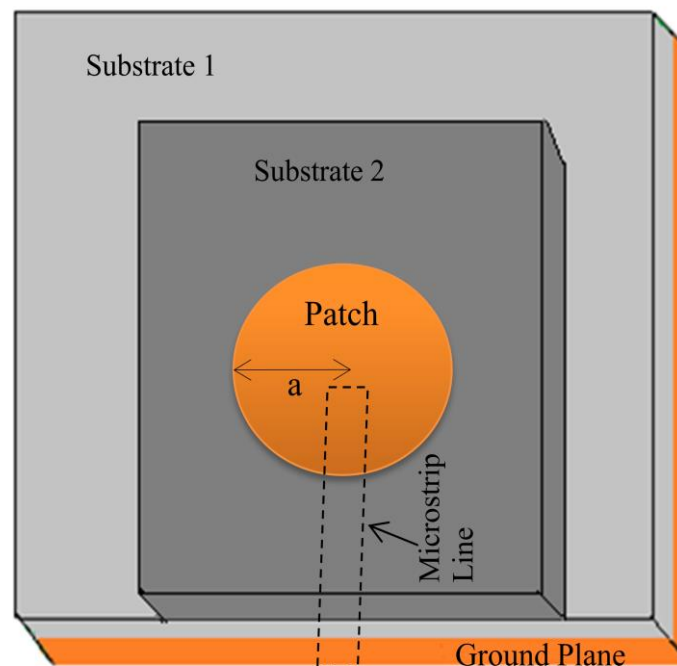
Fig. 1.4 Proximity coupled feed circular printable antenna.

1.2.4   Aperture Coupled Feed Technique

It is also non-contacting feed technique as shown in Fig. 1.5, where the ground plane is sandwiched by two substrates. There is microstrip line in 1st substrate and patch is grown on the 2nd substrate. The slot is design on ground plane through which the line is coupled to get radiation. The advantage of this symmetrical design is that the two dielectrics can be selected separately to optimize the patch radiation and lower cross-polarization. This technique avoids use of soldering and minimizes the chance of leakage current from feed. It also reduces the reactance of feed and also exhibits wide bandwidth in comparison with other feeding techniques. However, the fabrication is difficult compare to all other technique as structure is multilayer. Also, back radiation increases in such structures.

6
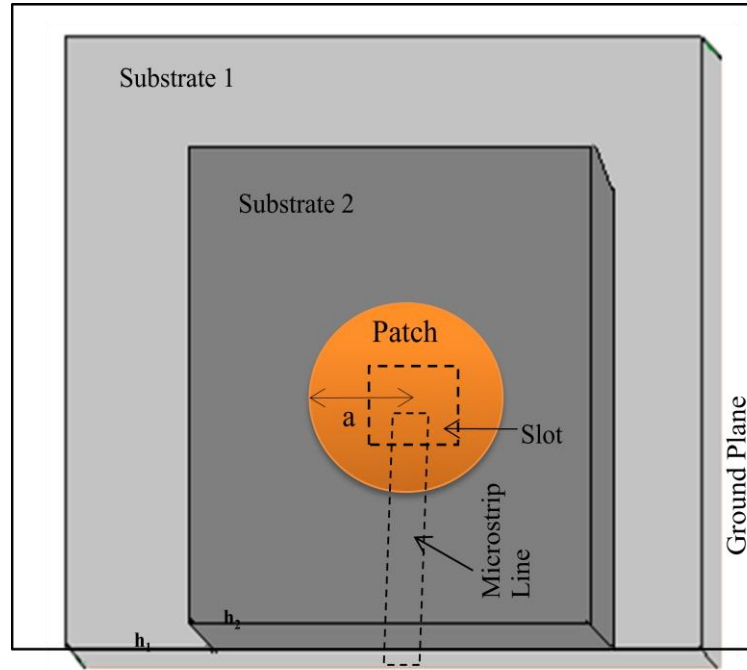
Fig. 1.5 Aperture coupled feed circular printable antenna.

1.3   Radiation Characteristics

Multiple radiation characteristics like co-polarization gain, beam width, co-polarization radiation to cross polarization radiation isolation (polarization purity)of microstrip antenna has been studied in [29]-[68], where techniques like dielectric cover over the patch [29], laminated ground plane [30], LiTiMg Ferrite substrate[31], air substrate [32], electromagnetic band gap surface[33]is utilized to improve radiation performance of MA. The use of Green's function [34], finite ground plane [35], and neuro-spectral computation approach [36] have been reported to analyze the radiation characteristic of MA. Spiral geometry size of circular microstrip antenna (CMA) [37] and superstrates loaded CMA [38] have been employed to increase the gain and half power beam width of the antennas. The improvement of gain by employing different method has been reported in [39]-[58], Out of them, the use of superstrates on microstrip antenna [39]-[40], introduction of air gap [41]-[42] have been investigated successfully. Around 5-7 dBi gain has been achieved by surface waves suppression using electromagnetic band gap (EBG) structure in [43], photonic band gap (PBG) structure in [44] and partially etched substrate in [45]. The gain of the microstrip antenna can be also enhanced through

7

defected on the ground surface (DGS) that has been reported in [46]-[47] and slotted ground plane in [48] which yields 7.2-9.2 dBi gain.

The different techniques has been evoked to improve the gain of circular microstrip antenna that come into views in [49]-[56], such as in [49]-[50] aperture couple based slot loading technique, in [51]-[53] shorting pin. The employment of frequency selective surface [54], multishaped substrate [55] in MA reveals the techniques of gain enhancement of such antennas. Maximum 9 dBi gain with 90% efficiency has been achieved in above mentioned literatures. However, these investigations fail to address the improvement in polarization purity of MA. Polarization purity is another important part of radiation characteristics, that has been studied and improved in various ways in [56]-[77]. Suspended path with dual feed [56], Meander line feeding [57]-[58], W and U shaped ground plane [59], [60] have been reported which yields 18-20 dB polarization purity. The most effective techniques to improve polarization purity till date are the employment of DGS [61]-[71], defected patch structure [72]-[74], and shorting stripes or post [75]-[77] with MAs which can yield around 20 dB of polarization purity.

1.4   Choice of Patch Geometry: A Survey

Several types of patch geometries such as rectangular, circular, triangular, octagonal, hexagonal etc can be useful as radiating element of MA. All these geometries except rectangular and circular are complex in nature and there are no available well established theories which can be adopted easily in the industries for batch production. Therefore, to develop the MA in more cost effective way, rectangular and circular geometries are very popular and preferred [78]. Also industry prefers such rectangular and circular geometry for its simple design and ease to mount the antenna inside the device without much change in the device periphery. Again, the trouble shooting can be easily done due its wide versatility and concrete established theory with promising characteristics. The thorough investigation with such simple rectangular and circular geometries have gained potential demands to the researchers and finds plentiful applications in modern wireless technologies in last two decades. In this context, large number of traditional geometries such as rectangular and circular MAs, have been widely investigated,

8

explored [79]-[84] and implemented [85]-[90].

The resonance frequency of rectangular microstrip antenna (RMA) can be written as

$$f_r = \frac{c}{2L\sqrt{\varepsilon_r}}$$

(1.1)

where, L is the length of the patch, ε_r is the dielectric constant, c is the velocity of the light. While the same for circular microstrip antenna (CMA) is

$$f_r = \frac{1.84c}{2\pi a\sqrt{\varepsilon_r}}$$

(1.2)

where, a is the radius of the patch, ε_r is the dielectric constant and c is the velocity of the light.

Comparison of equation (1.1) and equation (1.2) reveals that the required redial dimension of CMA is smaller than RMA. Therefore, in the present scenario of miniaturization, CMA can be more effective in tinny electronic devices.

However, more miniaturization in antenna geometry is always preferred in the present era where, the tiny wireless communication devices are most effective and popular. Infact, in the present era, most of the hand held wireless communication devices are budding towards tininess and multi functionality for compatibility with MMIC.

Therefore, the occasions are there where the geometry other than the conventional rectangular and circular geometries is favorable.

Circular sector microstrip antenna (CSMA) is very advantageous where the space is the key factor to organize a patch with conventional geometry. In fact, around 60% of patch area reduction can be achieved by the suitable choice of sector angle for a particular resonant frequency compared to conventional circular patch geometry. Here, the through and elaborate investigation on CSMA is very much required also challenging to the antenna researchers. Therefore, through investigation on CSMA is the modern state- of –art research field of antenna engineering. The CSMA is highly usable as it requires less space compare to conventional circular patch antennas. Therefore, an accurate analysis of CSMA is one of the main concerns in the printed antenna research field. The formulation of resonance frequency (f_r) of CSMA based on conventional cavity model was first reported in [89]-[90]. Followed by them, further attempts were made to estimate the dominant mode and its resonance

frequency in [91]-[92]. However, in [92], radiation pattern of CSMA is reported based on simulation results. The radiation pattern of CSMA with 60^0 sector angle was reported in [92]. However,[89]-[92] predicts the resonance frequency of CSMA with large error of around 2.5% between simulation and quantitative estimation. The resonance frequency with 60^0 and 90^0 sector angle has been investigated in [91]-[96] through simulation and around 3.8% error has been reveled in predicting resonance frequency. Furthermore [91]-[92] fails to determine the accurate dominant mode of CSMA. As such the dominant mode of CSMA depends critically on the sector angle. The study of resonance frequency and radiation field of CSMA had been presented in [93]-[96] based on simulation. The array structure with CSMA for the C and X band was investigated and the effect of element number in the array was reported in [95]. A simulation study of CSMA with 70^0 sector angle for CSMA was reported in [96]. Some newer applications of CSMA on broadband, dual polarized, circularly polarized antenna have been reported in [97]-[100]. In [97] comparatively large sector angles 270^0 CSMA and 320^0 CSMA have been investigated to improve the gain around 7 dBi and to achieve bandwidth of around 500 MHz. Proximity fed CSMA with multiple sector angles 340^0, 350^0, 355^0 have been studied for broad banding more than 700 MHz in [101]. Moreover, application of dual mode wide banding and dual port CSMA has been reported in [102]-[103]. In [102] dual mode of 270^0 CSMA has been excited simultaneously and evolve bore sight gain of 8. 1dBi.The antenna has been minimized about 44% comparison to conventional CMA without improving the gain of CSMA and the cross pole comparison got more than 20 dB in [103]. Further, dual band meta loaded semicircular CSMA with operating frequency 4.1 GHz has been reported in [104]. The measured gain of this antenna is 5.82 dBi with bandwidth of 114 MHz only. Furthermore, the application of broad banding of 120^0 and 270^0 sectoral patch and circular polarization with the help of CSMA is documented in [105]-[109]. In [105] a compact size of 109^0 CSMA has been reported for application of Ku band. This antenna exhibits 6.57 dBi simulated gain with 5 dB cross polarization only. To achieve circular polarization, the study of 65^0 sectoral patch antenna has been reported in addition with arc shape slots and slits structure in [106]. Further, 270^0 sectoral patch with rectangular cut slot has been reported in [107], which yields 8.5 dBi peak gain. The study of proximity fed 120^0

CSMA has been reported for broad banding and yields broadside peak gain of about 9.2 dBi in [108]. The comparison between RMA and the CSMA in C band array has been reported in [109] but gain of this antenna is quite low and it is around 5 dBi. Nevertheless, all these investigations were initiated through simulation followed by measurements.

The above mention reports, mainly discuss the CSMA with specific sector angle and mostly in intuitive way. They failed to draw accurate theoretical and analytical studies which are very much required to understand the structural behavior of CSMA in details for the design engineers working with CSMA. Therefore, all this lacuna of earlier studies should be investigate elaborately to understand the exact behavior of CSMA.

1.5.   Preface of the Dissertation

In the dissertation, improvement of some input and output characteristics of CSMAs have been investigated theoretically and implemented practically.
This antenna has been attracted to the antenna community and manufacturer in this modern age due to its compact size requirement compare to conventional geometry like circular patch antenna. So as to prepare modern hand held wireless device, less size of the antenna is being required to keep the associated circuitry besides the antenna. CSMA is highly demandable in this context but accurate resonance frequency and lowest order mode determination of this antenna is still lacking.

In chapter 2, the resonance frequency has been analyzed accurately. The effect of the feed location of the modes has been investigated further to determine the lowest order dominant mode with variation of substrate height, substrate permittivity and air gap. The improved computer aided design (CAD) has been formulated which makes the CSMA more promising than ever before. Modified cavity model has been introduced to determine the lowest order modes in CSMA.

In Chapter 3, the feed-probeposition for excitations of desire mode has been investigated and presented theoretically and verified experimentally. To find a proper feed location for exciting a particular mode in a CSMA, the appropriate theoretical formulation is another basic requirement. In this context no well established theoretical formulation for exciting a dominant mode of a CSMA is available till

date. Therefore, the determination of modes of a CSMA as a function feed location has been investigated and a new theoretical approximation technique has been projected based on maximum E/H ratio in this chapter to excite a specific mode.

Indeed, CSMAs with different range of sector angles has been classified and discussed scientifically by the relation of E/H ratio. A particular range of $|E/H|$ has been prescribed on which a particular mode can be excited. Moreover, a range of feed location has been approximated across which a particular mode can be excited if probe is placed.

Previous two chapters have been concentrated only the investigation of input characteristics. So the radiation characteristics and gain of this antenna have been given empathies to explore the performance of the antenna in some extent. The Gain of this antenna is generally low (7.1 dBi) that has been improved (9.9 dBi) by introduce an air in the substrate. The quick hand empirical formula also has been prescribed in this chapter.

In chapter 4, the complete design guideline has been prescribed for the specific application. The behavior of CSMA is generally varied with sector angles due to its asymmetric structure. So numerous number of sector angles are there. Thus selection of sector angles as a function of operating mode and frequency & miniaturization has been described for better selection and comprehensive guideline has been prescribed in this chapter.

In chapter 5, CSMA of 180^0 sector angle has been considered for investigation in view of the replacement of CMA. The minimization of patch area is advantageous around 50% as compare to circular microstrip antenna but co-pole (CP) to cross pole (XP) isolation is not satisfactory. Therefore to minimize XP radiation in this chapter, the patch area has been defected judiciously. Further the effect of ground plane variation also studied.

Finally in chapter 6, a conclusion of complete work has been presented and the best choice of sector angle antenna has been identified which can be used for all perspective such as industrial applications along with research and future application.

References

[1] G. A. Deschamps, "Microstrip Microwave Antennas," *Third USAF Symposium on Antennas* 1953.

[2] J. Q. Howell, "Microstrip Antennas," *IEEE Transactions on Antennas and Propagation*, AP- 23, no.1, pp. 90-93, January 1975

[3] R. Munson, "Conformal microstrip antennas and microstrip phased arrays," in *IEEE Transactions on Antennas and Propagation*, vol. 22, no. 1, pp. 74-78, January 1974, doi: 10.1109/TAP.1974.1140723.

[4] T. Itoh and R. Mittra, "Analysis of microstrip disk resonator," Arch. Elek. Ubertagung, vol. 21, pp. 456–458, Nov.1973.

[5] A. Derneryd, "Linearly polarized microstrip antennas*," IEEE Trans. Antennas Propagat.*, vol. 24, no. 6, pp. 846–851, 1976.

[6] G. Dubost, M. Nicolas and H. Havot, "Theory and applications of broadband microstrip antennas," Proc. 6th European Microwave Conference, pp. 275–279, 1976.

[7] P. Agrawal and M. Bailey, "An analysis technique for microstrip antennas," *IEEE Trans. Antennas Propagat.*, vol. 25, no. 6, pp. 756–759, 1977.

[8] W. F. Richards, Y. T. Lo and D. D. Harrison, "Improved theory for microstrip antennas," *Electronics Letters*, vol. 15,no. 2, pp. 42–44, 1979.

[9] Y. T. Lo, D. Solomon and W. Richards, "Theory and experiment on microstrip antennas," *IEEE Trans. Antennas Propagat.*, vol. 27, no. 2, pp. 137–145, 1979.

[10] P. Hammer, D. V. Bouchaute, D. Verschraeven, and A.V. D. Capelle, "Amodel for calculating the radiation field of microstrip antennas," *IEEE Trans. Antennas Propagat.*, vol. 27, no. 2, pp. 267–270, 1979.

[11] K. Keen, "A planar log-periodic antenna," *IEEE Trans. Antennas Propagat.*, vol. 22, no. 3, pp. 489–490, 1974.

[12] D. T. Shahani and B. Bhat, "Network model for strip-fed cavity-backed printed slot antenna," Electronics Letters, vol. 14, no. 24, pp. 767–769, 1978.

[13] I. E. Rana and N. G. Alexopoulos, "On the theory of printed wire antennas," 9th European Microwave Conference, pp. 687–691, 1979.

[14] A. Mulyanto, and R. Vernon, "AV-shaped log-periodic printed-circuit antenna array for the 1 to 10 GHz frequency range," Antennas and Propagation Society Intl. Symp., vol. 17, pp. 392–395, 1979.

[15] I. J. Bahl and P. Bhartia, *Microstrip Antennas*, Artech House, 1980.

[16] J. R. James, P. S. Hall, and C. Wood, *Microstrip Antennas: Theory and Design,* London, UK, Peter Peregrinus, 1981.

[17] C. A. Balanis, *Antenna Theory: Analysis and Design,* John Wiley & Sons, NY, 1997.

[18] R. Garg, P. Bhartia, I. Bahl, and A. Ittipiboon, *Microstrip Antenna Design Handbook*, Artech House, Norwood, 2001.

[19]   D. Pozar, "An update on microstrip antenna theory and design including some novel feeding techniques,"*IEEE Antennas and Propagation Society Newsletter*, vol. 28, no. 5, pp. 4-9, 1986.

[20]   A. Mandal, A. Ghosal, A. Majumdar, A. Ghosh, A. Das and S. K. Das, "Analysis of feeding techniques of rectangular microstrip antenna," *2012 IEEE International Conference on Signal Processing, Communication and Computing (ICSPCC 2012)*, pp. 26-31, 2012.

[21]   A. Arora, A. Khemchandani, Y. Rawat , S. Singhai , G. Chaitanya, "Comparative study of different Feeding Techniques for Rectangular Microstrip Patch Antenna," *International Journal of Innovative Research in Electrical, Electronics, Instrumentation and Control Engineering* , vol. 3, no. 5, pp. 32-35, 2015.

[22]   I. Singh, V. S. Tripathi, "Micro strip Patch Antenna and its Applications: a Survey"*Int. J. Comp. Tech. Appl.*, vol. 2, no 5, pp. 1595-1599,2011.

[23]   S. Bisht, S. Saini, V. Prakash , and B. Nautiyal, "Study The Various Feeding Techniques of Microstrip Antenna Using Design and Simulation Using CST Microwave Studio," *International Journal of Emerging Technology and Advanced Engineering,* vol. 4, no. 9, 2014.

[24]   H. K. Varshney, M. Kumar, A. K. Jaiswal, R. Saxena, and K. Jaiswal, "A Survey on Different Feeding Techniques of Rectangular Microstrip Patch Antenna," *International Journal of Current Engineering and Technology,*vol. 4, no. 3, pp. 1418-1423, 2014.

[25]   G. Singh, J. Singh, "Comparative Analysis of Microstrip Patch Antenna with Different Feeding Techniques," *International Conference on Recent Advances and Future Trends in Information Technology (iRAFIT 2014)*, pp. 18-22, 2014.

[26]   A. Kumar, J. Kaur , and R. Singh, "Performance Analysis of Different Feeding Techniques," *International Journal of Emerging Technology and Advanced Engineering*, vol. 3, no. 3, pp. 884-890, 2013.

[27]   P. J. Soh, M. K. A. Rahim, A. Asrokin, and M.Z.A Abdul Aziz "Design, Modeling, and performance Comparison of feeding techniques for a Microstrip Patch Antenna," *JurnalTeknogi,* vol 47, no. 1, pp. 103-119, 2007.

[28]   P. J. Soh, M. K. A. Rahim, A. Asrokin, and M. Z. A. A. Aziz, "Comparative radiation performance of different feeding techniques for a microstrip patch antenna," *Asia-Pacific Conference on Applied Electromagnetics,* pp. 6, 2005.

[29]   G. Qasim and S. Zhong, "Radiation characteristics of microstrip patch antennas with dielectric covers," *IEEE Antennas and Propagation Society International Symposium 1992 Digest*, pp. 2208-2211, 1992.

[30]   J.-F. Kiang, "Radiation characteristics of rectangular patch antennas with a laminated ground plane,"*IEE Proc.-Microw. Antennas Propag.,* vol. 143, no. 2, pp. 107-112, 1996.

[31]   N. K. Saxena, N. Kumar, and P. K. S. Pourush, "Radiation Characteristics of Microstrip Rectangular Patch Antenna Fabricated on LiTiMg Ferrite

Substrate," *AEU - International Journal of Electronics and Communications,* vol. 69, no. 12, pp. 1741-1744, 2015.

[32] C. Chandan, A. Ghosh, S. K. Ghosh, and S. Chattopadhyay, "Radiation characteristics of rectangular patch antenna using air substrates," *2009 International Conference on Emerging Trends in Electronic and Photonic Devices & Systems*, pp. 346-348, 2009.

[33] J. Liang and H. D. Yang, "Radiation Characteristics of a Microstrip Patch Over an Electromagnetic Bandgap Surface,"*IEEE Transactions on Antennas and Propagation*, vol. 55, no. 6, pp. 1691-1697, 2007.

[34] W. C. Chew and J. A. Kong, "Radiation characteristics of a circular microstrip antenna," *Journal of applied physics,* vol. 51, no. 7, pp. 3907-3915, 1980.

[35] A. K. Bhattacharyya, "Effects of finite ground plane on the radiation characteristics of a circular patch antenna," in *IEEE Transactions on Antennas and Propagation*, vol. 38, no. 2, pp. 152-159, 1990.

[36] S. Bedra, R. Bedra, "Radiation Characteristics of Circular Microstrip Patch Antenna with and Without Air Gap Using Neuro-Spectral Computation Approach," *IEEE Transactions on Antennas and Propagation*,vol. 38**.** no. 2. 1990.

[37] C. Y. Huang, J. Y. Wu, and K. L. Wong,"High-gain compact circularly polarized microstrip antenna,"*Electron Letter*, vol. 34, no. 3 pp. 712-715, 1998.

[38] C. Y. Huang, J. Y. Wu, C.F. Yang, and K. L. Wong,"Gain enhancement compact broadband microstrip antenna,"*Electron Letter,* vol. 34, no. 9, pp. 138-147, 1998.

[39] S. Park, C. Kim, Y. Jung, H. Lee, D. Cho, and M. Lee, " Gain enhancement of a microstrip patch antenna using a circularly periodic EBG structure and air layer,"*Int. J. Electron.Commun.(AEU),* vol. 64, no. 7, pp. 607-613, 2010.

[40] N. Llombart, A. Neto, G. Gerini, and P. de Maagt, "Planar circularly symmetric EBG structures for reducing surface waves in printed antennas," *IEEE Transactions on Antennas and Propagation*, vol. 53, no. 10, pp. 3210-3218, 2005.

[41] F. Abboud, J. P. Damiano, and A.Papeirnik, "A new model for calculating the input impedance of coax-fed circular microstrip antennas with and without air gaps,"*IEEE Trans Antennas Propag.,* vol. 38, no. 11,pp. 1882-1887, 1990.

[42] D. Guha, S.Chattopadhyay, and J. Y. Siddiqui, "Estimation of gain enhancement replacing PTFE by air substrate in a microstrip patch antenna," *IEEE Antennas and Propagation Mag*azine, vol. 52, no. 3, pp. 92-95, 2010.

[43] H. Boutayeb and T. A. Denidni, "Gain Enhancement of a Microstrip Patch Antenna Using a Cylindrical Electromagnetic Crystal Substrate,"*IEEE Transactions on Antennas and Propagation*, vol. 55, no. 11, pp. 3140-3145, 2007.

[44] Y-J. Park, A. Herschlein, and W. Wiesbeck, "A photonic bandgap (PBG) structure for guiding and suppressing surface waves in millimeter-wave antennas," *IEEE Transactions on Microwave Theory and Techniques*, vol. 49, no. 10, pp. 1854-1859, 2001.

[45] S. B. Yeap and Z. N. Chen, "Microstrip Patch Antennas with Enhanced Gain by Partial Substrate Removal," *IEEE Transactions on Antennas and Propagation*, vol. 58, no. 9, pp. 2811-2816, 2010.

[46] K. Mandal and P. P. Sarkar, "A compact high gain microstrip antenna for wireless applications," *Int. J. Electron Commun. (AEÜ),* vol. 67, no. 12, pp. 1010-1014, 2013.

[47] A. K. Arya, A. Patnaik, and M. V. Kartikeyan, "Gain Enhancement of Micro-strip patch antenna using Dumbbell shaped Defected Ground Structure"*International Journal of Scientific Research Engineering & Technology (IJSRET),*vol. 2, no.4, pp 184-188, 2013.

[48] J-S.Kuo and G-B. Hsieh, "Gain enhancement of a circularly polarized equilateral-triangular microstrip antenna with a slotted ground plane," *IEEE Transactions on Antennas and Propagation*, vol. 51, no. 7, pp. 1652-1656, 2003.

[49] S. K. Padhi, N. C. Karmakar, C. L. Law and S. Aditya, "A dual polarized aperture coupled circular patch antenna using a C-shaped coupling slot,"*IEEE Transactions on Antennas and Propagation*, vol. 51, no. 12, pp. 3295-3298, 2003.

[50] Y. Yusuf, H. Cheng, X. Gong, "Co-designed substrate-integrated waveguide filters with patch antennas, *IET Mirowave, antennas and propagation*, vol.7, no.7, pp.493-501,2013.

[51] S. Kojima, N. Shinohara and T. Mitani, "Integration of a Via-Loaded Annular-Ring Reduced-Surface-Wave Antenna and a Branch-Line Coupler," *IEEE Access*, vol. 8, pp. 133645-133653, 2020.

[52] S. M. Rathod, R. N. Awale, K. P. Ray, and S. S. Kakatkar, "Directivity Enhancement of a Circular Microstrip Antenna with Shorting Post," *IETE Journal of Research*, 2019.doi: 10.1080/03772063.2019.1612285.

[53] J-H. Ou, J. Huang, J. Liu, J. Tang, and X. Y. Zhang, "High-Gain Circular Patch Antenna and Array With Introduction of Multiple Shorting Pins," *IEEE Transactions on Antennas and Propagation*, vol. 68, no. 9, pp. 6506-6515, 2020.

[54] K. Xu and J. Shi, "High-efficiency circular dense dielectric patch antenna with frequency selectivity," *IET Electronic Letters*, vol. 54, no. 14, pp.861-862,2018.

[55] Md. A. K. Khan, T. A.Shaem, M. A. Alim, "Graphene patch antennas with different substrate shapes and materials," *Optik*, vol.202, 2020, doi: 10.1016/j.ijleo.2019.163700.

[56] Z. N. Chen and M. Y. W. Chia, "Broad-Band Suspended Probe-Fed Plate Antenna with Low Cross-Polarization Levels," *IEEE Transaction Antennas Propagt*. vol. 51, no. 2, pp. 345-346, 2003

[57]   P. Li, H. W. Lai, K. M. Luk, and K. L. Lau, "A wideband patch antenna with cross-polarization suppression," *IEEE Antennas Wireless Propag. Lett.,* vol. 3, pp. 211–214, 2004. doi: 10.1109/LAWP.2004.834937.

[58]   K. L. Wong, C. L. Tang, and J. Y. Chiou, "Broad-band probe-fed patch antenna with a W-shaped ground plane," *IEEE Trans. Antennas Propagt.,* vol. 50, no.6, pp. 827–831, 2002.

[59]   W. H. Hsu, and K. L. Wong, "Broad-band probe-fed patch antenna with a U-shaped ground plane for cross-polarization reduction," *IEEE Trans. Antennas Propagt.,* vol. 50, no.3, pp. 352–355, 2002.

[60]   D. Guha, M. Biswas, and Y. M. M. Antar, "Microstrip patch antenna with defected ground structure for cross polarization suppression," *IEEE Antennas Wireless Propag. Lett.,* vol. 4, pp. 455-458, 2005.

[61]   D. Guha, C. Kumar, and S. Pal, "Improved cross-polarization characteristics of circular microstrip antenna employing arc-shaped defected ground structure (DGS)," *IEEE Antennas Wireless Propag. Lett.,* vol. 8, pp. 1367-1369, 2009.

[62]   A. Ghosh, D. Ghosh, S. Chattopadhyay, and L. L. K. Singh, "Rectangular Microstrip Antenna on Slot Type Defected Ground for Reduced Cross Polarized Radiation," *IEEE Antenna and Wireless Propag. Letters,* vol. 14, pp. 321 – 324, 2015.

[63]   S. Chakraborty and S. Chattopadhyay, "Substrate fields modulation with defected ground structure: A key to realize high gain, wideband microstrip antenna with improved polarization purity in principal and diagonal planes," *International Journal of RF and Microwave Computer-Aided Engineering,* vol. 26, no.2, pp.174-181, 2016.

[64]   S. Chakraborty and S. Chattopadhyay, "Arc-cornered microstrip antenna with defected ground structure for broad banding and improved cross-polarization suppression over whole skew planes," *Int. Journal of Microwave and Wireless Technologies,* vol. 9, no. 2, pp. 437-446, 2017.

[65]   S. Chattopadhyay, and S. Chakraborty, "A physical insight into the influence of dominant mode of rectangular microstrip antenna on its cross-polarization characteristics and its improvement with T-shaped microstrip antenna", *IEEE Access,* 6, pp. 3594-3602, 2018.

[66]   A. Ghosh, S. Chakraborty, S. Chattopadhyay, A. Nandi, and B. Basu, " Rectangular microstrip antenna with dumbbell shaped defected ground structure for improved cross polarised radiation in wide elevation angle and its theoretical analysis," *IET Microwaves Antennas &Propag.,* vol. 10, no. 1, pp. 68-78, 2016.

[67]   A. Ghosh and B. Basu, "Triangular slotted Ground Plane: a Key to Realize High Gain, Cross- polarization Free Microstrip Antenna with Improved Bandwidth,"*Turkish Journal of Electrical Engineering & Computer Sciences,* vol. 27, no. 3, pp. 1559-1570, May, 2019.

[68]   A. Ghosh, S. Chattopadhyay, S. Chakraborty, and B. Basu, "Cross Type Defected Ground Structure Integrated Microstrip Antenna for Wide Band Width and Improved Polarization Purity", *Journal of Electromagnetic*

Waves and Applications (Taylor & Francis), vol. 31, no.5, pp.461-476, 2017.

[69] K. K. Naik and P. A. V. Sri, "Design of Hexadecagon Circular Patch Antenna with DGS at Ku Band for Satellite Communications," *Progress In Electromagnetics Research M,* vol. 63, pp. 163–173, 2018

[70] C. Kumar and D. Guha, "Asymmetric and compact DGS configuration for circular patch with improved radiations," IEEE AntennasWireless Propag. Lett., vol. 19, no. 2, pp. 355–357, Feb. 2020.

[71] T. Sarkar, A. Ghosh, L. L. K. Singh, S. Chattopadhyay, and C.-Y.-D. Sim,"DGS-integrated air-loaded wideband microstrip antenna for X- and Kuband," IEEE Antennas Wireless Propag. Lett., vol. 19, no. 1, pp. 114–118,Jan. 2020.

[72] A. Ghosh, S. K. Ghosh, D. Ghosh, and S. Chattopadhyay, "Improved polarization purity for circular microstrip antenna with defected patch surface," *Int. Journal of Microwave and Wireless Technologies*, vol. 8, no. 1, pp. 89-94, 2016.

[73] A. Ghosh, S. Chattopadhyay, L. L. K. Singh, and B. Basu,"Wide bandwidth microstrip antenna with defected patch surface for low cross polarization applications", *International Journal of RF and Microwave Computer-Aided Engineering* (Wiley), vol. 27, no. 8, pp. 1-10, 2017.

[74] A. Ghosh, S. Chakraborty, S. Chattopadhyay, A. Paul, S. Shivani, S. Sengupta, S. Banik, and S. Kumari, "Rectangular Microstrip Antenna with Defected Patch Surface for Improved Polarization Purity," *Proc. of 2015 Third Int Conf. on Computer, Communication, Control and Information Technology(C3IT)*, Howrah, India, pp. 7-8, 2015.

[75] D. Ghosh, S. K. Ghosh, S. Chattopadhyay, S. Nandi, D. Chakraborty, R. Anand, R. Raj, and A. Ghosh, "Physical and Quantitative Analysis of Compact Rectangular Microstrip Antenna with Shorted Non-Radiating Edges for Reduced Cross Polarized Radiation using Modified Cavity Model," *IEEE Antennas and Propagation Magazine*, vol.56, no.4, pp. 62-72, 2014.

[76] R. Poddar, S. Chakraborty, and S. Chattopadhyay, "Improved Cross Polarization and Broad Impedance Bandwidth from Simple Single Element Shorted Rectangular Microstrip Patch: Theory and Experiment," *Frequenz*, vol. 70, no. 1-2, pp. 1-9, 2016.

[77] Zonunmawii, A. Ghosh, L. L. K. Singh, S. Chattopadhyay, C-Y-D. Sim, "Reduced-Surface-Wave-Inspired Circular Microstrip Antenna for Concurrent Improvement in Radiation Characteristics", *IEEE Antenna & Wave Propagation Letter*, vol. 20, no. 5, pp. 858-862, 2021.

[78] M. U. Khan, M. S. Sharawi, and R. Mittra , "Microstrip patch antenna miniaturisation techniques: a review," *IET Microwaves, Antennas & Propagation,* vol. 9, no.9, pp. 913-922, 2015.

[79] H. Pues and A. V. Capelle, "accurate transmission line model for rectangular microstrip antenna," *IEE Proceedings H - Microwaves, Optics and Antennas*, vol. 131, no. 6, pp. 334-340, 1984.

[80] D. Guha and J. Y. Siddiqui, "Resonant frequency of circular microstrip antenna covered with dielectric superstrate," *IEEE Transactions on Antennas and Propagation*, vol.51, no.7, pp. 1649-1652, 2003.

[81] L. C. Shen, S. A. Long, M. Allerding, and M. Walton, "Resonant Frequency of a circular Disk Printed Circuit Antenna," *IEEE Transactions on Antennas and Propagation*, vol. 25, no.4, pp. 595-596, 1977.

[82] S. A. Long, L. C. Shen, and P.B. Morel, "Theory of Circular Disc Printed Circuit Antenna," *Proc. IEE*, vol.125, no.10, pp. 925-928,1978.

[83] G. A. Conway, S. L. Cotton, and W. G. Scanlon, "Design and characterization of integrated antennas for compact wearable wireless devices," *Proc. CNC/USNC North American Radio Science Meeting,* vol. 3, no. 8, pp. 1151–1156, 2007.

[84] S. Chattopadhyay, J. Y. Siddiqui, and D. Guha, "Rectangular Microstrip Patch on A Composite Dielectric Substrate for High Gain Wide Beam Radiation Patterns," *IEEE Trans. Antennas Propagation*, vol. 57, no. 10, pp. 3324-3327, 2009.

[85] R. Ranjan, M. K. Verma, S. Mukherjee, D. Ghosh and S. Chattopadhyay, "Rectangular Microstrip Antenna Using Inductive Septums for Dual Band Operation with a New Resonant Mode," *Journal of Electromagnetic Analysis and Applications*, vol.4, no.7, pp. 285-292, 2012.

[86] D. Guha, S. Chattopadhyay and J. Y. Siddiqui, "Estimation of Gain Enhancement Replacing PTFE by Air Substrate in a Microstrip Patch Antenna," *IEEE Antennas and Propagation Magazine*, vol. 52, no. 3, pp. 92-95,2010.

[87] J. K. Sah, S. Chatterjee, P. Bharati, D. Ghosh, A. Anand, and S. Chattopadhyay, "Rectangular Microstrip Antenna for Symmetrical 3-D Beam Widths for an Efficient Feed of Reflector Antenna and Its Quantitative Analysis," *Journal of Electromagnetic Analysis and Applications*, vol. 52, no. 6, pp. 230-234 , 2012.

[88] J. Colaco and R. Lohani. "Design & implementation of Microstrip patch antennas for 5G", *5th international conference on Communication & Electronics Systems (ICCES), pp.* 682-685,2020.

[89] W. F. Richards, J. D. Ou, and S.A. Long, "A Theoretical and Experimental Investigation of Annular Sector, and Circular Sector Microstrip Antennas," *IEEE Transactions Antennas and Propagation,* vol. 32, no. 8, pp. 864-867, 1984.

[90] A. K. Bhattacharya and R. Garg, "Analysis of Annular Sector and Circular Sector Microstrip Patch Antennas," *Electromagnetics*, vol. 6, no. 3, pp. 229-242, 1986.

[91] V. K. Tiwari, A. Kimothi, D. Bhatnagar , J. S Saini, V. K Saxsena, and P. Kumar, "Theoretical analysis on circular sector microstrip antennas ," *Indian Journal of Radio Space Physics*, vol. 35, no. 2, pp. 133-138, 2006.

[92] V. K. Tiwari, A. Kimothi, D. Bhatnagar , J. S Saini, and V. K Saxsena, "Theoretical and experimental investigations of circular sector microstrip

antennas," *Indian Journal of Radio Space Physics*, vol. 35, no. 3, pp. 206-211, June 2006.

[93] S. Bhattacharyya (Roy), D. Ghosh, G. K. Singh, R. Singh, A. Raj, M. Choudhury, S. Chattopadhyay, and A. Ghosh, "Accurate CAD Formulation for Resonant Frequency of Circular Sectorial Microstrip Antenna," *Proc.of IEEE International Conference on Microwave and Photonics*, 2013. doi: 10.1109/ICMAP.2013.6733513.

[94] A. Dalli, L. Zenkouar, and S. Bri, "Theoretical analysis and optimization of circular sector microstrip antenna," *Revue Méditerranéenne des Télécommunications*, vol. 2, no. 2, pp. 100-104, 2012.

[95] A. Dalli, L. Zenkouar, and S. Bri, "Conception of Circular Sector Microstrip Antenna and Array," *Inter.Jr. of Microwaves Applications,* vol.1, no.1, pp. 32-37, 2012.

[96] R. Agarwal and D. C. Dhubkarya, "Design and Simulation of circular sector microstrip antenna," *Int. Jr. of Knowledge Engineering and Technology*," vol. 1, 2012.

[97] A. Deshmukh, A. R. Jain, A. A. Joshi, T. A.Tirodkar, and K. P. Ray, "Broadband Proximity Fed Modified Circular Microstrip Antenna," *Proc. of Advances in Computing and Communications (ICACC),* 2013, doi: 10.1109/ICACC.2013.86.

[98] A. A. Deshmukh, V. Pandita, R. Colaco, and R. Doshi, "Dual band dual polarized modified circular microstrip antenna," Proc. Of Circuits, Systems, Communication and Information Technology Applications (CSCITA), 2014. doi: 10.1109/CSCITA.2014.6839285.

[99] A. A. Deshmukh and N. V. Phatak, "Broadband Sectoral Microstrip Antennas," *IEEE Antennas Wireless Propagation Leters*, vol. 14, pp. 727-730, Dec. 2014.

[100] S. Maddio "A Compact Circularly Polarized Antenna for 5.8-GHz Intelligent Transportation System,"*IEEE Antennas and Wireless Propagation Letters*, vol. 16,pp. 533 – 536, 2016.

[101] S. Naser ,N. Dib "A compact printed UWB Pacman-shaped MIMO antenna with two frequency rejection bands"*Applied Electrical Engineering and Computing Technologies (AEECT), 2015 IEEE Jordan Conference*,doi:10.1109/AEECT.2015.7360533 .

[102] W-J. L. Q. Li, S-G. Wang, and L. Zhu, "Design Approach to a Novel Dual-Mode Wideband Circular Sector Patch Antenna," *IEEE Transactions on Antennas and Propagation*, vol. 65, no.10, *pp.*4980-4990, 2017.

[103] D. D. Krishna,C. K. Aanandan,P. Mohanan , andK. Vasudevan "Circular microstrip antenna with a sector-slot for dual-port operation,"*Microwave and Optical Technology Letters,* doi: 10.1002/mop.21393, 2006.

[104] S. Yan, G. A. E. Vanderbosch, "Meta loaded CSMA," *progress In Electromagnetics Research*, vol. 156, pp. 37-46, 2016.

[105] G. K. Oguz, S. T. Imeci , "A Compact Size Circular Sector Patch Antenna For Ku-band Applications," *Applied Computational Electromagnetics Society Symposium - Italy (ACES),*2017.doi:10.23919/ROPACES.2017.7916057.

[106] A. A. Deshmukh, P. A. Kadam, A. Doshi, P. Kamble ,"Sectoral patch antenna embedded with arc shape slots and slits for circular polarized response,"*2018 International Conference on Communication information and Computing Technology (ICCICT),*2018. doi:10.1109/ICCICT.2018.8325897.

[107] A. A. Deshmukh, A. Jain, and K. P. Ray, "Broadband 270° sectoral microstrip antenna,"*Microwave and Optical Technology Letters,* 2014.doi: 10.1002/mop.28351.

[108] A. A. Deshmukh, P. Kamble, A. Doshi, D. Issrani, and K. P. Ray, "Proximity Fed broadband 120^0 sectoral Microstrip Antenna," *Procedia Computer Sciences* , vol. 115, no.10, pp.101-107, 2017.

[109] A. Dalli, L. Zenkouar, and S. Bri, "Comparison of Circular Sector and Rectangular Patch Antenna Arrays in C-Band," *Journal of Electromagnetic Analysis and Applications*, vol. 4, no. 11, pp. 457-467, 2012.

CHAPTER

2

Circular Sector Microstrip Antenna: Determination of Accurate Modes Using Modified Cavity Model

2.1   Introduction

In the modern era of wireless communications, the design and analysis of miniaturized and multifunctional antennas of different geometries continue to be the focus of state-of-the-art research. In this scenario, the most common geometries of microstrip antennas (MAs), such as rectangular and circular, have been extensively studied, analyzed and implemented for at least the last three decades as discussed in chapter 1.   However, in various practical wireless applications, radiators should be conformally mounted onto the previously existing structures, where space limitation is a crucial problem. In such applications, a circular sector microstrip antenna (CSMA) is highly advantageous because it requires less space than a conventional patch antenna of common geometries. Approximately more than 50% patch area reductions can be achieved with particular sector angles, compared with a conventional circular MPA. Therefore, an accurate analysis of CSMA is a priority in the present scenario of printed antenna research. In this context, a limited number of analyses [1]-[5] have been reported in which the computation of the accurate resonant frequency of CSMA with arbitrary sector angles has been dealt with. The formulation of the resonant frequency of a CSMA based on the cavity model was first reported in [1].   The electric field beneath the patch as well as the eigen functions of those antennas were also presented in [1]. In [2], a generalized transmission line modeling was used for computing the resonant frequency of a CSMA. However, the effect of fringing fields, which should be considered for the

accurate estimation of the resonant frequency of a CSMA, was not included in [1]-[2].

Recently, the theoretical and experimental analyses of CSMAs have been reported in [3]-[4]. In these works, the authors introduced the idea of fringing fields for computing the effective dimension of the patch required for calculating the resonant frequency of the antenna. However, the resonant frequency of the antenna could not be accurately predicted; and the dominant mode of CSMAs has been assumed to be similar to that of a conventional circular patch (TM_{11}), regardless of the sector angle in [3]-[4]. Nevertheless, the dominant mode of a CSMA should differ for different cavity dimensions (i.e., for changes in the sector angle) to satisfy the boundary conditions of electromagnetic fields beneath the patch.

Therefore, the identification of the mode of a CSMA with different sector angles is inappropriately reported in [3]-[4]. Moreover, the validation of the theories presented in [3]-[4] in terms of varying antenna parameters (such as substrate thickness, dielectric constant and air gap height) is not included. Furthermore, the higher modes were not investigated in those reports. In [5], Bhattacharya et al have computed the resonant frequency of the CSMA following the cavity model; however, they failed to identify the accurate dominant mode of the CSMA and predict its accurate resonant frequency. The study of the radiated field, resonant frequency and polarization of the CSMA was presented in [6]. The array structure with CSMA for the C and X band was investigated and the effect of element number in the array was reported in [7]. A simulation study of CSMA with 70^0 sector angle for CSMA was reported in [8]. Recently, some newer applications of CSMAs have been reported in [9]-[11], however, accurate dominant modes of the antenna were not emphasized in these reports. The resonant frequencies in these studies were based only on simulations. Therefore, neither the lowest order dominant mode, nor the corresponding resonant frequency of the CSMAs has been accurately determined in these previous investigations. Furthermore, in the study of a CSMA, the introduction of an air gap between the substrate and the ground plane, which offers the tunability of microstrip structures for rectangular and circular geometries, is very important [12]-[13].
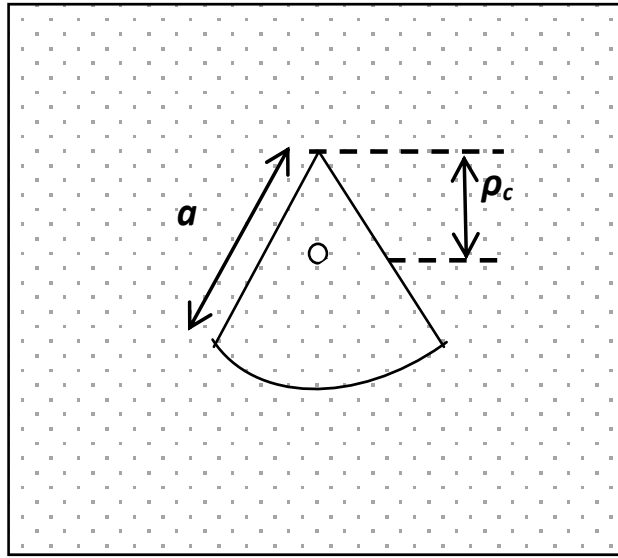
(a)
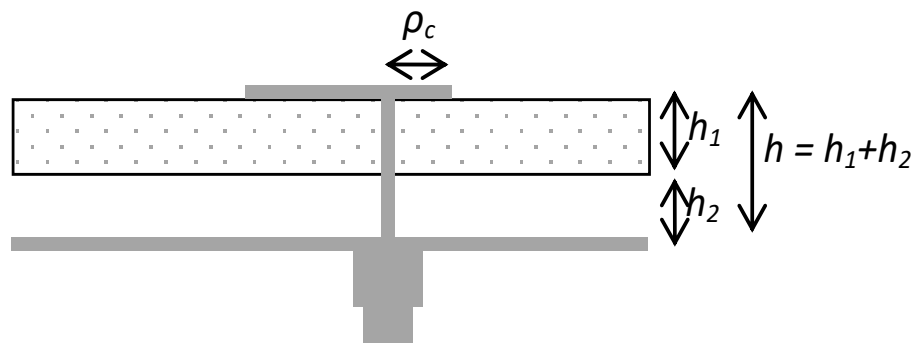
(b)
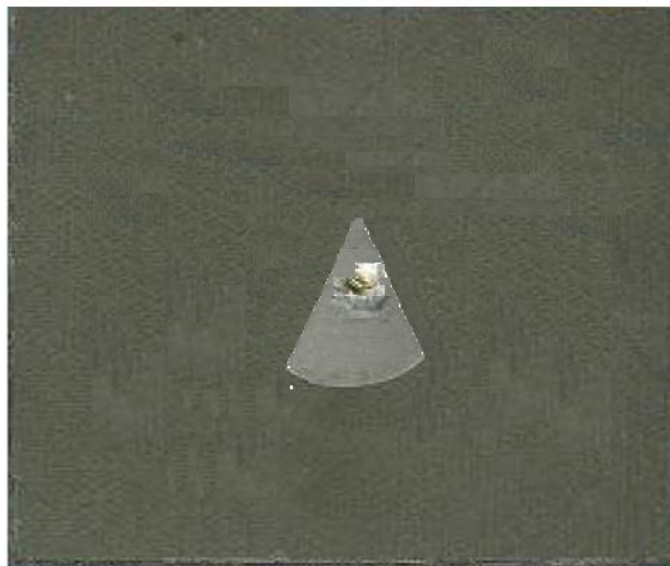
(c)
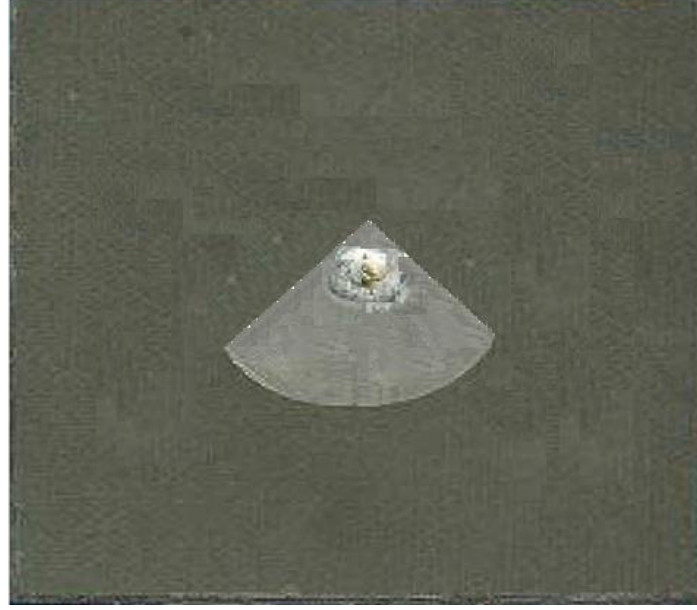
(d)
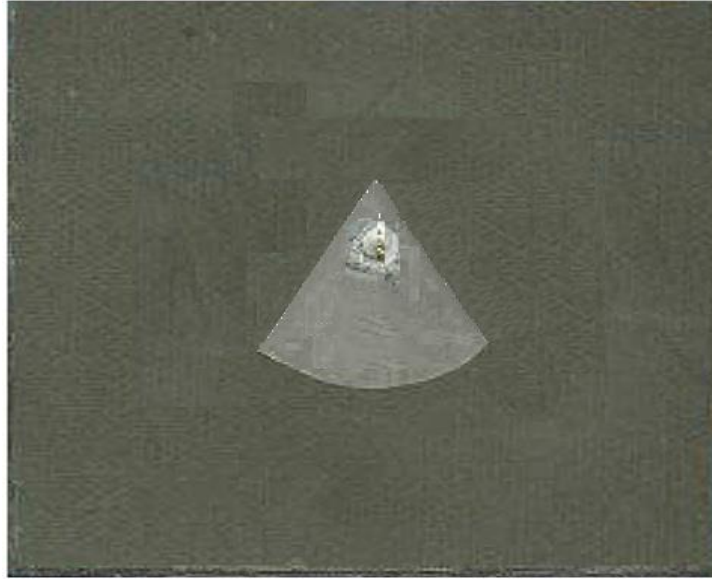
(e)

Fig. 2.1 Schematic representation of coax fed circular sectorial microstrip antenna (CSMA) (a) top view, (b) side view, some of the fabricated prototypes (c) 45^0 sector angle, (d) 90^0 sector angle, (e) 60^0 sector angle respectively.

However, the role of an air gap in the resonance behavior of the CSMA needs further investigation. To eliminate the lacunae of earlier works, the modal fields of the dominant as well as higher order modes of numerous CSMAs with different sector angles have been thoroughly studied. In this paper, an improved, accurate and comprehensive computer-aided design formulation for accurately determining the resonant frequency of a CSMA is proposed. The proposed formulation accurately

estimates the dominant and higher mode resonances in a CSMA with and without an air gap between the substrate and the ground plane. The mathematical derivations are based on the modified cavity model along with the accurate estimation of the effective permittivity and the effective antenna dimensions. The complete theory is presented meticulously in this paper for developing a concrete physical basis for the observed phenomenon. No published work that presents the variation of the resonant frequency of a CSMA with substrate thickness, air gap height, substrate permittivity, and the radial dimension of the antenna is available till date. Considering all the above-mentioned factors, the resulting variations of resonant frequencies as a function of the aforementioned parameters, have been included in the present study.

The theoretical formulation for the resonant frequency of a CSMA has been presented in section 2.2. The resonant frequency of a CSMA with varying sector angle and dielectric thickness is analyzed and a comprehensive and closed-form formulation is proposed in section 2.2.1. Therefore, an efficient equivalence relation is established and utilized for calculating the effective dimension of the patch has been described in section 2.2.2. Subsequently, the calculation of the effective dielectric constant of a CSMA has been presented in section 2.2.3. In section 2.3, the proposed theory has been validated against our simulation, the measurement data available in the literature, and our own measurement results. The resonant frequency of a CSMA as a function of substrate thickness, radial dimension of a patch and sector angle as well as the versatility of the present theory in determining the accurate higher order modes of CSMA for different sector angles are included in section 2.3. Section 2.4 contains the conclusions derived from the findings of the present work.

2.2   Theory

A coaxially fed CSMA with radial dimension a, printed on a substrate (ε_r) of thickness h_1 with an air gap of height (h_2) on the ground plane is shown in Fig. 2.1. The height of the air gap varies from zero to a certain finite value. The antenna is fed at a distance ρ_c from the apex of the conical shape as shown in Fig. 2.1 (a) using a coaxial probe. Some of the fabricated prototypes are shown in Fig. 2.1 (c). To calculate the resonant frequency of CSMA accurately, first the cavity model for

26

conventional circular patch has been utilized under the restriction of modified boundary conditions, as will be explained in section 2.2.1. This, in fact, provides a basic estimation of the resonant frequency of CSMA, with and without air gap. The fringing of the electric fields, at the edges of the patch, increases the effective dimension, which is accounted for in terms of a_{eff}. Indeed, this parameter needs to be determined precisely for accurate determination of antenna characteristics. Therefore, computations of effective dimension of the antenna and the effective dielectric constant are significant issues, which are discussed in section 2.2.2 and section 2.2.3.

2.2.1 Modified Cavity Model

Because of the narrowband resonant characteristics of their open radiating structures, microstrip antennas, can be viewed as lossy cavities. From this view point, cavity model is a very natural choice to analyze the modal fields of such antennas [14]. Classical description of using cavity model to determine the modal fields of conventional rectangular and circular patches can be found in [27]. Recently, cavity model analysis of shorted patch structure has been reported in [15]. In a very recent paper [16], exploitation of cavity model is documented for gain and bandwidth enhancement of a rectangular patch antenna.
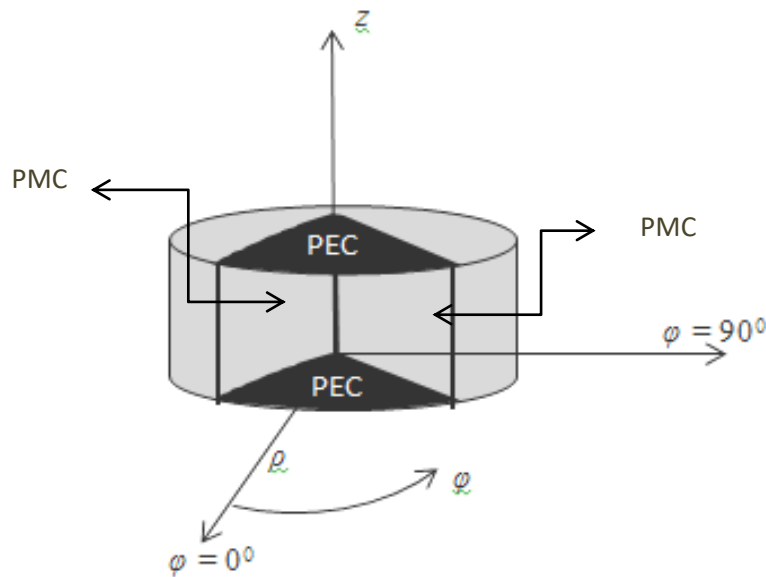
Fig. 2.2 The cavity model for CSMA.

The top and bottom walls (at *z = 0* and *h*) are perfect electric conductors (PEC), and three side walls are perfect magnetic conductors (PMC). Here, the normalized fields within the dielectric substrate (between patch and ground plane) can be determined accurately by treating the region as a cavity, bounded above and below by electric conductors (top and bottom plates, respectively) and along the periphery by magnetic walls. In the case of circular sector antenna, a modified cavity has been germinated whose top and bottom walls are perfect electric conductors (PEC), and the three side walls are perfect magnetic conductors (PMC).

The modified cavity model (MCM) is shown in Fig. 2.2.

The vector potential A_z must satisfy the homogeneous wave equation [17]

$$\nabla^2 A_z(\rho,\phi,z) + k^2 A_z(\rho,\phi,z) = 0 \tag{2.1}$$

where, A_z is given by [17] as

$$A_z = B_{mnp} J_m(k_\rho \rho)[A\cos(m\phi) + B\sin(m\phi)][\cos(k_z z)] \tag{2.2}$$

Therefore, the fields will be given by

$$
\left.
\begin{aligned}
E_\rho &= -\frac{j}{\omega\mu\varepsilon} \frac{\partial^2 A_Z}{\partial\rho\partial z} \\[6pt]
H_\rho &= \frac{1}{\mu}\frac{1}{\rho}\frac{\partial A_Z}{\partial\phi} \\[6pt]
E_\phi &= -\frac{j}{\omega\mu\varepsilon}\frac{1}{\rho}\frac{\partial^2 A_Z}{\partial\phi\partial z} \\[6pt]
H_\phi &= -\frac{1}{\mu}\frac{1}{\rho}\frac{\partial A_Z}{\partial\rho} \\[6pt]
E_z &= -\frac{j}{\omega\mu\varepsilon}\left(\frac{\partial^2}{\partial z^2}+k^2\right)A_Z \\[6pt]
H_z &= 0
\end{aligned}
\right\} \tag{2.3}
$$

Where ω, μ and ε are the frequency of the wave, permeability and permittivity of the medium respectively.

Based on the above equations, the resonant frequency of CSMA, with the widely used sector angles ($\phi_0 = 180^0$, 90^0 and 60^0) is documented in the following sections. Now, for the CSMA with arbitrary sector angle $\phi_0^{\;0}$;

$$H_\phi = 0; \left(\rho = a, 0 \leq \phi \leq \phi_0^0; 0 \leq z \leq h \right) \tag{2.4}$$

$$H_\phi(\rho = a) = -\frac{1}{\mu}\frac{\partial A_z}{\partial \rho} = -\frac{1}{\mu}B_{mnp}J_m'\left(k_\rho a\right)[A\cos m\phi + B\sin m\phi][\cos(k_z z)] = 0 \tag{2.5}$$

which signifies that,

$$J_m'\left(k_\rho a\right) = 0 \Rightarrow k_\rho a = \chi_{mn}' \Rightarrow k_\rho = {\chi_{mn}'}\big/{a} \tag{2.6}$$

where, J_m and J_m' are the Bessel functions of order m and its derivative respectively. χ_{mn}' is the nth zero of derivative of Bessel function of order m.

Again, the vanishing radial magnetic field boundary condition demands that,

$$H_\rho = 0; \left(\phi = 0, 0 \leq \rho \leq a; 0 \leq z \leq h \right)$$
$$H_\rho = 0; \left(\phi = \phi_0^0, 0 \leq \rho \leq a; 0 \leq z \leq h \right) \tag{2.7}$$

Thus,

$$H_\rho(\phi = 0) = \frac{1}{\mu}\frac{1}{\rho}\frac{\partial A_z}{\partial \phi} = \frac{1}{\mu}\frac{1}{\rho}B_{mnp}J_m(k_\rho \rho)[-mA\sin m\phi + mB\cos m\phi][\cos(k_z z)] = 0 \tag{2.8}$$

It is possible, if $B = 0$

Now,

$$H_\rho(\phi = \phi_0^0) = \frac{1}{\mu}\frac{1}{\rho}B_{mnp}J_m\left(k_\rho \rho\right)[-mA\sin m\phi_0][\cos(k_z z)] = 0 \tag{2.9}$$

It is possible, if

$$m\phi_0 = q\pi$$

$$m = \frac{q\pi}{\phi_0} \tag{2.10}$$

where $q = 0, 1, 2, 3,$ and all positive etc.

Again, the tangential electric field boundary condition requires that

$$E_\phi = 0; \left(z = 0, 0 \leq \rho \leq a; 0 \leq \phi \leq \phi_0^0 \right)$$
$$E_\phi = 0; \left(z = h, 0 \leq \rho \leq a; 0 \leq \phi \leq \phi_0^0 \right) \tag{2.11}$$

Therefore;

$$E_\phi(z = h) = \frac{j}{\omega\mu\varepsilon}\frac{1}{\rho}B_{mnp}J_m\left(k_\rho \rho\right)k_z(-mA\sin m\phi)\sin(k_z h) = 0 \tag{2.12}$$

It is possible if,

$$k_z = \frac{p\pi}{h}$$ (2.13)

Now, $k^2 = k_\rho^2 + k_z^2$ (2.14)

Where, k is the propagation vector and k_ρ, k_z are the propagation vectors along radial (ρ) and vertical (z) directions.

The resonance frequency (f_r) will be expressed as

$$f_r = \frac{1}{2\pi\sqrt{\mu\varepsilon}} \sqrt{\left(\frac{\chi'_{mn}}{a}\right)^2 + \left(\frac{p\pi}{h}\right)^2}$$ (2.15)

Considering that the patch is on thin substrate, the zeroth order resonance frequency (f_r) is

$$f_r = \frac{\chi'_{mn}}{2\pi a\sqrt{\mu\varepsilon}} = \frac{\chi'_{mn}c}{2\pi a\sqrt{\varepsilon_r}}$$ (2.16)

where, c is the free space velocity and χ'_{mn} is the nth zero of derivative of Bessel function of order m.

The parameter m is related to q by equation (2.10). The parameter n, in fact, denotes the number of radial variations, and q the number of circumferential variations.

Now considering the fringing effect around the patch periphery, the dimension a will be replaced by the effective dimension a_{eff}; and the dielectric constant ε_r by effective dielectric constant ε_{reff}.

Thus equation (2.16) becomes

$$f_r = \frac{\chi'_{mn}c}{2\pi a_{eff}\sqrt{\varepsilon_{reff}}}$$ (2.17)

The calculation of effective dimension a_{eff}; and the effective dielectric constant ε_{reff} is shown in section 2.2.2 and section 2.2.3, respectively.

30

Case-I: 180^0 circular sector patch antenna ($\varphi_0 = \pi$)

For semicircular patch, $\phi_0 = \pi$, and equation (2.10) becomes $m = q$. Thus, the possible values of m will be any positive integer greater than zero.

Following the roots of the derivative of Bessel function, the lowest value of $\chi'_{mn} = 1.84$ occurs when $m = 1$, $n = 1$.

Therefore, according to equation (2.17), the lowest order resonant mode (dominant mode) of semicircular patch becomes TM_{11} and hence its frequency is

$$f_r = \frac{\chi'_{11}c}{2\pi a_{eff}\sqrt{\varepsilon_{reff}}} = \frac{1.84c}{2\pi a_{eff}\sqrt{\varepsilon_{reff}}}$$

(2.18)

Case-II: 90^0 circular sector patch antenna ($\varphi_0 = \pi/2$)

For 90^0 circular sector, $\phi_0 = \pi/2$, and equation (2.10) becomes

$$m = 2q.$$

(2.19)

Thus, it is the possible that $m = 0, 2, 4, 6$, etc.

Following the roots of the derivative of Bessel function, the lowest value, $\chi'_{mn} = 3.05$, occurs when $m = 2$, $n = 1$.

Therefore, following equation (2.17), the lowest order resonant mode (dominant mode) of 90^0 circular sector patch becomes TM_{21} and its frequency

$$f_r = \frac{\chi'_{21}c}{2\pi a_{eff}\sqrt{\varepsilon_{reff}}} = \frac{3.05c}{2\pi a_{eff}\sqrt{\varepsilon_{reff}}}$$

(2.20)

Case-III: 60^0 circular sector patch antenna ($\varphi_0 = \pi/3$)

For 60^0 circular sector, $\phi_0 = \pi/3$, and equation (2.10) becomes

$$m = 3q$$

(2.21)

Thus, it is possible that $m = 0, 3, 6, 9$, etc.

Following the roots of the derivative of Bessel function, the lowest value, $\chi'_{mn} = 3.83$, occurs when $m = 0$, $n = 1$.

Therefore, following equation (2.17), the lowest order resonant mode (dominant mode) of 60^0 circular sector patch becomes TM_{01} and its frequency

$$f_r = \frac{\chi'_{01}c}{2\pi a_{eff}\sqrt{\varepsilon_{reff}}} = \frac{3.83c}{2\pi a_{eff}\sqrt{\varepsilon_{reff}}}$$

(2.22)

It may be noted that for 60^0 circular sector, no circumferential variation occurs when one radial variation exists beneath the patch. This can be proved pictorially also by observing the magnitude of the dominant mode electric field distribution on the surface of the patch (Fig. 2.3). This, in fact, produces a broadside radiation like circular patch with TM_{11} mode, but with lower gain. The gain can be enhanced by introducing a cavity beneath the patch as in [18] or by changing the substrate permittivity.

Suitable utilization of equation (2.3) reveals that, for a circular sector patch, the fields are

$$E_\rho = 0\,;\;\; E_\phi = 0\,;\; H_z = 0\,;$$

$$E_z = B_{mnp}A\cos(m\phi)J_m(k_\rho\rho)\cos(k_z z)$$

$$H_\rho = \frac{1}{\mu\rho}B_{mnp}J_m(k_\rho\rho)(-mA\sin m\phi)\cos(k_z z)$$

$$H_\phi = -\frac{1}{\mu}B_{mnp}A\cos(m\phi)J'_m(k_\rho\rho)\cos(k_z z)$$

(2.23)

Thus, in the dominant TM_{01} mode, the field components for 60^0 circular sector patch, are as follows:

$$E_\rho = 0\,;\;\; E_\phi = 0\,;\; H_{z=0}\,;\; H_\rho = 0$$

$$E_z = B_{010}AJ_0(k_\rho\rho)\cos(k_z z)$$

$$H_\phi = -\frac{1}{\mu}B_{010}AJ'_0(k_\rho\rho)\cos(k_z z)$$

(2.24)

Fig. 2.4 confirms the existence of only two field components beneath the patch for the dominant mode (TM_{01}), for 60^0 circular sector. This further corroborates the fact that TM_{01} is the dominant mode for 60^0 circular sector.

It may be noted that the electric field component does not vary with φ, as can be seen from equation (2.24) and from Fig. 2.3.

Hence, in the dominant mode of CSMA (for 60^0 sector angle), only two field components exist, namely E_z and H_φ. As all microstrip patch structures are fabricated

32

on a thin substrate, the variation along z direction is not considered. Therefore, the variations of E_z and H_φ components of the dominant TM_{01} mode are dependent mainly on $J_0(k_\rho\rho)$ and $J_0'(k_\rho\rho)$, respectively. The variations of $J_0(k_\rho\rho)$ and $J_0'(k_\rho\rho)$, as a function of ρ, ensure that E_z becomes maximum at $\rho = 0$, $\rho = a$ and minimum near about the centre. On the contrary, H_φ becomes maximum near the centre and minimum near the edges ($\rho = 0$ and $\rho = a$).
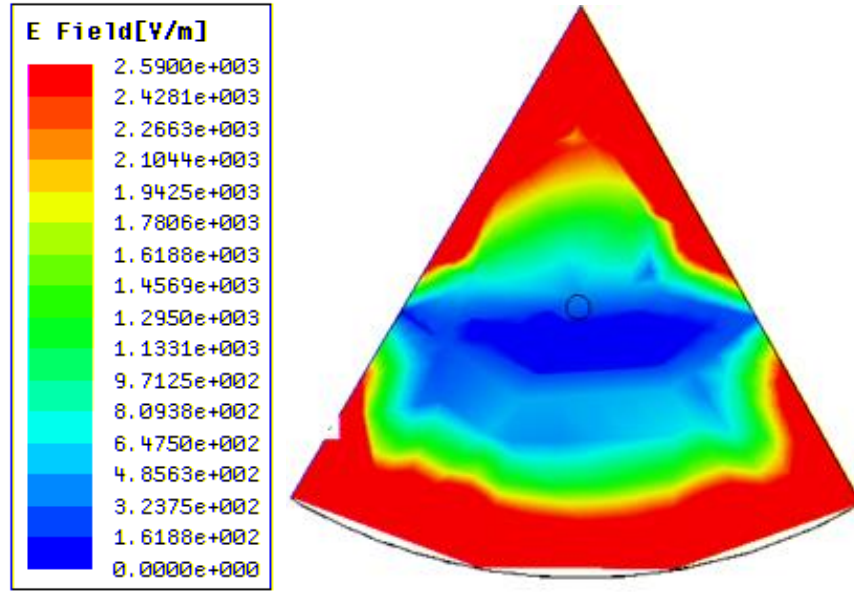
Fig. 2.3 Electric field magnitude over the patch surface of CSMA (for 60^0 sector angle) for the dominant TM_{01} mode (f = 3.76 GHz). Parameters: a = 30 mm, h_1 = 1.575 mm, h_2 = 0, ε_r = 2.33.

(a)

(b)
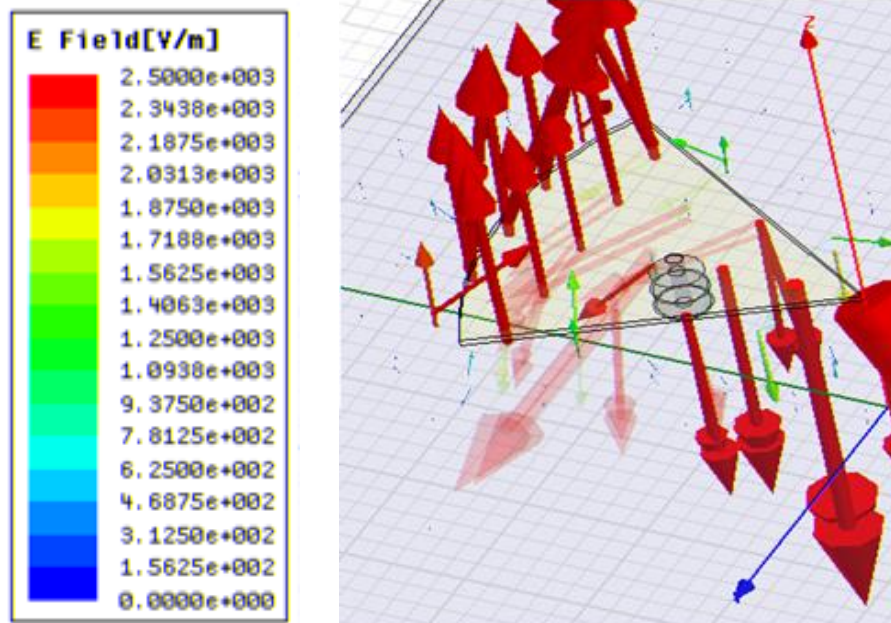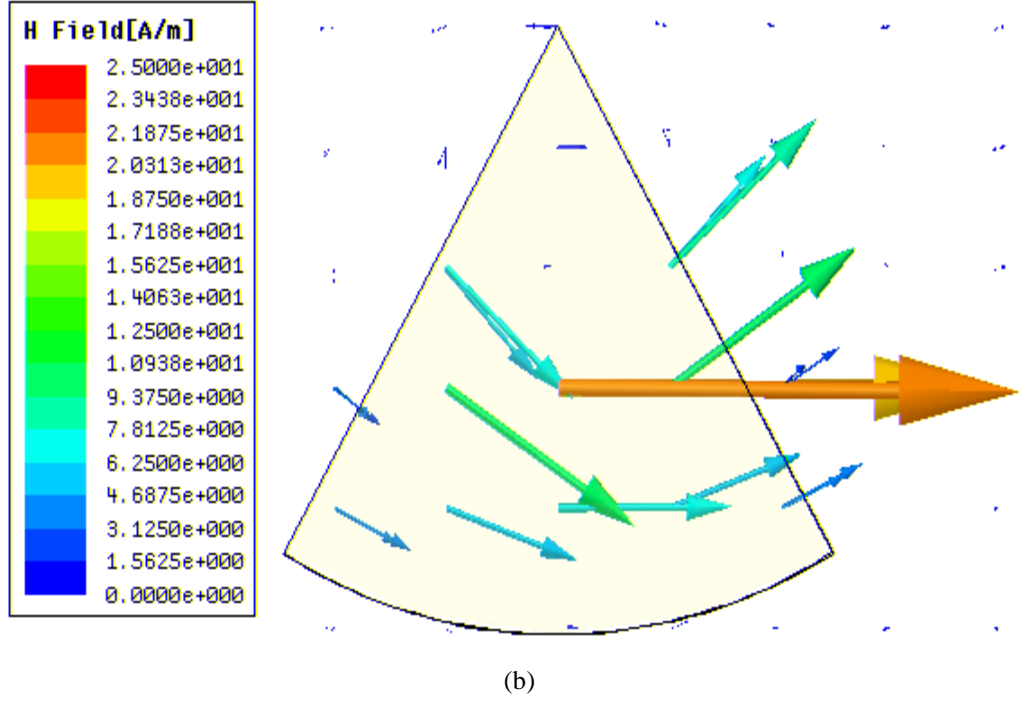
Fig. 2.4 Field components of CSMA (for 60^0 sector angle) for the dominant TM_{01} mode ($f = 3.76$ GHz) (a) z component of electric field, (b) φ component of magnetic field. Parameters: $a = 30$ mm, $h_1 = 1.575$ mm, $h_2 = 0$, $\varepsilon_r = 2.33$.

2.2.2   Calculation of Effective Dimension

The effective dimension of the antenna (a_{eff}) can be calculated according to [19], thus

$$a_{eff} = a\sqrt{(1+q_1)}$$

(2.25)

Where q_1 is the fringing factor, which can be obtained from [19]. On the other hand, the calculation of fringing factor is very important for accurate estimation of the resonant frequency of the antenna. This is crucial, because the effective dimension of the antenna and the effective dielectric constant directly affect the resonant frequency. Thus, based on the following [12], [27], [28], an equivalent circular patch with radius a_c has been consider, resonating at the same zero order frequency as does the sector patch antenna with radial dimension a. This helps to establish a relationship amongst the dimensions of both the geometries in a simplified way. Equating the zero order resonant frequencies [4], [24] of both the patches and it can be represents as

34

$$f_{0,r} = \frac{\chi'_{11} c}{2\pi a_c \sqrt{\varepsilon_r}} = \frac{\chi'_{mn} c}{2\pi a \sqrt{\varepsilon_r}} \qquad (2.26)$$

$$a_c = \frac{\chi'_{11}}{\chi'_{mn}} a = \frac{1.84a}{\chi'_{mn}} \qquad (2.27)$$

$\chi'_{mn} = 1.84$ when $\phi_0 = 180^0$, as suggested in section 2.2.1, Case-I (semicircular patch),

$\chi'_{mn} = 3.05$ when $\phi_0 = 90^0$, as suggested in section 2.2.1, Case-II (90^0 circular sector patch),

$\chi'_{mn} = 3.83$ when $\phi_0 = 60^0$, as suggested in section 2.2.1, Case-III (60^0 circular sector patch).

Thus, the fringing factor q_1 can be calculated from the circular patch [28], equivalent to the CSMA, as done in [13] for a RMA. Therefore, equation (2.26) has been established to correlate with the sector patch with circular patch. It may be noted that (q_1), in case of circular sector patch, is determined from the corresponding fringing factor of the circular patch [28]. This fringing factor (q_1) is utilized in equation (2.25) to obtain the effective dimension (a_{eff}) of circular sector patch.

2.2.3 Calculation of Effective Dielectric Constant

An effective dielectric constant can be calculated, based on static and dynamic capacitances [20]-[21]. When an air gap of height h_2 is introduced between the substrate (thickness h_1, dielectric constant ε_r) and the ground plane as shown in Fig. 2.1, the equivalent dielectric constant of the medium below the patch becomes

$$\varepsilon_{re} = \frac{\varepsilon_r \left(1 + h_2/h_1\right)}{\left(1 + \varepsilon_r \, h_2/h_1\right)} \qquad (2.28)$$

The dynamic dielectric constant ε_{rdyn} is given by

$$\varepsilon_{rdyn} = \frac{C_{dyn}(\varepsilon = \varepsilon_0 \varepsilon_{re})}{C_{dyn}(\varepsilon = \varepsilon_0)} \qquad (2.29)$$

where, C_{dyn} is the total dynamic capacitance [20], which can be expressed as

$$C_{dyn} = C_{0,dyn} + C_{e,dyn} \qquad (2.30)$$

Here, $C_{0,dyn}$ is the dynamic capacitance for the fields stored under the disc i.e. the case with no fringing and $C_{e,dyn}$ is the dynamic fringing capacitance that arises from fringing effect.

Now following [20], $C_{0,dyn}$ can be written as

$$C_{0,dyn} = \frac{\varepsilon_0 \varepsilon_r \pi a_c^2}{\delta h} \left[1 - \frac{J_{m-1}(\chi'_{mn}) J_{m+1}(\chi'_{mn})}{J_m^2(\chi'_{mn})} \right]$$

$$= \gamma_m C_{0,stat}$$

(2.31)

where,

$$\delta = 1 \text{ for } m = 0 \text{ and } \delta = 2 \text{ for } m \neq 0. \ C_{0,stat} = \frac{\varepsilon_0 \varepsilon_r \pi a_c^2}{\delta h}$$

(2.32)

and

$$\gamma_m = \left[1 - \frac{J_{m-1}(\chi'_{mn}) J_{m+1}(\chi'_{mn})}{J_m^2(\chi'_{mn})} \right]$$

(2.33)

Here, γ_m is the factor by which the dynamic capacitance for the fields stored under the disc can be computed and it is strictly depends on mode number m.

Therefore, using the equations (2.21)-(2.24), equation (2.20) may be expressed as

$$\varepsilon_{rdyn} = \frac{\varepsilon_{re} \left[\gamma_m + \dfrac{q_1}{2} \right]}{\left[\gamma_m + \dfrac{q_{01}}{2} \right]} \text{ (for } m \neq 0)$$

(2.34)

$$\varepsilon_{rdyn} = \frac{\varepsilon_{re} [\gamma_m + q_1]}{[\gamma_m + q_{01}]} \text{ (for } m = 0)$$

(2.35)

$$\gamma_m = 1.0 \text{ for } m = 0$$

$$= 0.3525 \text{ for } m = 1$$

$$= 0.2865 \text{ for } m = 2$$

$$= 0.2450 \text{ for } m = 3$$

and, q_{01} is the fringing factor when $\varepsilon_r = 1$.

Thus, the effective dielectric constant ε_{reff} becomes, as in [19],

$$\varepsilon_{reff} = \frac{4\varepsilon_{re}\varepsilon_{rdyn}}{\left(\sqrt{\varepsilon_{re}} + \sqrt{\varepsilon_{rdyn}}\right)^2} \qquad\qquad (2.36)$$

2.3   Results and Discussions

In this section, the data obtained by using the proposed formulation is compared with the data obtained by simulation, measurement and other available theories or formulations in literature. The experiments have carried out with different prototypes and the results obtained are presented here to validate the present formulation.

In Fig. 2.5, the calculated resonant frequencies of S band CSMA for different air gap heights are compared with the simulation results [22] and some own measurement. Fig. 2.5 shows that the average percentage (%) deviations of simulation and theoretical results, with respect to the measurement results, are around 0.40% and 0.65% respectively, for 60^0 sector. The corresponding deviations for 90^0 sector are 0.59% and 0.81%, respectively. There is a good agreement amongst simulation, theoretical and measurement results for both the sector angles.

The tunability of the CSMA, as a function of the air gap height, is also revealed to be the same as what is expected from the patch antennas with conventional geometry. In fact, the introduction of air gap between the substrate and the ground plane effectively increases the air content between the patch and the ground plane. This, in turn, reduces the effective dielectric constant of the substrate which increases the resonant frequency of a antenna structure. The proposed formulation is compared with some previously published formulations [3]-[5] in Table 2.1. The proposed formulation is found to offer minimum average percent error of 0.95%, in comparison to simulation.
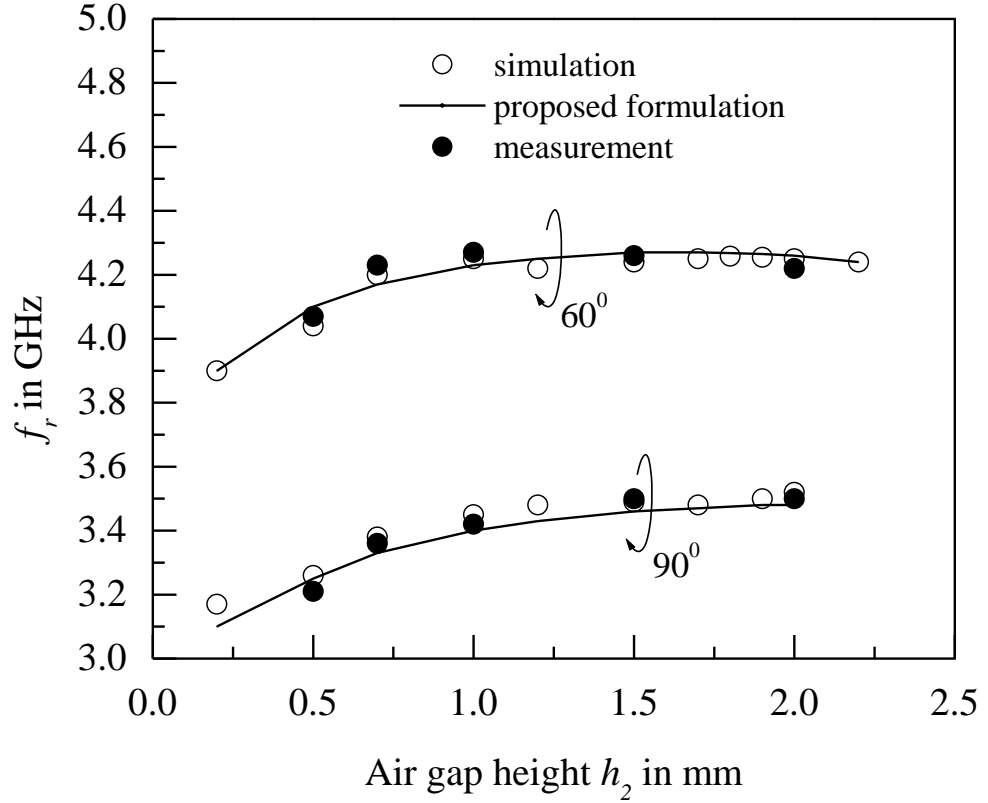
Fig. 2.5 Variation of resonant frequency of CSMA (for two sector angles) as a function of air gap height h_2 with $a = 30$ mm, $h_1 = 1.575$ mm, $\varepsilon_r = 2.33$.

Some measured results are also incorporated in this table for further validation of the proposed formulation. The data presented in Table 2.1 reveals a close agreement between the proposed formulation and the measurement results.

It further reveals that, in comparison with the measurement results, the proposed formulation offers only around 0.75% error in estimating the resonant frequencies of CSMA, while the errors reported in [3]-[4] are around 3.95%. Therefore, from an examination of the data presented in Table 2.1, it follows that the proposed formulation offers minimum % error with respect to both simulation [22] and measurement results, as also the results of earlier theories. The validity of modified formulation in the case of CSMA with substrates of different electrical thicknesses has been verified. In Fig. 2.6 the verification reveals an excellent agreement between simulated, theoretically computed results and measured results for two different sector angles. However, there is a visible deviation in predicted resonant frequency in the figure when $h_1 = 4$ mm, in comparison to full wave simulation.

TABLE 2.1 Comparison of the computed [proposed formulation] resonant frequencies of CSMA for different sector angle with that of earlier theories and simulation; $h_2 = 0$, $h_1 = 1.575$ mm.

φ_0 (degree)	a (mm)	Permittivity (ϵ_r)	f_r (GHz) [22]	f_r (GHz) Calculated [3]-[4]	f_r (GHz) [5]	f_r (GHz) [measured, present]	f_r (GHz) [proposed formulation]
60	30	2.55	3.59	3.95 (10.02%)	3.67 (2.2%)	-	3.57 (0.55%)
60	30	2.33	3.70	4.17 (12.70%)	3.83 (3.5%)	3.70	3.72 (0.54%)
90	30	2.55	2.90	2.90 (0%)	2.78 (4.1%)	-	2.92 (0.68%)
90	30	2.33	3.08	3.03 (1.62%)	2.90 (5.8%)	3.06	3.05 (0.31%)
90	31.6	2.33	2.87	2.88 (0.34%)	2.76 (3.8%)	2.89	2.9 (1.04%)
180	30	2.33	1.88	1.82 (3.19%)	-	1.88	1.86 (1.06%)
180	20	2.33	2.82	2.81 (0.35%)	-	2.74	2.75 (2.48%)
% relative error with respect to simulation [22]			-	4.03%	3.8%	-	0.95%

In general, when the thickness of the substrate exceeds about 2% of the free space wavelength, the cavity model starts giving inaccurate results, because of the breakdown of the basic assumptions of the cavity model, as indicated clearly in [25].

Moreover, a simple cavity model does not account for the fringing effect along the periphery of the patch. Therefore, in the proposed formulation, the fringing fields along the periphery of the patch have taken care by appropriately modeling the cavity boundary.
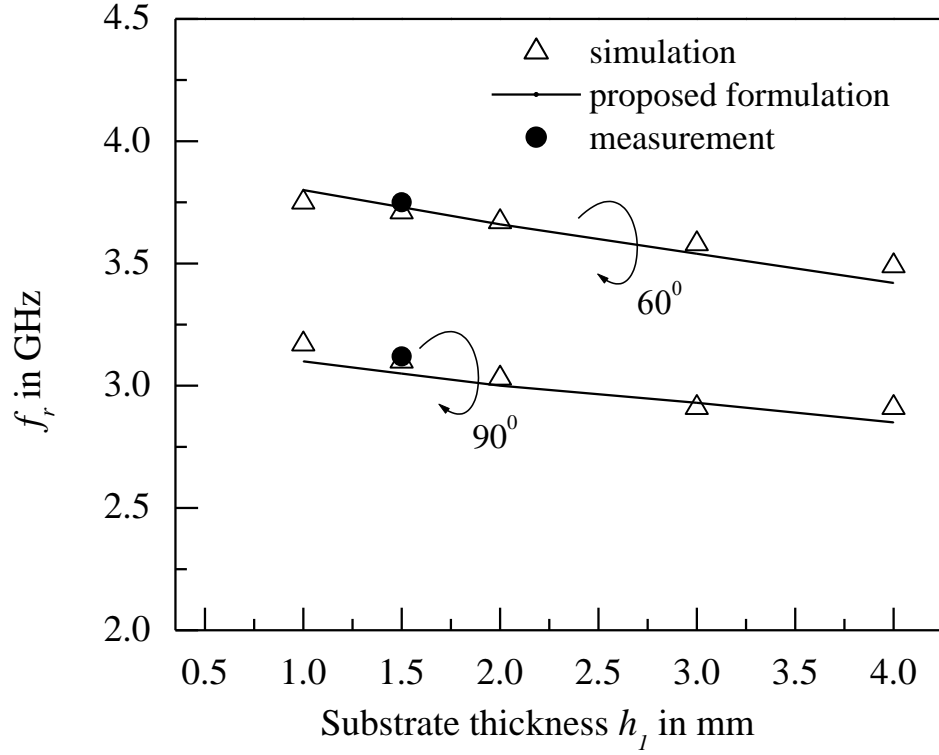
Fig. 2.6 Variation of resonant frequency of CSMA (for two sector angles) as a function of substrate thickness h_1 with $a = 30$ mm, $h_2 = 0$, $\varepsilon_r = 2.33$.
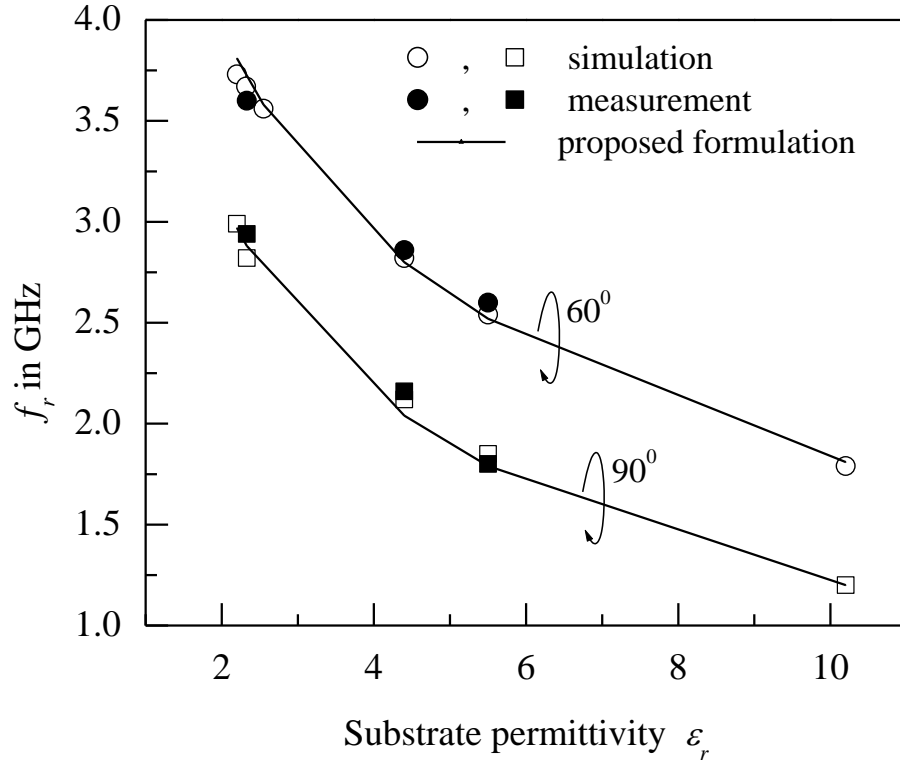
Fig. 2.7 Variation of resonant frequency of CSMA (for two sector angles) as a function of dielectric constant of the substrate with $a = 30$ mm, $h_1 = 1.58$ mm, $h_2 = 0$.

40

However, when the thickness becomes too large, i.e., when it exceeds 4.0% of free space wavelength; the results show around 1.7-2.0% deviation of resonant frequency in comparison to that of full wave simulation. However, this much of deviation in the prediction of resonant frequency is acceptable for a microstrip patch etched over a thick substrate. Unfortunately, reports dealing with resonant frequencies of CSMA over thick substrates are rather scarce. The resonant frequencies of CSMA with widely varying substrate permittivity (ε_r varying from 2.2 to 10.2) are shown in Fig. 2.7.

The values computed from the proposed formulation are compared with the results obtained from [22] and from measurement. Excellent agreement between the present theory and simulation [22] and measured results are revealed. Superiority of the proposed formulation in addressing the resonant frequency of CSMA with different radial dimensions for two different sector angles has been examined through Fig. 2.8.
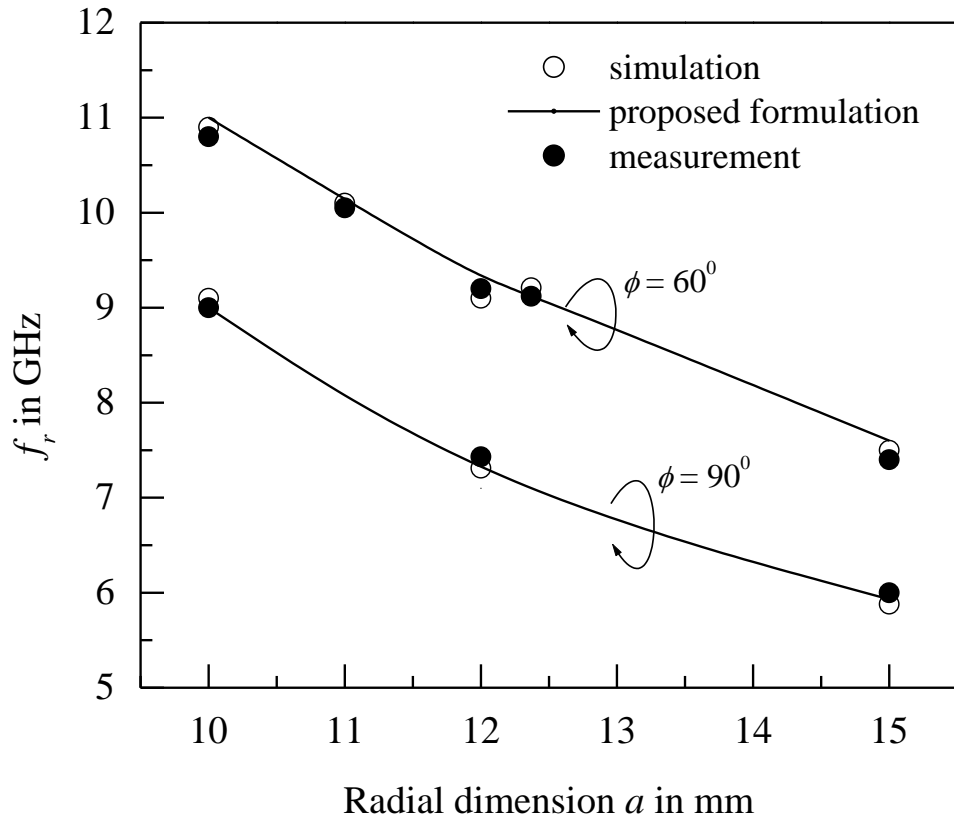
Fig. 2.8 Variation of resonant frequency of CSMA (for two sector angles $\phi = 60^0$ and 90^0) as a function of radial dimension a of the antenna with $h_1 = 0.787$ mm, $h_2 = 0$, $\varepsilon_r = 2.2$.

41

Some of the own measurement results are also incorporated in the same plot in support of the proposed formulation and to unravel the close agreement between the theoretical, simulation and measurement results. For further corroboration of the proposed formulation, some simulated and results are presented in Table 2.2 & Table 2.3 for $\varphi = 60^0$, 30^0 and 45^0.

TABLE 2.2 Comparison of the simulated, and computed [proposed formulation] resonant frequencies of CSMA for 60^0 sector angle with air gap; $\varepsilon_r = 2.2$, h_2 = variable.

Sector patch radius a (mm)	Air gap h_2 (mm)	Substrate thickness h_1 (mm)	f_r (GHz) [22]	f_r (GHz) [proposed formulation]
34.57	0	0.787	3.42	3.43
34.57	1.0	0.787	4.10	4.11
34.57	1.8	0.787	4.09	4.09
25.22	0	0.787	4.63	4.66
25.22	0.5	0.787	5.41	5.35
25.22	1.0	0.787	5.44	5.46
25.22	1.8	0.787	5.39	5.39
15.36	0	0.787	7.49	7.46
15.36	0.5	0.787	8.36	8.37
15.36	1.0	0.787	8.39	8.39
15.36	1.8	0.787	8.15	8.09
12.37	0	0.787	9.10	9.14
12.37	1.0	0.787	10.15	10.19
12.37	1.8	0.787	9.40	9.40
% relative error with respect to simulation [22]			-	0.40% (w.r.t sim)

The ability of the proposed formulation in addressing and identifying the higher order modes for different sector angles, with and without air gap, is also investigated and the results are presented in Table 2.4. The investigation has been performed on CSMAs having different dielectric constants. Comparison of the proposed formulation results with those of the simulation in each case reveals excellent conformity between the two.

TABLE 2.3 Comparison of the measured and computed [proposed formulation] dominant mode resonant frequencies of CSMA for 30^0 and 45^0 sector angles with air gap.

Sector angle (φ_0) degree	a (mm)	Substrate thickness h_1 (mm)	Air gap h_2 in (mm)	ε_r	f_r GHz (TM$_{01}$) [measured present]	f_r GHz (TM$_{01}$) [proposed formulation]
30^0	10	1.575	0	2.33	9.95	9.90
		1.575	1	2.33	10.43	10.41
		0.787	0	2.2	10.72	10.90
		0.787	1	2.2	12.00	11.92
	15	1.575	0	2.33	6.90	6.92
		1.575	1	2.33	7.61	7.56
		0.787	0	2.2	7.60	7.55
		0.787	1	2.2	8.48	8.50
45^0	20	1.575	0	2.33	5.40	5.35
		1.575	1	2.33	5.90	5.95
		0.787	0	2.2	5.72	5.76
		0.787	1	2.2	6.71	6.65
	25	1.575	0	2.33	4.36	4.36
		1.575	1	2.33	5.00	4.92
		0.787	0	2.2	4.65	4.66
		0.787	1	2.2	5.49	5.47
% relative error with respect to measurement					-	0.67%

All the simulation results of the investigation have been obtained by keeping the feed location at the matched position for the dominant mode. As such, the S_{11} minima corresponding to all the higher modes, have had no sufficient dip, as a result of which, it might have lost the order of accuracy in indicating simulated resonant frequency That explains why, in a few cases presented in Table 2.4, the simulation results show a slight deviation with respect to the values computed, using the proposed formulation.

TABLE 2.4 Comparison of the simulated and computed [proposed formulation] resonant frequencies of higher order modes for CSMA for different sector angles and different substrate permittivity.

φ_0 (degree)	h_1 (mm)	a (mm)	ε_r	h_2 (mm)	Modes (TM_{mn})	Simulated f_r (GHz) [22]	Computed f_r (GHz) [proposed formulation]
60	1.58	30	2.33	0	TM_{01}	3.76	3.73
					TM_{31}	4.14	4.2
					TM_{02}	7.04	6.80
					TM_{61}	7.23	7.25
					TM_{62}	11.00	10.62
				1	TM_{01}	4.23	4.23
					TM_{31}	4.63	4.69
					TM_{61}	7.80	7.70
					TM_{03}	9.80	9.60
60	1.58	20	4.4	0	TM_{01}	4.05	4.03
					TM_{31}	4.71	4.62
					TM_{02}	7.3	6.98
					TM_{61}	8.05	7.97
90	1.58	20	4.4	1	TM_{21}	4.65	4.62
					TM_{01}	5.61	5.49
					TM_{41}	7.52	7.48
45	1.58	30	2.33	0	TM_{01}	3.60	3.68
					TM_{41}	5.10	4.97
					TM_{02}	6.15	6.40

By solving the field equations and observing the roots of the derivative of the Bessel function (χ'_{mn}) in order, the higher order modes are theoretically evaluated. For visualization-based understanding of the dominant and higher order modal fields, the magnitudes of electric fields over the patch surface, for a few higher modes, have been presented in Fig. 2.9 for a few higher order modes listed in Table 2.4.

(a)

(b)

(c)
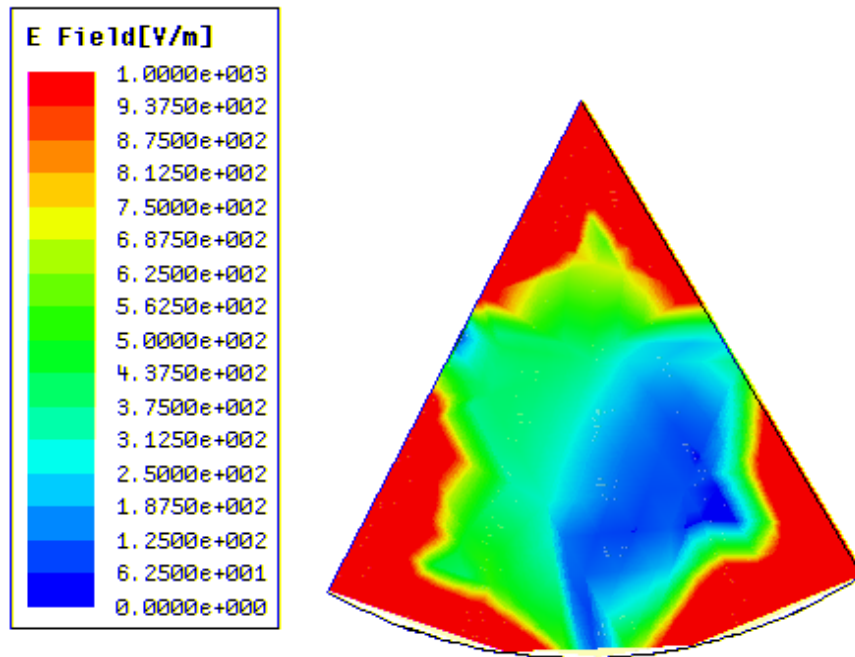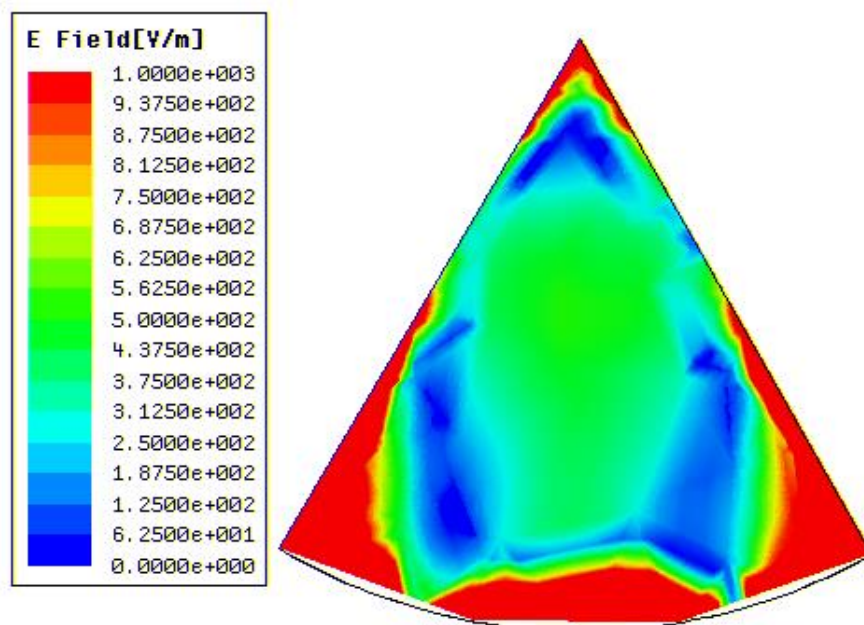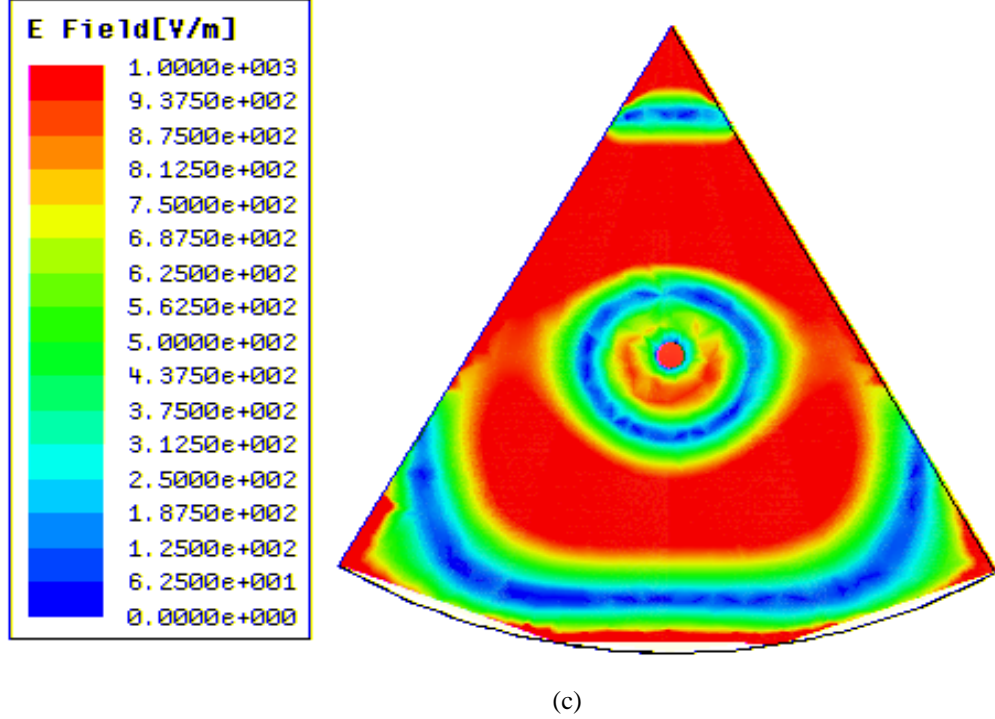
Fig. 2.9 Electric Field magnitude over the patch surface of CSMA (with 60^0 sector angle) for higher order modes (a) TM_{31} mode (f = 4.14 GHz), (b) TM_{61} mode (f = 7.23 GHz), (c) TM_{62} mode (f = 11.0 GHz), Parameters: a = 30 mm, h_1 = 1.575 mm, h_2 = 0, ε_r = 2.33.

Following [26], the higher order modes of CSMA, for $\varphi = 60^0$, have been identified. According to the discussions presented in section 2.2.1, the number of variations in electric field along the radial direction (along ρ direction) is n and that along the circumferential direction (along φ direction) is q ($m = 3q$; for $\varphi = 60^0$). Therefore, by inspecting the number of electric field variations along ρ and φ variations the mode TM_{mn} can be identified.

In Fig. 2.9 (a), one radial variation (n =1) and one circumferential variation ($q = 1$; $m = 3$) are evident, as expected for TM_{31} mode. Similarly, two circumferential variations ($q = 2$; $m = 6$) and one radial variation ($n = 1$) corresponding to TM_{61} mode, and two circumferential variations ($q = 2$; $m = 6$) and two radial variations ($n = 2$) corresponding to TM_{62} mode are manifested in Fig. 2.9 (b) and 2.9 (c), respectively. Compared to Fig. 2.9, Fig. 2.3 shows one variation ($n = 1$) in electric field along the radial direction, corresponding to TM_{01} mode, but no variation along the circumference ($q = 0$; $m = 0$). This observation is remarkably in tune with what has been discussed in the theoretical part (section 2.2.1, Case-III). Besides, it further

46

corroborates the superiority of the proposed formulation in predicting the dominant and higher order modes for sector patch antennas, with and without air gap.

TABLE 2.5 Comparison of the simulated measured and computed [proposed formulation] resonant frequencies of dominant and higher order modes of CSMA for different sector angles

Sector angle φ_0 (degree)	a (mm)	h_1 (mm)	ε_r	Mode	Simulated f_r (MHz) [10] **, [present]	Measured f_r (MHz) [present], [23] *	Computed f_r (MHz) [proposed formulation]
**240^0	20	1.6	2.33	1st	2290	2315	2300
				2nd	3700	3690	3680
				3rd	5000	4945	4900
270^0	40	1.6	4.4	1st	810	808	805
				2nd	1285	1280	1275
				3rd	1750	1746	1743
300^0	40	1.6	4.4	1st	760	750	753
				2nd	1200	1210	1199
				3rd	1615	1615	1611
330^0	40	1.6	4.4	1st	726	721	719
				2nd	1115	1122	1118
				3rd	1505	1501	1498
* 65^0	45	1.6	4.4	1st	-	1944	1944
% of relative error with respect to measurement						-	0.32%

The reliability of the proposed formulation is thus established for designing the CSMA, with and without air gaps. For further confirmation, the predicted results, based on the proposed formulation, have been compared with the simulated and our own measured results.

TABLE 2.6 Comparison of the measured and computed [proposed formulation] resonant frequencies of dominant modes of CSMA for different sector angles and substrate thicknesses $h_1 \sim 3$ mm.

Sector angle φ_0 (degree)	a (mm)	ε_r	Measured f_r (MHz) [11], [24] **	Computed f_r in MHz [proposed formulation]
340^0	70	1	778	780
** 120^0	21.9	2.55	3181	3183

Measured data from some earlier reports has also been included in the comparative study to verify the validity of the proposed formulation (Tables 2.5 and Tables 2.6).

The comparative study reveals an excellent agreement amongst the measured, simulated and theoretically computed results. The theoretical and measurement results for dominant mode resonant frequencies of CSMA (printed on widely available polytetrafluorethylene (PTFE) substrate; $\varepsilon_r = 2.33$, $h_1 = 1.59$ mm) for wide variety of sector angles are presented in Fig. 2.10.
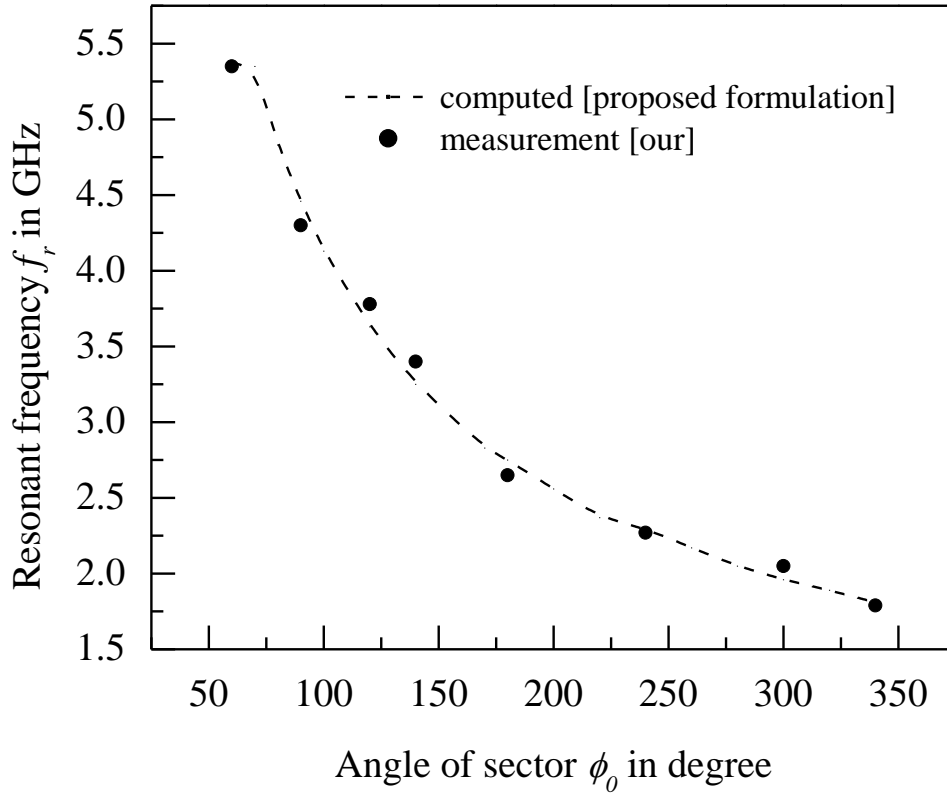
Fig. 2.10 Comparison of computed and measured dominant mode resonant frequency of CSMA with different sector angles (φ_0). Parameters: $a = 20$ mm, $h_1 = 1.58$ mm, $h_2 = 0$, $\varepsilon_r = 2.33$.

It may be noted that, the present approach may be extended to compute the dominant mode frequency of circular patch.

In fact, the CSMA with $\varphi = 2\pi$ degree degenerates to conventional circular patch where, the radial component of magnetic fields (H_ρ) at $\varphi = 0^0$ and $\varphi = 2\pi$ are continuous with the boundary condition of continuity of tangential component of magnetic fields. Following the same, the lowest order mode of CSMA with $\varphi = 2\pi$ degree (circular patch) becomes TM_{11}. The present investigation ought to be very

much useful to the scientific community for quick and accurate calculations of lowest order resonant frequency of CSMA of any sector angle.

2.4.   Conclusion

CSMA with and without air gap has been thoroughly studied. An improved CAD formulation is proposed for accurate prediction of its resonant frequency. The proposed formulation is validated thoroughly for CSMAs with widely varying antenna parameters by several measurement and simulation data. The proposed formulation can efficiently compute the dominant mode along with the higher order modes of CSMA with any sector angle. The proposed CAD formulation appears to be much improved, versatile and simple compared to the earlier reported theories. However, the effect of feed location on the modes and its frequency is a critical issue which will be addressed thoroughly in a separate investigation.

References

[1]   W. Richards, J-D. Ou, and S. Long, "A theoretical and experimental investigation of annular, annular sector, and circular sector microstrip antennas," *IEEE Transactions on Antennas and Propagation*, vol. 32, no. 8, pp. 864-867, 1984.

[2]   A. K. Bhattacharya, and R. Garg, "Analysis of Annular Sector and Circular Sector Microstrip Patch Antennas," *Electromagnetics*, vol. 6, no 3, pp. 229-242, 1986.

[3]   V. K. Tiwari, A. Kimothi, D. Bhatnagar, J. S Saini, V. K Saxsena, and P. Kumar, "Theoretical analysis on circular sector microstrip antennas," *Indian Journal of Radio Space Physics*, vol. 35, pp. 133-138, 2006.

[4]   V. K. Tiwari, A. Kimothi, D. Bhatnagar, J. S. Saini, and V. K Saxsena, "Theoretical and experimental investigations of circular sector microstrip antennas," Indian *Journal of Radio Space Physics*, vol. 35, pp. 206-211, 2006.

[5]   S. Bhattacharyya, D. Ghosh, G. K. Singh, R. Sing, A. Raj, S. Chattopadhyay, A. Ghosh, and S. Chakravorty, "Accurate CAD formulation for resonant frequency of circular sectorial microstrip antenna," *International Conference on Microwave and Photonics (ICMAP)*, pp. 1-3, Dhanbad, India, 2013.

[6]   A. Dalli, L. Zenkouar, and S. Bri, "Theoretical analysis and optimization of circular sector microstrip antenna," *Revue Méditerranéenne des Télécommunications,* vol. 2, no. 2, 2012.

[7]   A. Dalli, L. Zenkouar, and S. Bri, "Conception of Circular Sector Microstrip Antenna and Array," *International Journal of Microwaves Applications*, vol.1, no. 1, pp. 32-37, 2012.

[8]   R. Agarwal and D. C. Dhubkarya, "Design and Simulation of circular sector microstrip antenna," *International Journal of Knowledge Engineering and Technology*, vol. 1, no. 1, 2012.

[9]   A. A. Deshmukh, A. R. Jain, A. A. Joshi, T. A. Tirodkar, and K. P. Ray, "Broadband Proximity Fed Modified Circular Microstrip Antenna," *Third International Conference on Advances in Computing and Communications*, Cochin, India, pp. 404-407, 2013.

[10]   A. A. Deshmukh, V. Pandita, R. Colaco, and R. Doshi, "Dual band dual polarized modified circular microstrip antenna," *International Conference on Circuits, Systems, Communication and Information Technology Applications (CSCITA)*, Mumbai, India, pp. 347-352, 2014.

[11]   A. A. Deshmukh and N. V. Phatak, "Broadband Sectoral Microstrip Antennas," in *IEEE Antennas and Wireless Propagation Letters*, vol. 14, pp. 727-730, 2015.

[12]   S. Chattopadhyay, M. Biswas, J. Y. Siddiqui, and D. Guha, "Rectangular Microstrips with Variable Air-Gap Varying Aspect Ratio: Improved Formulation and Experiments," *Microwave Optical Tech. Letter*, vol.51, no. 1, pp. 169-173, 2009.

[13]   S. Chattopadhyay, M. Biswas, J. Y. Siddiqui, and D. Guha, "Input Impedance of Probe-Fed Rectangular Microstrip Antennas with Variable Air-Gap and Varying Aspect Ratio," IEE *Microwaves, Antennas Propagation*, vol. 3, no. 8 , pp. 1151-1156, 2009.

[14]   Y. Lo, D. Solomon, and W. Richards, "Theory and experiment on microstrip antennas," *IEEE Transactions on Antennas and Propagation*, vol. 27, no. 2, pp. 137-145, 1979.

[15]   D. Ghosh, S. K. Ghosh, S. Chattopadhyay, and S. Banerjee, "Physical and Quantitative Analysis of Compact Rectangular Microstrip Antenna with Shorted Non-Radiating Edges for Reduced Cross-Polarized Radiation Using Modified Cavity Model," *IEEE Antennas and Propagation Magazine*, vol. 56, no. 4, pp. 61-72, 2016.

[16]   S. Chakraborty and S. Chattopadhyay, "Substrate Fields Modulation with Defected Ground Structure: A Key to Realize High Gain, Wideband Microstrip Antenna with Improved Polarization Purity in Principal and Diagonal Planes," *Int. Journal of RF, Microwave and Computer Aided Engineering*, vol. 26, no. 2, p. 174-181 , 2015.

[17]   C. A. Balanis, "Antenna Theory and Design," 3rd edition, John Wiley & Sons, Inc., New York, 2004.

[18]   K. Malakar, J. Nandi, S. Mitra, P. Gorai, S. Chattopadhyay, and S. Banerjee, "Rectangular Microstrip Antenna with Air Cavity for High Gain and

Improved Front to Back Ratio," *Journal of Electromagnetic Analysis and Applications*, vol. 3 no. 9, pp. 368-372, 2011.

[19]   D. Guha, "Resonant frequency of circular microstrip antennas with and without air gaps," in *IEEE Transactions on Antennas and Propagation*, vol. 49, no. 1, pp. 55-59, 2001.

[20]   I. Wolff and N. Knoppik, "Rectangular and Circular Microstrip Disk Capacitors and Resonators," *IEEE Transactions on Microwave Theory and Techniques*, vol. 22, no. 10, pp. 857-864, 1974.

[21]   F. Abboud, J. P. Damiano, and A. Papiernik, "A new model for calculating the input impedance of coax-fed circular microstrip antennas with and without air gaps," *IEEE Transactions on Antennas and Propagation*, vol. 38, no. 11, pp. 1882-1885, 1990.

[22]   HFSS: High Frequency Structure Simulator, Ansoft Corp, 2014, USA.

[23]   W. H. Hsu and K. L. Wong, "Circularly-polarised disk-sector microstrip antenna," *Electron Letter,* vol. 34, no, 23, pp. 2188-2190, 1998.

[24]   Eswarappa, K. C. Gupta, and R. Raghuram, "Mixed Boundary Semicircular and 120^{0} – Sectoral Microstrip Antennas," *Antennas and Propagation Symposium Digest*, San Jose, CA, USA, 1989.

[25]   K. F. Lee and K. M. Luk, "Microstrip Patch Antennas, Imperial College Press," London, 2011.

[26]   S. Biswas, D. Guha, and C. Kumar, "Control of Higher Harmonics and Their Radiations in Microstrip Antennas Using Compact Defected Ground Structures," *IEEE Transactions on Antennas and Propagation*, vol. 61, no. 6, pp. 3349-3353, 2013.

[27]   R. Garg, P. Bhartia, I. Bahl, and A. Ittipiboon, Microstrip Antenna Design Handbook, Artech House, Norwood, 2001.

[28]   D. Guha and J. Y. Siddiqui, "Resonant frequency of circular microstrip antenna covered with dielectric superstrate," *IEEE Transactions on Antennas and Propagation*, vol. 51, no. 7, pp. 1649-1652, 2003.

CHAPTER

3

Insightful Exploration of Feed Dependent Modes of Circular Sector Microstrip Antenna

3.1.   Introduction

In the recent years, there is a growing inclination on exploring and enhancing the radiation and input characteristics of circular sector microstrip antenna (CSMA) for modern applications due to its conformality over curved surfaces, and better compactness in comparison with other regular shaped patch geometries such as rectangular, circular as is discussed in Chapter 1. This circular sector microstrip antenna with and without variable air-gap height, has been documented in Chapter 2. The accurate determination of lowest order dominant and its frequency along with determination of higher mode has been methodically discussed in previous chapter. Apart from that, the accurate estimation of the feed-probe position for the excitation of desired modes in a CSMA is another basic design requirement.

In the recent years, significant works [1]-[4] has been reported on CSMA for yielding circular polarization well as multibanding. Notably, all these reported works, the measurement has been instigated on based on appropriate simulation to optimize the proposed CSMA structure. The possibility of using fractional modes in CSMA has been demonstrated in few literatures [5]-[6], to excite multiple higher order modes simultaneously. This has been done by optimizing sector angle of the CSMA, which yields dual resonances or broadband characteristics without focusing the feed location dependency on the excited mode. The feed locations were elected along the middle line of the sector (bi sector line) to ease the feeding of a CSMA structure and hence could not excite the lowest order mode. Also, to achieve

desirable characteristic of CSMA, feed locations have been elected intuitively. Notably, in [7]-[11] the CSMA has been investigated to determine its resonant frequency. The effects of feed point for excitation of different modes have been rigorously analyzed for Circular microstrip antenna (CMA) [12]. It is observed that the excitation of dominant mode TM_{11} is always strong when it is feeding centrally or near to the centre of the patch. When the patch was fed near the edges the higher order TM_{21} mode has a tendency to be excited. Nevertheless, the peak excitation of that TM_{21} mode was always below 24 dB than the TM_{11} mode. In case of rectangular microstrip antenna two orthogonal resonance (TM_{10} and TM_{01}) modes can be simultaneously excited by feeding it from two sides [13]. Similarly, the feed-probe position of a CSMA also has a substantial effect on the excitation of a desired mode. Consequently, the serious attention and thorough methodical investigations are required to correctly understand the modal behavior of the CSMAs as a function of feed position. In this context no such open-literatures are available till date. Therefore, the simple, quick hand, but accurate technique must have been explored to excite its proper mode and to understand the influence of feed positions on modal characteristics of a CSMA for a number of sector angles (ϕ_0). From the view of less space requirement, CSMAs with sector angle (ϕ_0) less than 180^0 have been considered here in Fig. 3.1.

Unlike earlier investigations, in which researchers used the trial-and-error approach to design a CSMA for particular applications based on simulations, here, the investigations on modal properties as a function of feed location has been carried out methodically and an quick hand empirical but accurate technique has been proposed to estimate the feed location to excite a particular mode in CSMAs.

Unlike CMA, the impedance variations of a CSMA when tuning the feed position do not happen only along the radial distance but also along the azimuth angle. Till date, no accurate impedance formulation for a CSMA is available. Hence, the E/H ratio has been exploited to find a proper feed location for exciting a particular mode.

The determination of modes of a CSMA based on feed location investigated in this work is not reported elsewhere.

The effects of feed location on the polarization of antenna have been for the first time documented for a CSMA. It would be helpful for future designs for using a CSMA in polarization reuse or polarization diversity applications.

In a CSMA, a little change of the sector angles several modes can be generated. By using single feed with no perturbation in the patch structure, higher order modes can be generated in a CSMA as is documented in this chapter.

Fed along the edge
($\phi_f = \phi = 0°$ line)

Fed along the central symmetrical position
($\phi_f = \phi = \phi_0/2$line)

Feeding points
either 1 or 2 ($\phi_f = 0°$ or $\phi_0/2$)

Fig. 3.1 Schematic representation of a CSMA for two different feed-probe positions. (The substrate and ground plane are not shown in the figure).

In the present chapter, first at section 3.2, the theoretical insight of the study has been presented. Here, to excite a particular mode the relation between $|E/H|$ and the CSMA parameters has been established. In section 3.3.1 and section 3.3.2 the detail discussion of CSMA with numerous numbers of sector angles with different characteristics as a function of feed location has been categorized. Next, in section 3.4, the feed location has been approximated to excite a particular mode in CSMA, based on the theoretical insight presented in section 3.2. A specific range of $|E/H|$ has been predicted in this section for which a particular mode can be excited. In section 3.5 the proposed technique has been validated through experimental measurements. At last, the overall conclusion as findings documented in the section 3.6.

3.2   Theoretical Insight

A CSMA resonates at its lowest order primary dominant mode which depends critically on both the radial dimension of the patch and sector angle. The field distributions within the substrate can be written as [11]

$$
\left.
\begin{aligned}
&\overline{E}_z = B_{mnp} A \cos(m\phi) J_m(k_\rho \rho) \cos(k_z z) \\[2em]
&\overline{H}_\rho = \frac{-j}{\omega\mu\rho} B_{mnp} J_m(k_\rho \rho)(mA \sin m\phi)\cos(k_z z) = \frac{1}{\omega\mu\rho} B_{mnp} J_m(k_\rho \rho)(mA \sin m\phi)\cos(k_z z) e^{-j\frac{\pi}{2}} \\[2em]
&\overline{H}_\phi = -j\frac{k_\rho}{\omega\mu} B_{mnp} A \cos(m\phi) J'_m(k_\rho \rho)\cos(k_z z) = \frac{k_\rho}{\omega\mu} B_{mnp} A \cos(m\phi) J'_m(k_\rho \rho)\cos(k_z z) e^{-j\frac{\pi}{2}}
\end{aligned}
\right\}
\quad (3.1)
$$

Where, $k_\rho = \chi'_{mn}/a$; a = radial dimension of a CSMA, and χ'_{mn} is constant. Here, ρ is defined as radial dimension from the apex of the patch to the edge of patch such that $0 < \rho \leq a$, where a is the maximum radial dimension of the patch. k_ρ is the propagation constant along the radial dimension (ρ) and k_z is the propagation constant along the z direction. J_m and J'_m are the Bessel function and derivative of Bessel function of order m in relation to ($k_\rho \rho$), respectively. μ refers to the permeability of the medium, and ω is the angular frequency. A and B_{mnp} are constants, m is ((number of circumferential variation $\times \pi$)/φ_0) and n is the root of derivative of Bessel function of order m in relation to ($k_\rho \rho$). In equation (3.1), $\overline{H}_\rho$ and $\overline{H}_\phi$ are radial and circumferential components of magnetic field $\overline{H}$. Therefore, at a particular point, the magnitude of magnetic field is

$$
\left|\overline{H}\right| = \frac{1}{\omega\mu} B_{mnp} A \left[\frac{m^2}{\rho^2} J_m^2(k_\rho \rho)\sin^2(m\phi) + k_\rho^2 J_m'^2(k_\rho \rho)\cos^2(m\phi)\right]^{1/2}
\tag{3.2}
$$

and the phase is $-\pi/2$.

Hence, $\dfrac{\overline{E}_z}{\omega\mu\overline{H}} = \dfrac{\cos(m\phi)J_m(k_\rho\rho)}{\left[\dfrac{m^2}{\rho^2}J_m^2(k_\rho\rho)\sin^2(m\phi)+k_\rho^2 J_m'^2(k_\rho\rho)\cos^2(m\phi)\right]^{1/2}}e^{j\frac{\pi}{2}}$ (3.3)

Therefore, the magnitude of equation (3.3) can be written as,

$\left|\dfrac{\overline{E}_z}{\omega\mu\overline{H}}\right| = \dfrac{\left|\cos(m\phi)J_m(k_\rho\rho)\right|}{\left[\dfrac{m^2}{\rho^2}J_m^2(k_\rho\rho)\sin^2(m\phi)+k_\rho^2 J_m'^2(k_\rho\rho)\cos^2(m\phi)\right]^{1/2}}$ (3.4)

and the phase of equation (3.4) is π/2, as is expected from a parallel resonating circuit. This is customary as the basic microstrip antennas are modeled with parallel resonating circuits. Notably, this phase shift of π/2 in between the electric and magnetic field is constant, and it is not the function of the CSMA parameters. In [13], the input impedance of a circular patch has been thoroughly analyzed by modeling the feed probe (using the current ribbon model), and it has exhibited similar and constant phase difference of *π/2* between the input voltage *V* and current *I*, which is in agreement with our concept. Therefore, to avoid further complexity, the phase shift between *E* and *H* is not considered in the further analysis.

This electric to magnetic field ratio (*E/H* ratio) beneath the patch is noteworthy to understand the impedance behavior, as well as to excite a particular mode in a CSMA with specific sector angle. The input impedance of the CSMA at a particular feeding position must depend on this *E/H* ratio at that point. In a more compact form, equation (3.4) is denoted as

$\left|\overline{E}_z\big/\omega\mu\overline{H}\right|^{-2} = \left(\dfrac{m^2}{\rho^2}\right)\tan^2(m\phi)+k_\rho^2\dfrac{J_m'^2(k_\rho\rho)}{J_m^2(k_\rho\rho)}$ (3.5)

The resonant frequency of a CSMA can be obtained from [11] using modified cavity model (with boundary of PEC walls at top and bottom and PMC walls along sector edges where $H_\rho=0$ at $\phi = 0°$ and $\phi = \phi_0$ and $H_\phi = 0$ at $\rho = a$ for $\phi = 0°$ to ϕ_0) as

$f_r = \dfrac{\chi'_{mn}c}{2\pi a_{eff}\sqrt{\varepsilon_{reff}}}$ (3.6)

Where, $\varkappa'_{mn}$ is the nth root of derivative of Bessel function of order m in relation to $(k_\rho\rho)$, a_{eff} is the effective dimension of the antenna with fringing, and ε_{reff} is the effective dielectric constant which includes the static and dynamic capacitance of patch. These capacitances are the function of physical dimensions i.e radial dimension a, sector angle ϕ_0, and the substrate thickness h. Therefore, the above parameters will affect the mode and it's frequency.

The effective power ($P_{excited}$) delivered by the feed-probe to the patch corresponding to a particular mode is

$$P_{excited} = \int \bar{E} \bullet \bar{J} dv \tag{3.7}$$

Where $\bar{J}$ is the excitation of feed-probe current density and $\bar{E}$ is the induced electric field. Therefore, to excite the specific mode in the CSMA, the coaxial feeding probe (current source) must be placed at the position that has sufficient electric field.

3.3   Modal Characteristics of a CSMA

The CSMAs with different range of sector angles with different characteristics as a function of feed location has been investigated thoroughly. Based on through and methodical investigation with different sector angles have been categorized and discussed in the following section.

3.3.1   CSMA with Sector Angle $0^0 < \phi_0 \leq 60^0$

The dominant mode of a CSMA with sector angle $0^\circ < \phi_0 \leq 60^\circ$ is TM_{01} ($m = 0$ and $n = 1$) [11]. When $m = 0$, the E/H ratio is independent of azimuthal angle ϕ and it solely depends on the Bessel function of order m and argument $(k_\rho\rho)$, as seen in Eq. (3.5). Therefore, it varies along the radial direction and there is no variation along the circumferential direction ϕ. The computed (based on Eq.3.5) variation of $(E/\omega\mu H)$ ratio as a function of radial dimension is shown in Fig. 3.2 (a) at $\phi = 0^\circ$ and $\phi_0/2$ for 45° CSMA at dominant TM_{01} mode. It is found that the variation is identical for both the cases with feeding along the $\phi_f = \phi = 0^\circ$ line or along the $\phi_f = \phi = \phi_0/2$ line. Therefore, whether the CSMA is fed along central symmetrical position ($\phi_f = \phi = \phi_0/2$ line) or along the edge ($\phi_f = \phi = 0^\circ$ line); the feed-probe would experience similar type of impedance variation, and hence only TM_{01} mode is excited in the

CSMA. Thorough investigations via [14] with all sector angles up to 60^0 shows that the dominant TM_{01} mode can always be excited in the CSMA and it is independent of azimuthal feed-probe location ϕ_f. Furthermore, the resonant frequency of the CSMA with $0^\circ < \phi_0 \le 60^\circ$ is fully dependent on the radial dimension (ρ) of the patch and not on the sector angle ϕ_0. The fields beneath the patch for the mode with $m = 0$ resonates along the x-x' direction, its E and H planes are corresponding to x-z and y-z respectively. Consequently, the radiated electric field for such CSMAs is x polarized.

3.3.2   CSMA with Sector Angle $60^\circ < \phi_0 \le 170^\circ$

In case of CSMAs with sector angles $60^\circ < \phi_0 \le 170^\circ$, the dominant modes have $m \ne 0$. It is realized from Eq. (3.5) that when $m \ne 0$, the E/H ratio depends on both the azimuth angle ϕ and the Bessel function of order m and argument ($k_\rho\ \rho$). Therefore, the impedance variation for the mode with $m \ne 0$ within the CSMA is of complex nature and it varies along the radial direction ρ, as well as the circumferential direction ϕ. Furthermore, when the antenna is fed along the central symmetrical $\phi = \phi_0/2$ line, it would encounter different impedance variation compared to the one that fed along the $\phi = 0^\circ$ line as this E/H ratio is closely related to V/I ratio, i.e., the impedance at the feed-probe location.

Thorough investigations via [14] shows that for the CSMAs with sector angles $60^\circ < \phi_0 \le 110^\circ$, the dominant modes of the CSMAs are fractional modes and can only be excited when the CSMA is fed along the edge i.e. along $\phi = 0^\circ$ line. When the patches are fed along the central symmetrical $\phi = \phi_0/2$ line; the excited modes are the next higher order TM_{01} mode. Hence, to excite the proper lowest order dominant mode, the CSMA should be fed along the edge i.e. $\phi_f = \phi = 0^\circ$ line. The variation of ($E/\omega\mu H$) ratio as a function of radial dimension (ρ) for 90° CSMA at its dominant TM_{21} mode is shown in Fig.3.2(b) for different azimuth angle of feeding values (ϕ_f) i.e. from edge ($\phi_f = 7^\circ$) to $\phi_f \approx \phi_0/2$. Notably, the slope of ($E/\omega\mu H$) ratio as a function of ρ is not the same for different feeding angle ϕ_f. The maximum value of the ratio is obtained at the edge i.e at $\rho = a$ for all ϕ_f values. However, these maximas are different for different ϕ_f. This indicates that, for different ϕ_f, one needs to optimize the feed position as a function of ρ. It is also noted from Fig. 3.2. (b) that the E/H

ratio exhibits it's higher value near the edge of the CSMA, i.e., along $\phi_f = 7°$, as compared to other ϕ_f values, and there is not much variation of E/H ratio beyond $\phi = 25^0$ in the case of 90^0 CSMA, as there is null electric field at the central region of the patch (that is $\phi_0/2$) for TM_{21} mode. Therefore, optimizing the feed location as a function of ρ becomes useless to excite the dominant TM_{21} mode in $90°$ CSMA if it is fed along the central $\phi_f = \phi_0/2$ line. Interestingly, if the feed probe is placed along the $\phi_f = \phi_0/2$ line, the next higher order mode TM_{01} can easily be excited in the 90^0 CSMA. This behavior of CSMA is valid for all the sector angles with $60° < \phi_0 \leq 110°$.
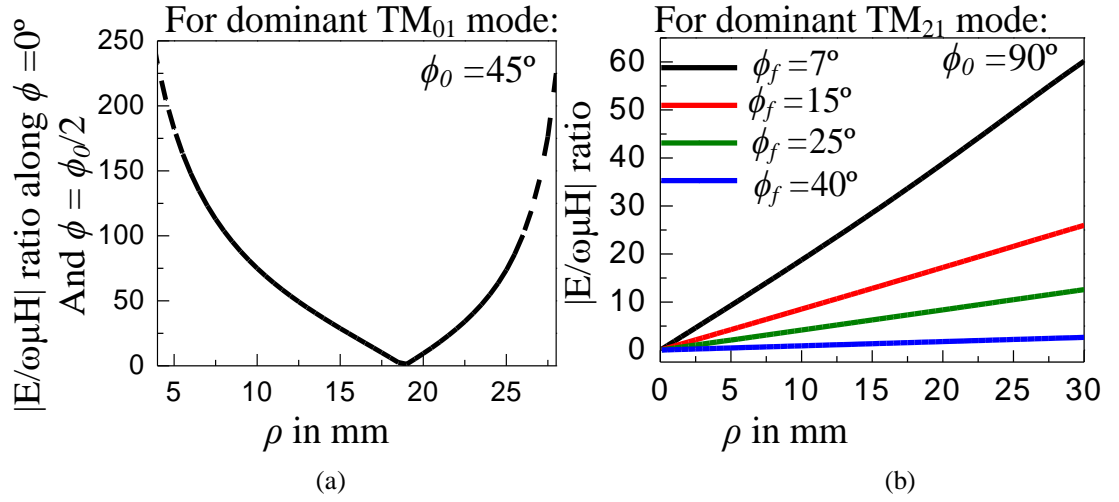
Fig. 3.2 Variation of $(E/\mu\omega H)$ ratio as a function of radial dimension for CSMA with (a) $\phi_0 = 45^0$ and (b) $\phi_0 = 90^0$. (CSMA parameters: radius $a = 30$ mm, $\varepsilon_r = 2.33$, substrate height $h = 1.575$ mm.)

Therefore, for all such centrally fed ($\phi_f = \phi_0/2$) CSMAs ($60° < \phi_0 \leq 110°$), the excited mode is the same i.e. TM_{01} and consequently its frequency is solely dependent on the radial dimension of the patches and is independent of the sector angle of the CSMA. Nevertheless, if those CSMAs are fed along the edge (near $\phi = 0^0$ line), the proper dominant mode (e.g $TM_{2.25\ 1}$ for $80°$, TM_{21} for $90°$, $TM_{1.63\ 1}$ for $110°$ and so on) can be excited. In those cases, the fields beneath the patches for the mode with either $m = 2.25$ or 2 or 1.63; the number of circumferential variation $q = 1$ and resonates along the $y\text{-}y'$ direction and hence its E and H planes are corresponding to $y\text{-}z$ and $x\text{-}z$, respectively. Consequently, the radiated electric field for such cases is y polarized. On the contrary, if the same patches ($60° < \phi_0 \leq 110°$) are fed along the central symmetrical $\phi = \phi_f = \phi_0/2$ line, the fields beneath the patches for TM_{01} mode

resonates along the *x-x'* direction and the radiated electric field for such cases is *x* polarized. The simulated reflection coefficient profiles for $90°$ CSMA fed at different ϕ_f are shown in Fig. 3.3. Here, the excitation of higher order TM_{01} mode is exhibited, instead of the dominant TM_{21} mode beyond $\phi_f = 25°$. Similar to the previous cases, the dominant modes of the CSMAs ($110° < \phi_0 \leq 170°$) can also be excited when the patch is fed along the edge i.e., along $\phi = 0°$ line.
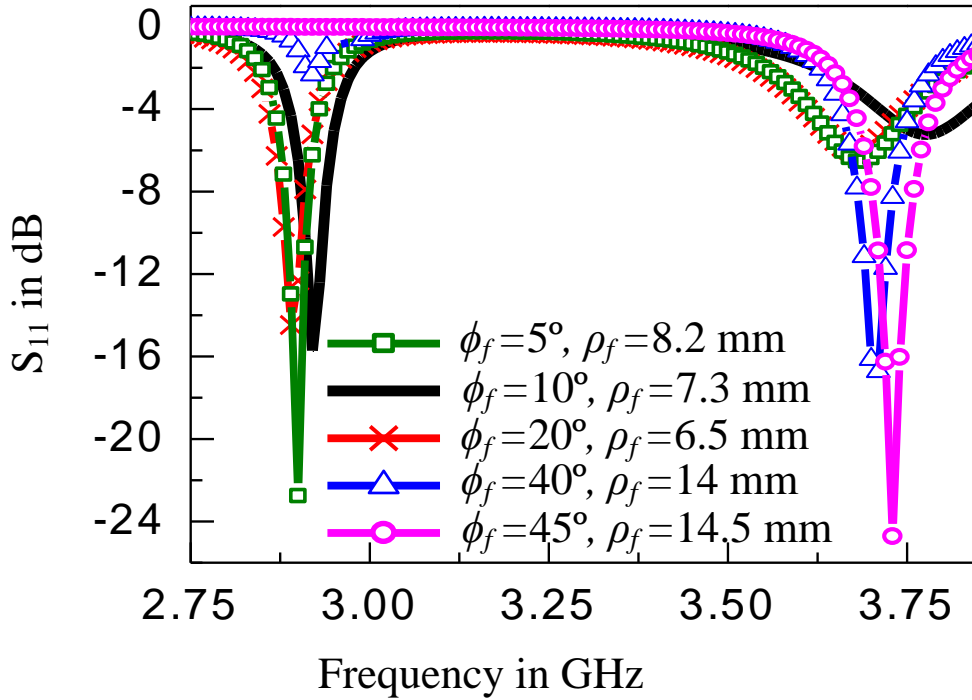
Fig. 3.3 Simulated S_{11} profile for a CSMA with $\phi_0 = 90^0$ fed along different azimuthal feed locations ϕ_f. (CSMA parameters: radius $a = 30$ mm, $\varepsilon_r = 2.33$, substrate height $h = 1.575$ mm.)

Once the CSMAs of such angles are fed along the central symmetrical $\phi = \phi_f = \phi_0/2$ line; they will exhibit the next higher order modes ($TM_{2m\,n}$) that are not the same for different sector angles ϕ_0 and they are not similar to TM_{01} mode (independent of ϕ_0 as was the above case for CSMAs with $60° < \phi_0 \leq 110°$).

Consequently, the CSMAs with $110° < \phi_0 \leq 170°$ exhibit their proper dominant modes (e.g $TM_{1.5\,1}$ for $120°$, $TM_{1.2\,1}$ for $150°$, $TM_{1.05\,1}$ for $170°$ and so on) when they are fed along the $\phi_f = \phi = 0°$ line, and in that case, the fields beneath the patches resonates along the *y-y'* direction and hence, the radiated electric field for such cases is *y* polarized. On the contrary, the centrally fed CSMAs ($\phi_f = \phi_0/2$ line) with such sector angles exhibit the next higher order $TM_{2m\,n}$ modes (e.g TM_{31} for $120°$, $TM_{2.4\,1}$

for $150^{°}$, $TM_{2.1\ 1}$ for $170^{°}$ and so on). The variation of ($E/\omega\mu H$) ratio for $120^{°}$ CSMA as a function of radial dimension (ρ) and azimuth angle at its dominant mode have exhibited similar profiles as in Fig. 3.2 (b). The simulated electric field distributions of the patch for three group of sector angles are presented in Fig. 3.4.

(a)

(b)

(c)

(d)

(e)

(f)
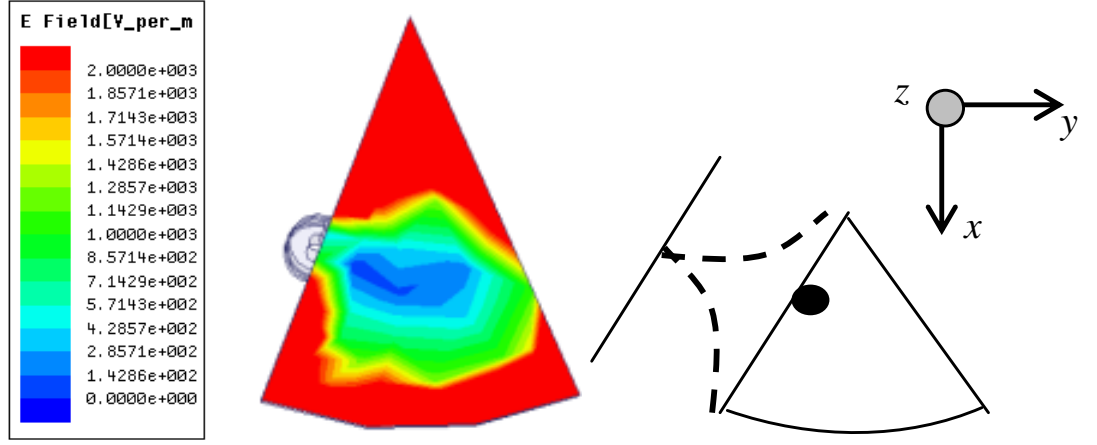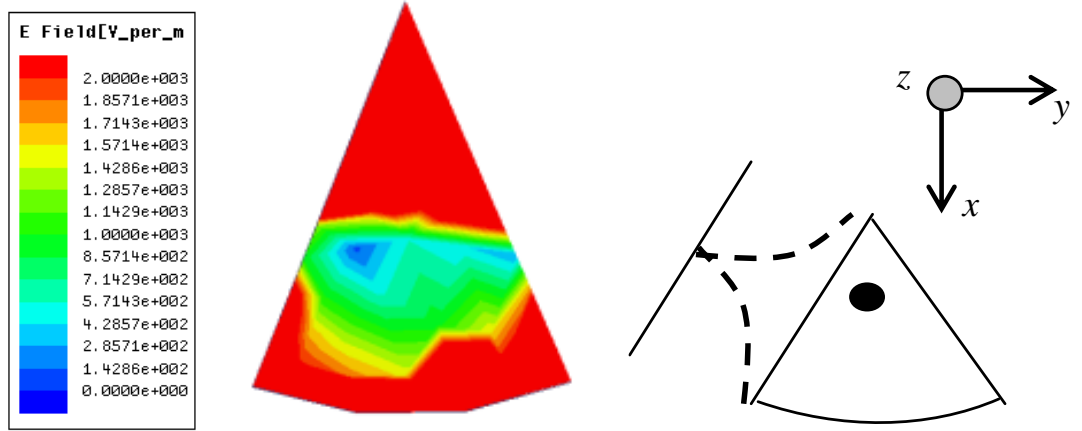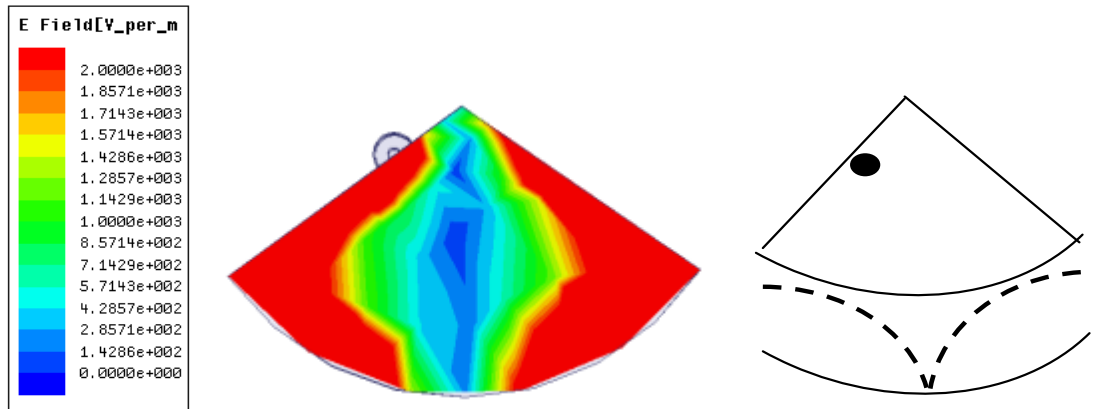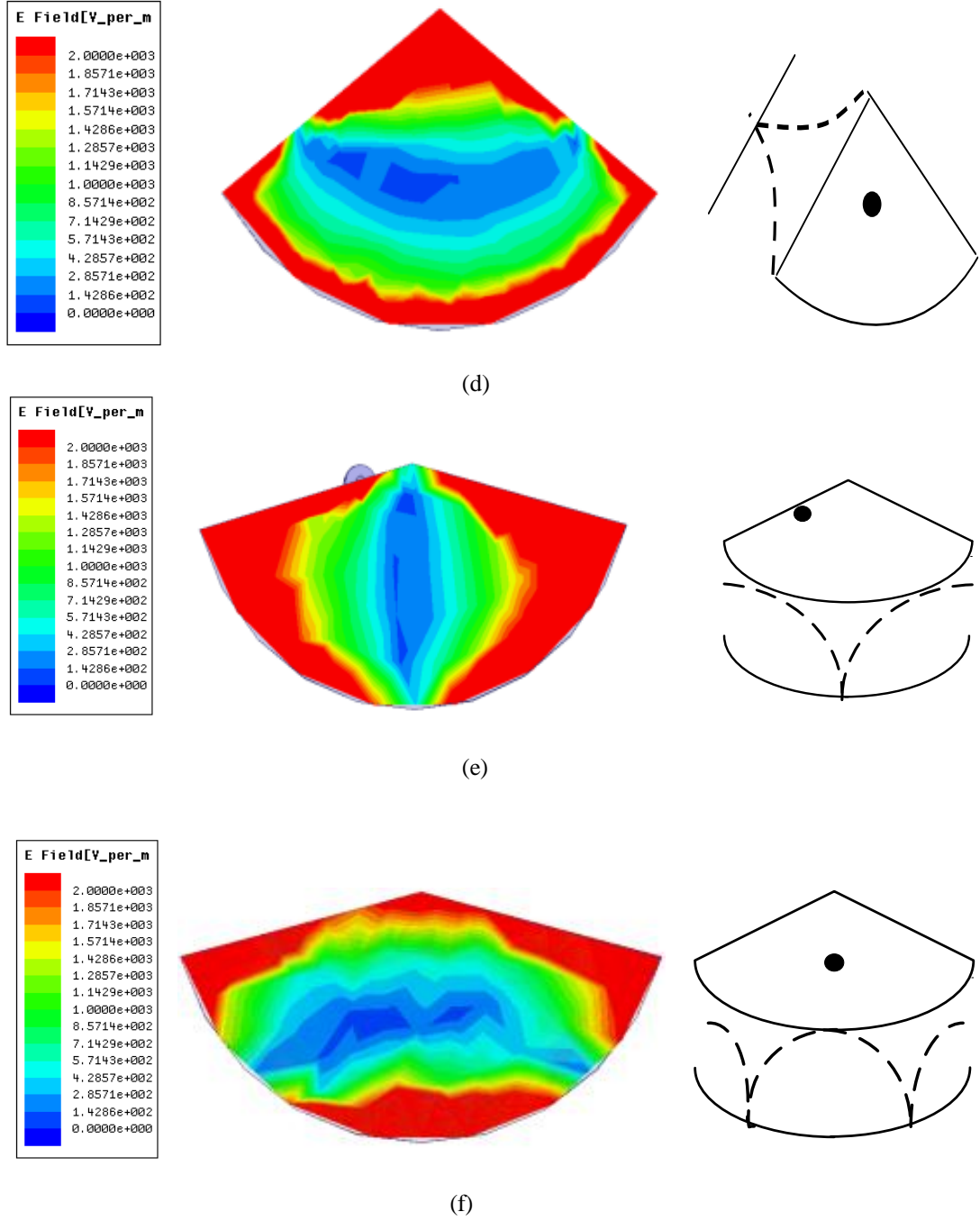
Fig. 3.4 The magnitude of electric field distribution on patch surface of CSMA and the corresponding standing wave pattern between the patch and ground plane for two feed-probe positions.(Scales are same in all the plots), (CSMA parameters: radius $a = 30$ mm, $\varepsilon_r = 2.33$, substrate height $h = 1.575$ mm.) (a) CSMA with $\phi_0 = 45^0$ fed along $\phi = 0^0$ line, (b) CSMA with $\phi_0 = 45^0$ fed along $\phi = \phi_0/2$ line, (c) CSMA with $\phi_0 = 110^0$ fed along $\phi = 0^0$ line, (d) CSMA with $\phi_0 = 110^0$ fed along $\phi = \phi_0/2$ line. (e) CSMA with $\phi_0 = 150^0$ fed along $\phi = 0^0$ line, (f) CSMA with $\phi_0 = 150^0$ fed along $\phi = \phi_0/2$ line.

62

For the cases when the CSMA is fed along the central symmetrical line or along the edge, it confirms the aforementioned observation. The corresponding standing wave distributions between the patch and ground plane have also been indicated in the same figure which corroborates the above explanations of different resonating profiles for the CSMAs as a function of azimuthal feed probe locations ϕ_f. This indeed, substantiates that, the fields beneath the patch resonates laterally along y-y' direction which gives birth to y polarized electric fields for all edge fed CSMAs (fed along or near $\phi_f = \phi = 0°$ line). In that case, the resonating dimension of a CSMA is along the circumference and hence the length of the arc is nearly half wavelength i.e $\rho\phi_0 \approx \lambda_g/2$. On the contrary, the fields beneath the patch resonate longitudinally along the x-x' direction that gives birth to x polarized electric fields for the centrally fed CSMAs except those with $110° < \phi_0 \leq 170°$. For CSMAs with $60° < \phi_0 \leq 110°$, the resonating dimension of the CSMA is the length of the radial dimension i.e $\rho = \lambda_g/2$. In case of the centrally fed CSMAs with $110° < \phi_0 \leq 170°$, the fields resonates along both the lateral and longitudinal direction and hence produces a mixed polarization and hence not useful for linearly polarized applications. It is also clearly observed in Fig. 3.4 that in all the cases, the feed-probe is to be located between successive minima and maxima standing wave patterns of the corresponding excited mode. Hence, it may be concluded that, to excite the proper lowest order dominant mode of a CSMA, it should be fed near the edge (along $\phi = 0°$ line). Nevertheless, feeding along the $\phi = 0°$ line is difficult from practical point of view. Therefore, a rigorous investigation has been performed to find the position (azimuth) up to which the CSMA can be fed to excite its lowest order dominant mode. Each CSMA of different sector angles have been studied through simulation and it is noted that, in each case, the lowest order dominant mode for a particular sector can surely be excited up to $\phi_f = 0.20\phi_0$. Although, the optimization of feed location along the central symmetrical $\phi = \phi_0/2$ line is easy, a CSMA with sector angle $60° < \phi_0 \leq 170°$ should not be fed along the central symmetrical $\phi = \phi_0/2$ line, as it excites the next higher order mode rather than the proper dominant mode. It may be noted that all the observations are similar for different substrate heights of the CSMA.

3.4   Determination of Approximate Feed Location

In all the cases investigated above; Eq. (3.5) is utilized to investigate the range of ($E/\omega\mu H$) ratio for which the dominant mode is excited. It is observed that the impedance of the CSMA varies both along the radial distance and azimuth angle. This in turn develops complexity in finding proper feed location to excite the proper lowest order mode.
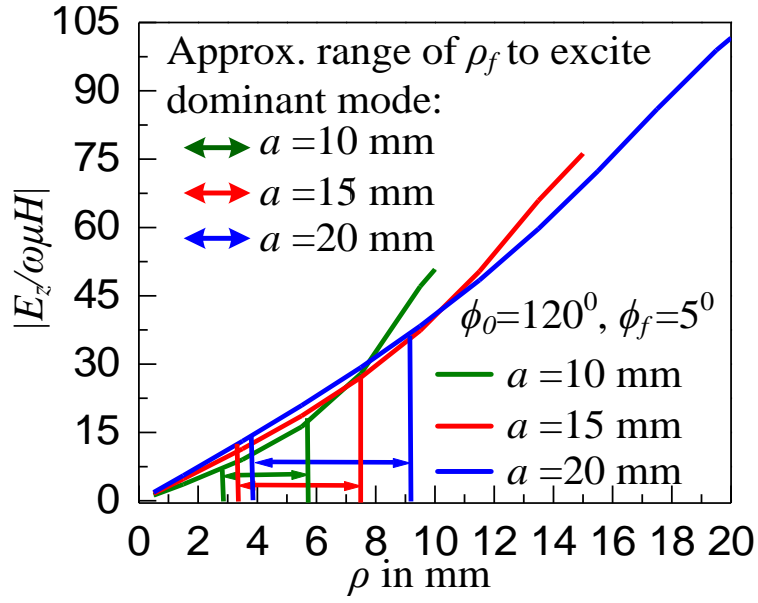
(a)
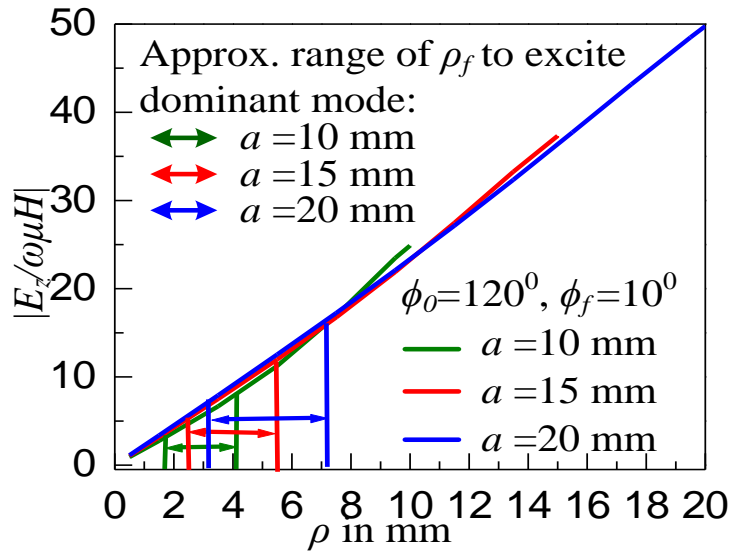
(b)

Fig. 3.5 Predicted radial feed location (ρ_f) ranges of 120° CSMA of a =10 mm, 15 mm, 20 mm based on Eq. (3.5) and ($E_z/\omega\mu H$)$_{max}$ (obtained from Eq. (3.5) by putting $\rho = a$) for (a) ϕ_f =5°, (b) ϕ_f =10°.

The range of radial feed location ρ_f for $\phi_f = 5°$ and $\phi_f = 10°$ is different for a CSMA with particular radial dimension a. Till date, no accurate impedance formulation for a CSMA is available from which a particular 50 Ω point can be determined. Hence, the E/H ratio has been exploited to find a proper feed location for exciting a particular mode. In fact, the input voltage to current ratio (input impedance) of the patch must contain the signature of the E/H ratio at that particular point beneath the patch.

It is observed that the $(E_z/\omega\mu H)$ ratio for which the CSMA is excited at a particular mode varies within a particular range and that is approximately from $0.15(E_z/\omega\mu H)_{max}$ to $0.35(E_z/\omega\mu H)_{max}$ maximum radial dimension of a CSMA).

Therefore, using Eq. (3.5) an approximate range of feed location can be predicted across which a particular mode can be excited. Therefore, using the same concept, a $120°$ CSMA with three different radial dimensions have been investigated for two feed locations (in terms of azimuth), namely, $\phi_f = 5°$ and $\phi_f = 10°$, and they are presented in Fig. 3.5. It is observed that the range of feed locations to excite its dominant mode are different for the same patch with feed locations at $\phi_f = 5°$ and $\phi_f = 10°$. For further corroboration of the observation, the approximate range of feed positions is determined (using Eq. (3.5)) for a CSMA with different ϕ_0, and are presented in Table 3.1. Notably, the simulated resonant frequencies and its corresponding S_{11} values are also incorporated in the table to validate the excitation of the dominant and next higher order modes within the predicted range of feed locations. The theoretical prediction shows good agreement with simulation.

3.5   Experimental Results and Discussions

The experiments were carried out with the prototypes having patch radial dimension $a = 29.7$ mm fabricated on thin PTFE substrate ($\varepsilon_r = 2.33$, thickness $h = 1.58$ mm). The patch is fed by an SMA feed-probe (Radiall R125.403.000) with probe diameter of 1.2 mm. One sample of fabricated prototype of a CSMA with $\phi_0 = 110°$ is presented in Fig. 3.6. Microstrip patch with thin substrate has been preferred to avoid the complexity in feed inductance which causes problem in optimal matching.

Some representative measured results of reflection coefficient profiles are presented in this section.

TABLE 3.1 Predicted feed-probe positions for a CSMA with different sector angles for excitation of particular modes. (CSMA parameters: radius a = 30 mm, ε_r = 2.33, substrate height h = 1.575 mm.), f_r: Resonant frequency of particular mode, ϕ_f. Feed angle in terms of azimuth. Range of $(E_z/\omega\mu H)$:0.15$(E_z/\omega\mu H)_{max}$ to 0.35$(E_z/\omega\mu H)_{max}$.

ϕ_0	Feed angle ϕ_f	Computed range of ρ_f (mm) (Approx)	ρ_f (mm) to excite dominant mode [Sim]	S_{11} (dB) [Sim]	f_r (GHz) [Sim]	f_r (GHz) [11] And related mode
85^0	5^0	4.8-12.6	6.8	-10.5	2.99	3.12 $TM_{2.12\ 1}$
			8.5	-12.3	3.0	
			10.5	-14.0	2.99	
			11.1	-21.0	3.11	
			12.2	-13.1	3.0	
	42.5^0	10.2-15.8	14.5	-21	3.70	3.78 TM_{01}
105^0	5^0	5.0-11.9	6.0	-10	2.71	2.67
			7.0	-14.2	2.70	
			8.0	-20.1	2.70	
			9.0	-23.0	2.69	
			10.6	-14.0	2.68	$TM_{1.68\ 1}$
			11.2	-10.9	2.71	
	53.5^0	10.2-15.8	13.5	-23	3.78	3.78 TM_{01}
115^0	5^0	4.6-11.8	5.0	-9.99	2.51	2.50
			6.0	-11	2.50	
			7.0	-15	2.41	
			8.0	-20	2.49	$TM_{1.56\ 1}$
			9.0	-24	2.46	
			10.0	-15	2.43	
	57.5^0	-	13.5	-21	3.40	3.31 $TM_{3.12\ 1}$
125^0	5^0	5.5-12.0	6.0	-10.4	2.40	2.38
			7.5	-26.7	2.39	
			8.5	-17.1	2.35	$TM_{1.44\ 1}$
			9.5	-14.1	2.32	
			10.5	-10.2	2.28	
			11.0	-9.8	2.30	
	62.5^0	-	12.0	-25	3.74	3.9 $TM_{2.88\ 1}$

In Fig. 3.7, the theoretically predicted feed location range of a CSMA with $\phi_0 = 110^{\circ}$ to excite the dominant $TM_{1.63\ 1}$ mode has been examined through measurements for azimuthal feed angle $\phi_f = 10^{\circ}$. The antenna has been tested for four different radial feed locations ρ_f and two of them are within the predicted range, while the

others are outside the range. Thus, the predicted feed location range is in good agreement with the measurements.
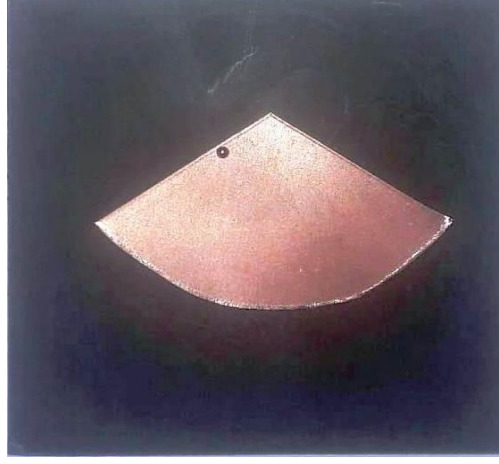
(a)

(b)

Fig. 3.6 Fabricated prototype of CSMA with $\phi_0 = 110°$ (a) top and (b) back view.

In Table 3.2, the excited modes and their measured resonant frequencies of a CSMAs with different sector angles ($\phi_0 = 45°$, $60°$, $90°$, $110°$, $150°$ and $160°$) are presented for theoretically predicted feed locations. In each case, the approximate ranges of radial feed locations ρ_f for specific azimuthal feed angle ϕ_f are determined based on the theoretical prediction presented in section 3.2.1 and section 3.2.2. The experimental radial feed position ρ_f at same feed angle ϕ_f for every sector angle ϕ_0 along with the excited mode and its frequency are presented in Table 3.2. In all the cases, the experimental and simulated feed locations are in good agreement with the theoretically predicted range to excite a particular mode. Each CSMA with a specific

sector angle is fed at different feed locations; in which some are near the edge lines (near and along $\phi = 0°$ line) and some are at $\phi_f > 0.2\ \phi_0$. Based on the theoretical predictions, the CSMAs are fed to excite dominant or next higher order modes.
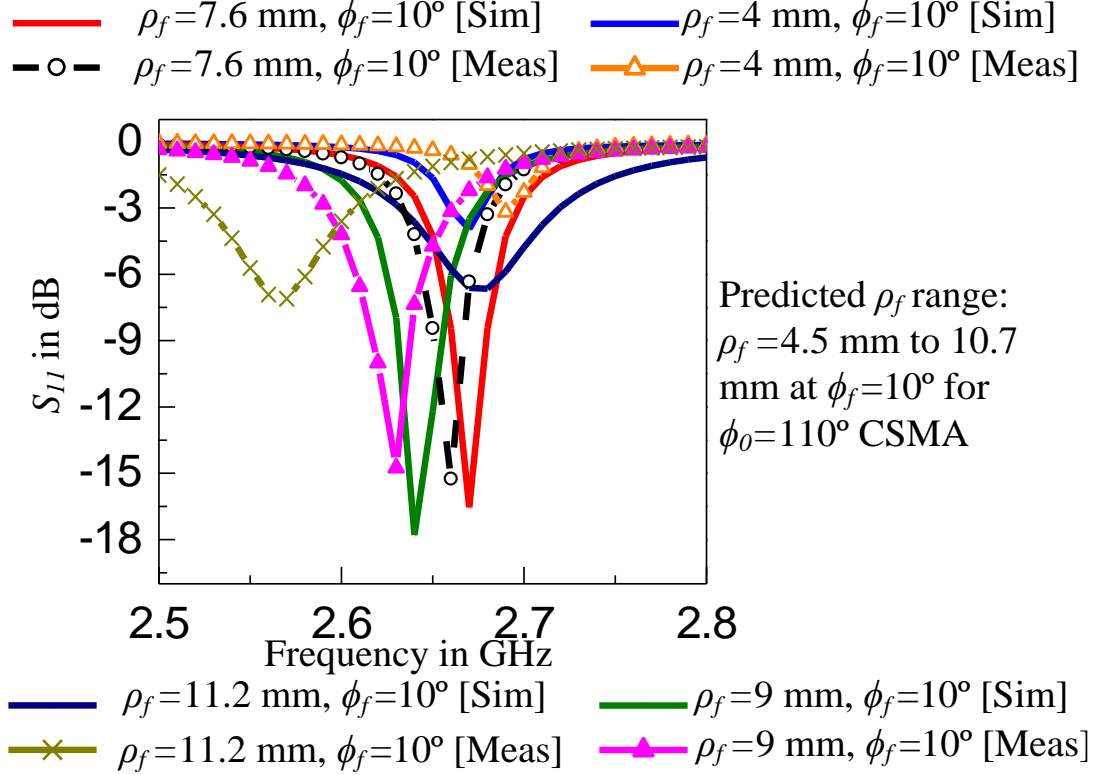
Fig. 3.7 Comparison of measured and simulated S_{11} profiles for CSMA with $\phi_0 = 110^0$, $\phi_f = 10^0$ at theoretically predicted radial feed locations ρ_f (CSMA parameters: radius $a = 30$ mm, $\varepsilon_r = 2.33$, substrate height $h = 1.575$ mm.)

It confirms that the excited modes for CSMAs with sector angle $\phi_0 = 45°$ and $60°$ are not dependent on the azimuthal feed positions that validate the observation presented in section 3.3.1. Moreover, in both the cases, the excited mode (TM_{01}) and its frequency is similar (~3.7 GHz). Therefore, it confirms that the lowest order mode and its frequency of a CSMA with $\phi_0 \leq 60°$ is independent of sector angle ϕ_0, and its frequency is exclusively dependent on the radial dimension of the patch, as well as the dielectric constant of the substrate. In the cases of CSMAs with $\phi_0 = 90°$ and $110°$, the excited modes significantly depend on the azimuthal feed locations. In these cases, when the CSMAs are fed within 0.2 ϕ_0, the lowest order modes are excited. However, the lowest order modes are different in each case and it depends on the sector angle ϕ_0 of the CSMA.

TABLE 3.2 Comparison between predicted and measured feed-probe positions to excite a particular mode and corresponding resonant frequencies for CSMA with different sector angles. (CSMA parameters: radius a = 30 mm, ε_r = 2.33, substrate height h = 1.575 mm.)

| Range of $E_z/\omega\mu H$ | Patch with sector angle ϕ_0 | Feed Location | | | | Excited Mode | Computed Frequency (GHz) of respective modes [11] | Measured Frequency (GHz) |
		Feed Location in terms of azimuth angle ϕ_f	Approximate range of Radial distance ρ_f in mm (from apex)	Simulated radial distance ρ_f in mm (from apex) (for best matching)	Experimental radial distance ρ_f in mm (from apex)			
0.15 $(E_z/\omega\mu H)_{max}$ to 0.35$(E_z/\omega\mu H)_{max}$	45⁰	5⁰ $(\phi_1 < 0.5\ \phi_0)$	10.2-15.8	14.8	15.1	TM_{01}	3.70	3.75
		15⁰ $(\phi_1 < 0.5\ \phi_0)$	10.2-15.8	14.6	15.0	TM_{01}	3.70	3.78
		22⁰ $(\phi_1 \approx 0.5\ \phi_0)$	10.2-15.8	15	14.2	TM_{01}	3.70	3.72
	60⁰	5⁰ $(\phi_1 < 0.5\ \phi_0)$	10.2-15.8	13.5	14	TM_{01}	3.70	3.73
		15⁰ $(\phi_1 < 0.5\ \phi_0)$	10.2-15.8	14.2	15	TM_{01}	3.70	3.72
		30⁰ $(\phi_1 \approx 0.5\ \phi_0)$	10.2-15.8	15.4	15.5	TM_{01}	3.70	3.70
	90⁰	7⁰ $(\phi_1 < 0.2\ \phi_0)$	4.8-10.9	8.2	9	TM_{21}	3.00	2.90
		15⁰ $(\phi_1 < 0.2\ \phi_0)$	3.9-9.1	7	7.2	TM_{21}	3.00	2.92
		40⁰ $(\phi_1 > 0.2\ \phi_0)$	10.2-15.8	14	14	TM_{01}	3.70	3.70
		45⁰ $(\phi_1 \approx 0.5\ \phi_0)$ (i.e $> 0.2\ \phi_0$)	10.2-15.8	14.5	15	TM_{01}	3.70	3.67
	110⁰	5⁰ $(\phi_1 < 0.2\ \phi_0)$	5.3-11.2	7	7.6	$TM_{1.63\ 1}$	2.60	2.61
		10⁰ $(\phi_1 < 0.2\ \phi_0)$	4.5-10.7	8	8.9	$TM_{1.63\ 1}$	2.60	2.56
		50⁰ $(\phi_1 > 0.2\ \phi_0)$	10.2-15.8	14.2	14.6	TM_{01}	3.70	3.76
		55⁰ $(\phi_1 \approx 0.5\ \phi_0)$ (i.e $> 0.2\ \phi_0$)	10.2-15.8	13	13.8	TM_{01}	3.70	3.79

		Feed Location						
Range of $E_z/\omega\mu H$	Patch with sector angle ϕ_0	Feed Location in terms of azimuth angle ϕ_f	Approximate range of Radial distance ρ_f in mm (from apex)	Simulated radial distance ρ_f in mm (from apex) (for best matching)	Experimental radial distance ρ_f in mm (from apex)	Excited Mode	Computed Frequency (GHz) of respective modes [11]	Measured Frequency (GHz)
0.15$(E_z/\omega\mu H)_{max}$ to 0.35$(E_z/\omega\mu H)_{max}$	150°	5^0 ($\phi_1 < 0.2\,\phi_0$)	4.8-11.7	6.8	7.2	$TM_{1.2\ 1}$	2.13	2.08
		23^0 ($\phi_1 < 0.2\,\phi_0$)	4.1-9.85	7	6.7	$TM_{1.2\ 1}$	2.13	2.06
		57^0 ($\phi_1 > 0.2\,\phi_0$)	-	14.6	15	$TM_{2.4\ 1}$	3.50	3.43
		75^0 ($\phi_1 \approx 0.5\,\phi_0$) (i.e $> 0.2\,\phi_0$)	-	15	16	$TM_{2.4\ 1}$	3.50	3.41
	160°	5^0 ($\phi_1 < 0.2\,\phi_0$)	5.1-11.9	5.8	6.1	$TM_{1.12\ 1}$	2.00	2.01
		21^0 ($\phi_1 < 0.2\,\phi_0$)	3.8-9.7	4.9	5.2	$TM_{1.12\ 1}$	2.00	1.99
		52^0 ($\phi_1 > 0.2\,\phi_0$)	-	16.4	17	$TM_{2.25\ 1}$	3.30	3.23
		80^0 ($\phi_1 \approx 0.5\,\phi_0$) (i.e $> 0.2\,\phi_0$)	-	15	16	$TM_{2.25\ 1}$	3.30	3.19

Consequently, the frequencies of the excited lowest order modes are different. The dominant mode resonant frequencies also depend on the sector angle, radial dimension of the patch, as well as the dielectric constant of the substrate. However, when the same CSMAs ($\phi_0 = 90^\circ$ and 110°) are fed beyond 0.2 ϕ_0 or fed centrally; the next higher mode TM_{01} will be excited. The higher order mode is same in these cases and independent of the sector angle ϕ_0 and its frequency is exclusively dependent on the radial dimension of the patch, as well as the dielectric constant of the substrate. Hence, these phenomena of CSMAs with $60^\circ \leq \phi_0 \leq 110^\circ$ agree with our predictions presented in section 3.3.2. Similar observations are revealed for CSMAs with $\phi_0 = 150^\circ$ and 160°. However, such CSMAs when centrally feed ($\phi_f = 0.5\phi_0$) or feed at $\phi_f > 0.2\ \phi_0$ excite different higher order modes and this is a key difference with CSMAs

with $60° < \phi_0 \leq 110°$, as have been discussed in section 3.3.2. Moreover, the next higher order modes are TM_{21} instead of TM_{01} mode.

Nevertheless, it is very clear from the investigation that the dominant mode for a CSMA with specific sector angle (with $\phi_0 > 60°$) can be excited only up to $\phi = 0.2 \ \phi_0$. When the same CSMA is fed at $\phi_f > 0.2 \ \phi_0$ and typically along central line i.e $\phi_f = 0.5 \ \phi_0$; the dominant modes are not excited. Instead, the next higher mode will be excited. In each of the cases in Table 3.2, it is revealed that within the predicted feed location ranges, the experimental and simulated feed-probe locations for the excitation of specific mode are in excellent agreement.

(a)

(b)

71
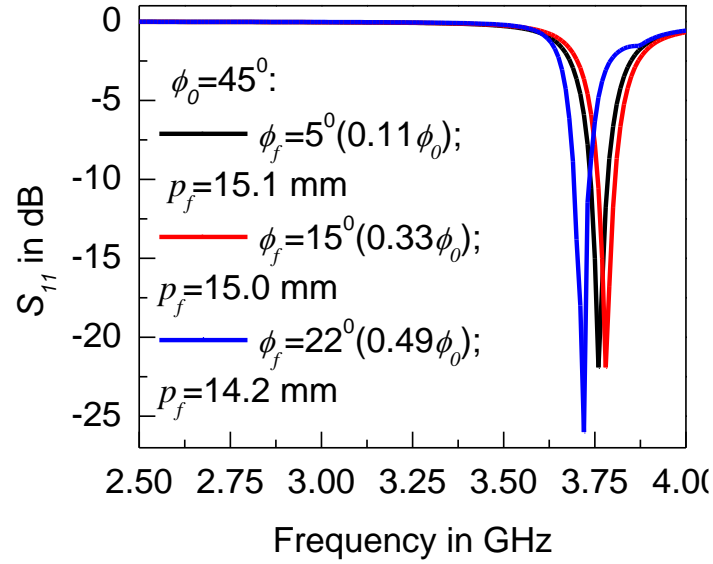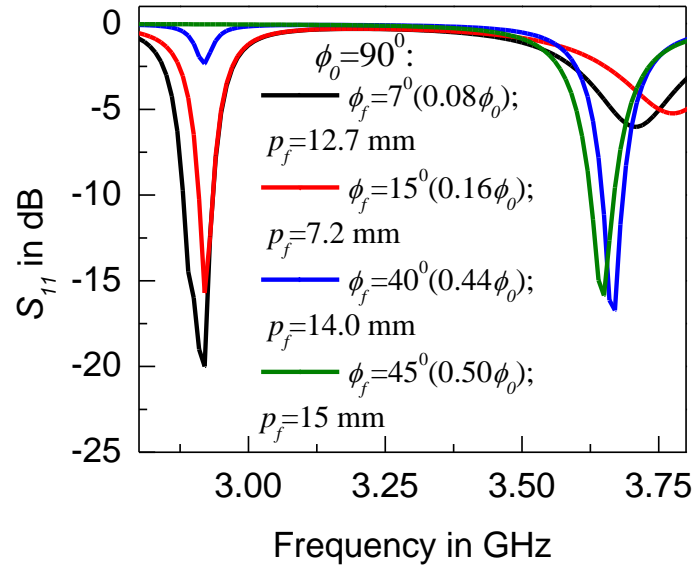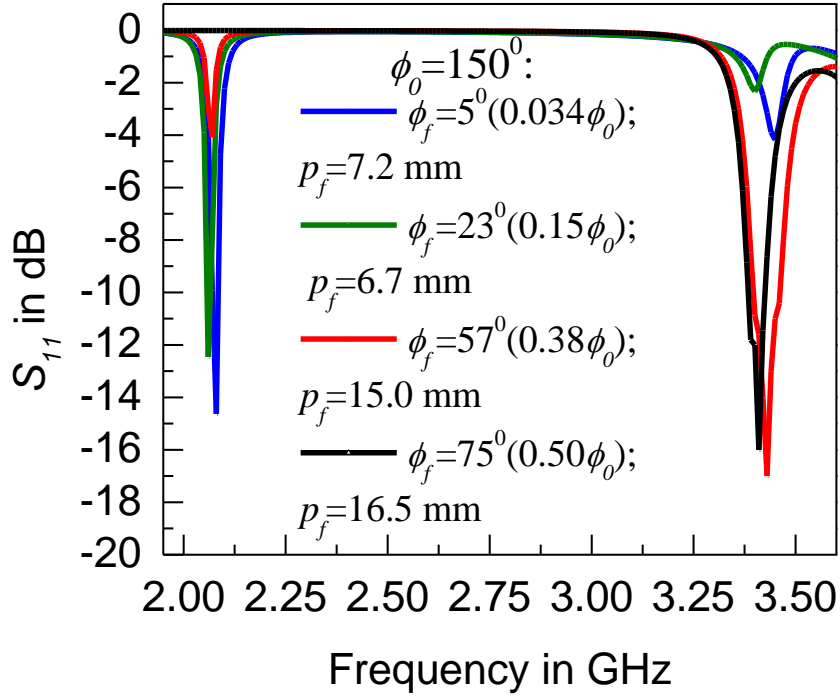
(c)

Fig. 3.8 Measured S_{11} profile for a CSMA with different sector angles fed along different ϕ line. (CSMA parameters: radius $a = 29.7$ mm, $\varepsilon_r = 2.33$, substrate height $h = 1.575$ mm.), (a) sector angle $\phi_0 = 45^0$, (b) sector angle $\phi_0 = 90^0$, (c) sector angle $\phi_0 = 150^0$.

However, for centrally fed CSMAs with sector angles of $120^\circ \leq \phi_0 \leq 170^\circ$, the approximate range of feed locations has not been predicted with the present theory as they produce different higher order modes with complex field configuration. The S_{11} profiles for some of the cases shown in Table 3.2 for different feed probe locations are presented in Fig. 3.8. This gives a clear visualization of varying S_{11} profiles as a function of feed probe locations in a CSMAs with $\phi_0 = 45^0$, 90^0 and 150^0. Hence, it is observed from measurements that in all the cases, the feed locations to excite a particular mode in a specific CSMA with specific sector angle ϕ_0 can be predicted easily with the help of the proposed technique.

Hence the influence of the feed-probe as a function of modes of CSMA has been investigated thoroughly. The particular position of feed probe to excite particular mode including the lowest order dominant mode has been established. The radiation characteristic of CSMA as a function of feed position is equally important and has been documented in the following section.

3.6   Radiation Characteristics of CSMA as a Function of Feed Position

The radiation characteristics of 90^0 CSMA for two feed positions have been investigated further. The CSMAs with a small sector angle $\phi_0 = 90^0$ has been considered in the present investigation in view of lesser space requirement compared to CMA. As observed from section 3.3.2, 90^0 CSMA has the lowest order dominant TM_{21} and that can only excited when it is fed along it's edge. If the 90^0 CSMA is fed along central symmetrical line, it excites next higher TM_{01} mode. Therefore, depending on the feed probe location, two modes can be excited as Antenna#1 (feed probe along central symmetrical line, $\phi = \phi_0/2$) and Antenna #2 (feed probe along central symmetrical line, $\phi = 0^0$). Based on theory presented in section 3.4 Antenna#2 is fed at $\phi_f = 5^0$ and $\rho_f = 5$ mm. The simulated field distribution for Antenna#1 and Antenna#2 has been depicted in Fig. 3.9. The figure confirms the proposed analysis documented up to section 3.5. If the 90^0 CSMA is fed along central symmetrical line, it excites next higher TM_{01} mode. Therefore, depending on the feed probe location, two modes can be excited as Antenna#1 (feed probe along central symmetrical line, $\phi = \phi_0/2$) and Antenna#2 (feed probe along central symmetrical line, $\phi = 0^0$). Based on theory presented in section 3.4 Antenna#2 is fed at $\phi_f = 5^0$ and $\rho_f = 5$mm. The simulated field distribution for Antenna#1 and Antenna#2 has been depicted in Fig. 3.9. The figure confirms the proposed analysis documented up to section 3.5.

(a)
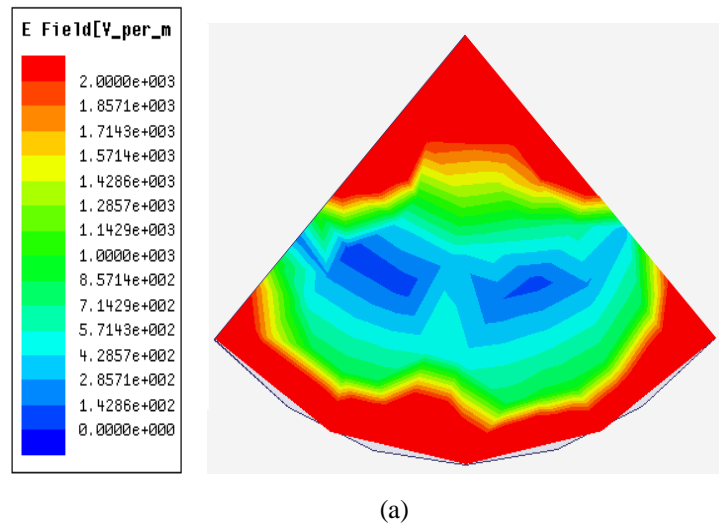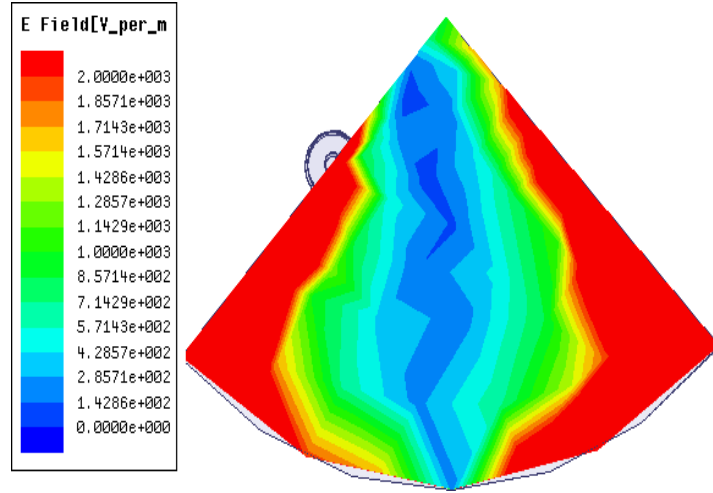
(b)

Fig. 3.9 The magnitude of simulated [18] electric field distribution over patch surface of CSMA for two feed-probe positions. (CSMA parameters: radius a = 10 mm, ε_r = 2.33, substrate height h = 1.575 mm.) (a) CSMA with ϕ_0 = 90^0 fed along ϕ = $\phi_0/2$ line (b) CSMA with ϕ_0 = 90^0 fed along ϕ = 0^0 line.

3.6.1 Antenna#1: 90^0 CSMA with Feed -Probe along Central Symmetrical $\phi = \phi_0/2$ line

The simulated [14] reflection coefficient of Antenna#1 has been presented in Fig 3.10. The Antenna#1 exhibits around 9 % impedance bandwidth.

f_r = 10.59 GHz
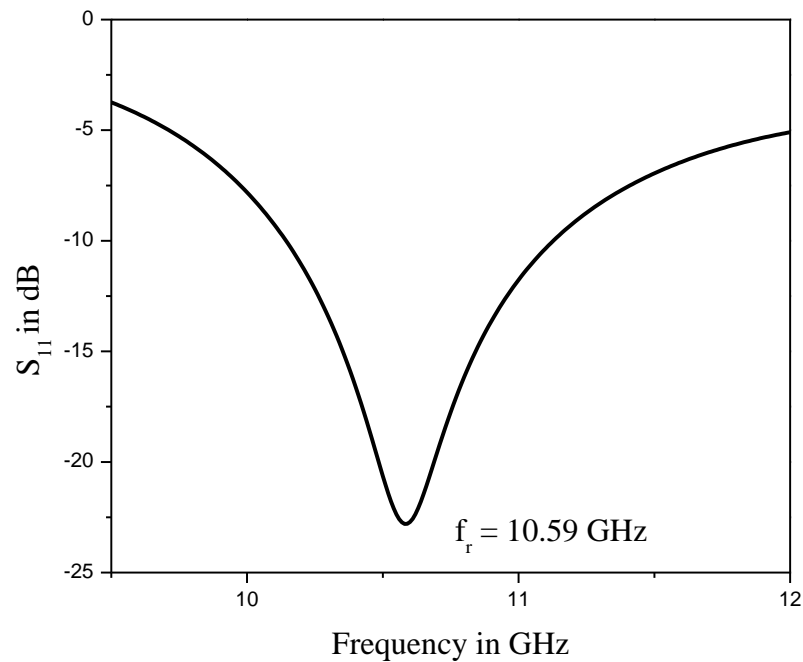
Fig. 3.10 Simulated reflection co-efficient profile for Antenna#1 (center fed 90^0 CSMA)

The H plane and E plane co-pole radiation pattern are presented in Fig. 3.11. It is observed that the Antenna#1 show broadside radiation pattern and have good radiation characteristics. The 3dB beam widths of both the antennas are around 70^0 and 95^0 in H and E-plane, respectively
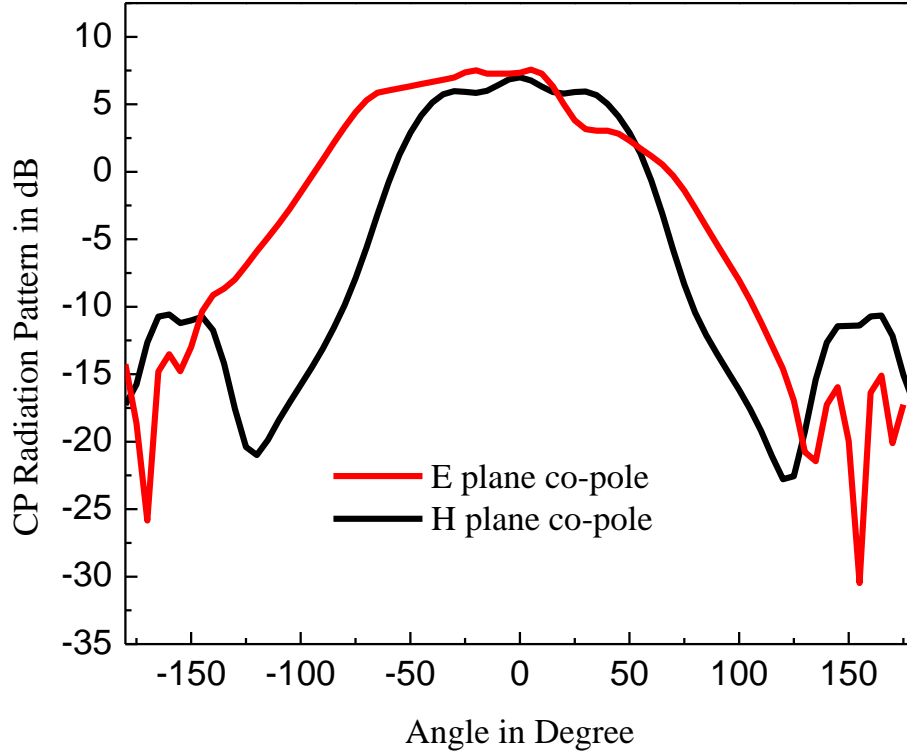
Fig. 3.11 CP Radiation patterns for Antenna#1 at TM_{01} mode (f_r = 10.59 GHz) in both E and H plane

3.6.2 Antenna#2: 90^0 CSMA with Feed -Probe along Edge ($\phi = 0^0$ line)

Now, the same CSMA is fed along edge ($\phi = 5^0$ line) by a feed-probe. It is observed that instead of TM_{01} mode, dominant TM_{21} mode is excited. It is further observed that TM_{21} is excited up to the feed-probe position $\phi_1 = 30^0$ line and beyond that this mode ceases to exist. The simulated [18] reflection coefficient is presented in Fig 3.12. The CSMA exhibits around 5% impedance bandwidth. The simulated [18] CP E plane and H plane radiation patterns are presented in Fig. 3.13.
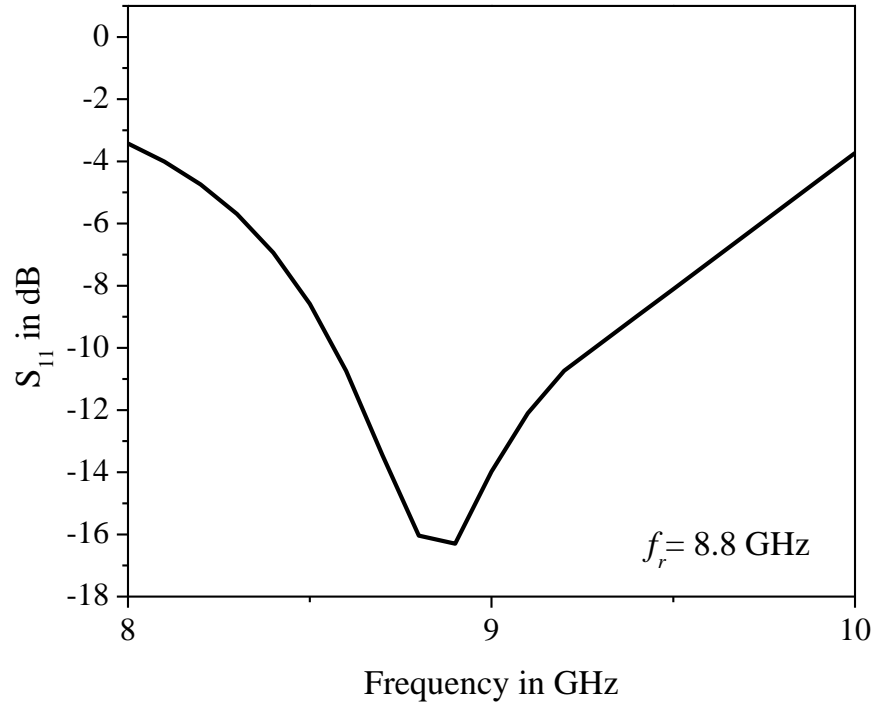
Fig. 3.12 Simulated reflection co-efficient profile for Antenna#2 (edge fed 90⁰ CSMA)
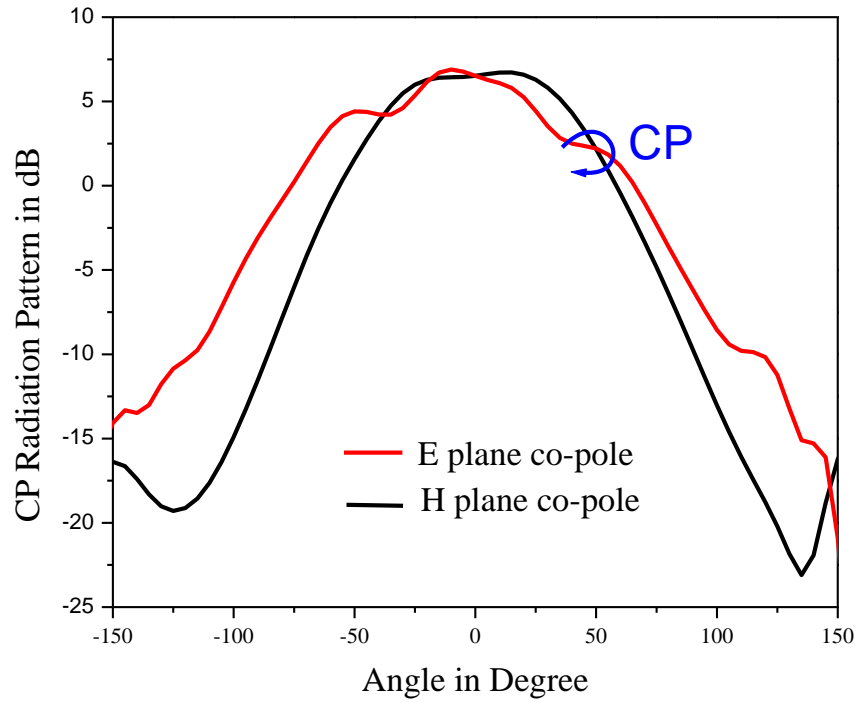
Fig. 3.13 CP Radiation patterns for Antenna#2 at TM_{21} mode (f_r = 8.8 GHz) in both E and H plane.

3.7 An Attempt to Enhance of Gain in CSMA

The study of gain enhancement of 90^0 CSMA has not been reported earlier. Thus, the study of gain improvement is important to understand the radiation characteristics of CSMA. The detailed study of improvement of gain in 90 CSMA has been discussed in this section. Although the 90^0 CSMA attains miniaturization, gain of such antenna is not satisfactory in comparison with conventional CMA. However, gain improvement is one of the primary requirements of modern antenna technology. Therefore, the gain can be enhanced in such antennas if the conventional dielectric substrate (PTFE) is replaced by simple air substrate. Although several attempts have been made to use CSMA in modern wireless communications for different applications, the issue of gain enhancement in such small antennas has not been properly addressed in the open literatures. The use of air substrate in microstrip antennas of common geometries is the common and popular technique to enhance the gain.

In this section, the air substrate has been utilized instead of PTFE substrate and an improvement of gain is observed like other geometries. Further, a quick hand formulation has been established to estimate the gain enhancement of CSMA with air substrate compared to standard CSMA on PTFE substrate. In this present study, a edge fed 90° CSMA ($\phi_0 = 90^0$) of radius $a = 30$ mm on PTFE ($\varepsilon_r = 2.33$) and air substrate ($\varepsilon_r = 1$) with $h = 1.575$ mm has been investigated on 60×60 mm^2 ground plane. Both the antennas excite its dominant TM_{21} mode as discussed in the earlier section of this chapter. The schematic representation of the structure is shown in Fig. 3.14.

The change in gain (ΔG) and effective radiating area (A_{eff}) of a microstrip patch antenna is related as follows.

$$\Delta G[dB] = 10\log_{10}\left[\frac{\left(\dfrac{A_{eff}}{\lambda_0^2}\right)_{air}}{\left(\dfrac{A_{eff}}{\lambda_0^2}\right)_{ref}}\right] \tag{3.8}$$

where, $A_{eff} = \frac{(a_{eff}^2 \varphi_0)}{2}$ for CSMA where $\phi_0 = 1.57$ radian,

$\quad a_{eff} = (a \times \sqrt{(1+q)})$,

$\quad$ q = fringing factor and obtained from chapter 2.

$\quad \lambda_0$ = operating wavelength of the respective radiator.

As soon as the conventional PTFE substrate is replaced by air substrate, the electric field becomes loosely bound. It results in wider effective area, and hence provides better gain.

(a)

(b)
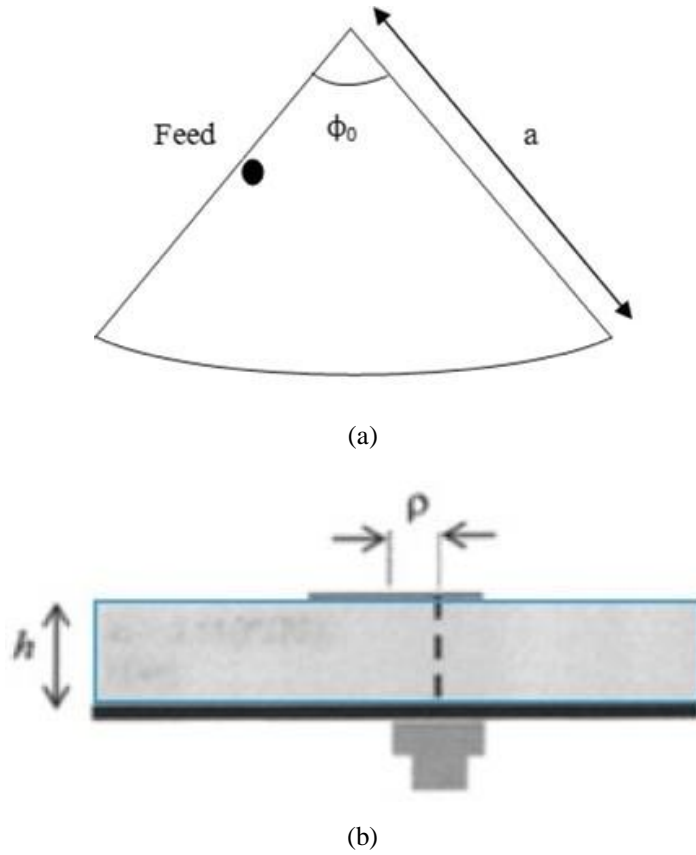
Fig. 3.14. Schematic diagram of 90° CSMA (a) top view (b) cross-sectional views.

The simulation study has been carried out using commercially available HFSS (v.14). The reflection coefficient profiles for both the CSMAs (with PTFE and air substrates) have been presented in Fig. 3.15. As expected, the resonant frequency of CSMA with air substrate has been shifted towards the higher side of the spectrum in comparison with CSMA on PTFE substrate. The resonant frequency of CSMA with air substrate is around 4.4. GHz while the same with PTFE substrate is around 2.9 GHz. Moreover, the bandwidth in case of the air substrate is better (6% more) as compare to PTFE substrate.
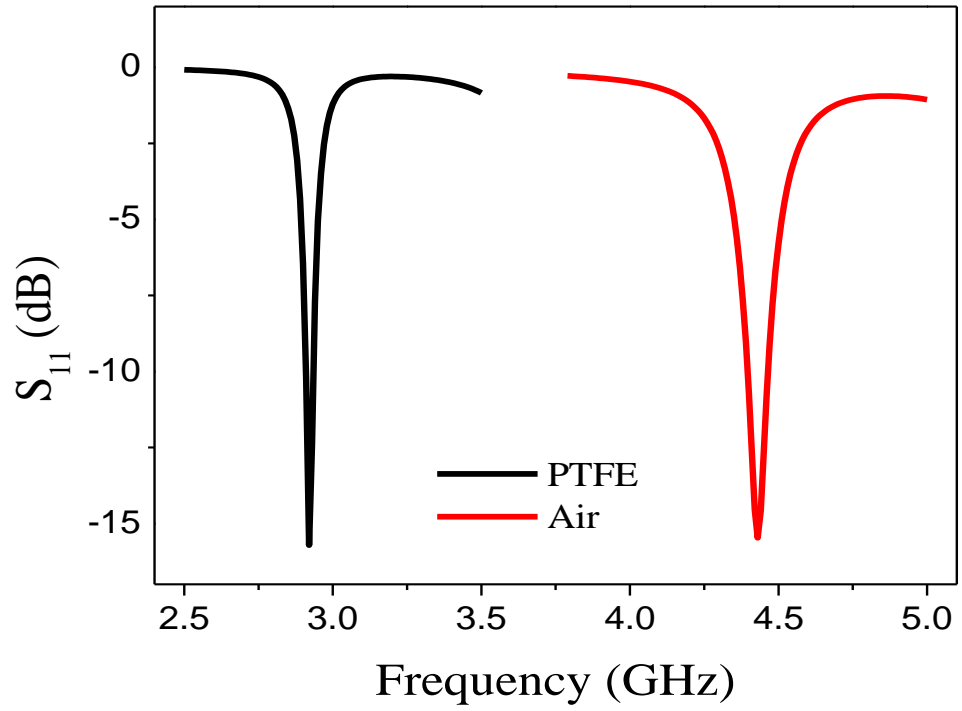
Fig. 3.15 Reflection coefficient profile of 90° CSMA with PTFE substrate and air substrate
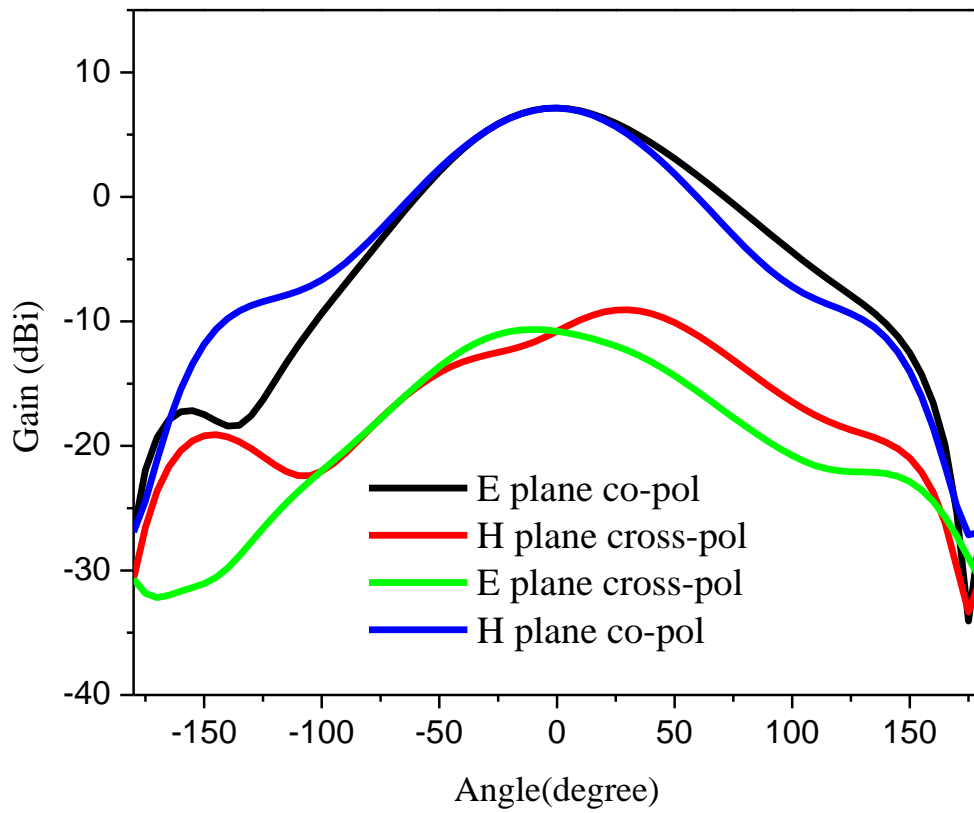
Fig. 3.16 Radiation pattern (co-pol and cross-pol) of CSMA with PTFE substrate
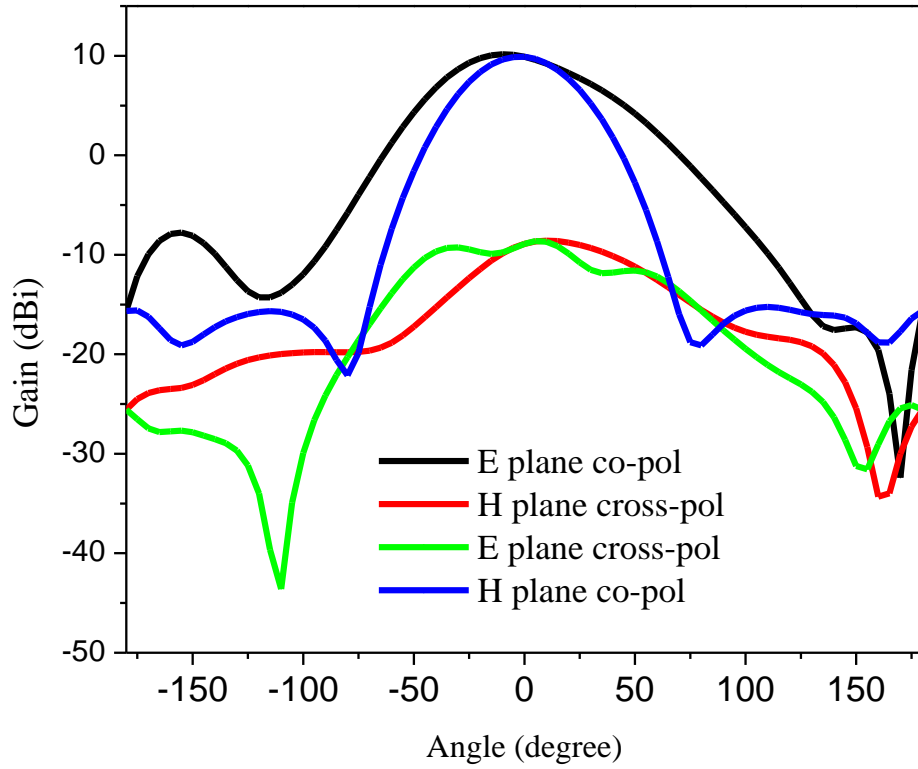
Fig. 3.17 Radiation pattern (co-pol and cross-pol) of CSMA with air substrate

It is observed that the co-pol gain of CSMA with air substrate is around 9.9 dBi whereas; the same with PTFE substrate is only 7.1 dBi. 2.8 dBi of gain improvement is revealed from the proposed technique.

The comparison of simulated and calculated gain enhancement of CSMA with air substrate has been presented in Table 3.3. A close agreement has been reveled between computed and simulated result.

TABLE 3.3 The calculated values of the effective patch dimensions and gain enhancement compared with the measured results.

Substrate	Resonance frequency (GHz)	Effective radial dimension (a_{eff})	Simulated gain (dBi)	$\Delta G[dB]$	
				Simulated	Calculated
PTFE	2.92	32.49	7.1	2.8	3.14
Air	4.43	33.94	9.9		

3.9   Conclusion

The influence of the feed-probe on the modes of CSMA has been investigated thoroughly and methodically. The fractional / dominant mode as well as the higher

order modes as a function of feed location in the CSMAs with different range of sector angles from 0^0 to 170^0 has been categorized and discussed in detail. The polarization of those has also been explained with the help of standing wave patterns observing beneath the patch. Finally, based on maximum *E/H* ratio an accurate but quick hand approximate theoretical technique has been anticipated to determine the feed location of a CSMA which can excite a specific mode. Consequently, 90^0 CSMA with air and PTFE substrate has also been thoroughly investigated for gain enhancement. A quick hand formulation has also been developed to estimate the gain enhancement which is in close agreement with simulated results. The proposed techniques to estimate the gain enhancement for CSMA with air substrate is very easy and simple which will be surely beneficial for scientist and practicing engineers looking for high gain simple CSMA. As such, the design issues of CSMA and determination of modes are critical and complex. The issue of miniaturization with respect to the radial dimension and active patch area is vital to choose a specific sector angle of CSMA. Therefore, compact design issues are very important for practicing and design engineers which will be discussed in the next chapter.

References

[1]   W. H. Hsu and K. L. Wong, "Circularly-polarised disk-sector Microstrip antenna," *Electron. Letter*, vol. 34, no. 23, pp. 2188–2190, 1998.

[2]   A. A. Deshmukh and N. V. Phatak, "Broadband sectoral microstrip antennas," *IEEE Antennas Wireless Propagation Letter,* vol. 14, pp. 727–730, Dec. 2014.

[3]   A. A. Deshmukh and P. Verma, "Multi-band dual polarized variations of modified circular microstrip antennas," *IETE Journal of Research*, pp 1-9, 2019 doi:10.1080/03772063.2019.1604179.

[4]   A. A. Deshmukh, P. Kamble, A. Doshi, D. Israni, and K. P. Ray, "Proximityfed broad band 120° sectoral microstrip antenna," *Procedia Comput. Sci.*, vol.115, pp. 101–107, 2017.

[5]   W-J. Lu, Q. Li, S. G. Wang, and L. Zhu, "Design approach to a novel dual mode wide band circular sector patch antenna," *IEEE Trans. Antennas Propag.*, vol. 65, no. 10, pp. 4980–4990, 2017.

[6]   W-J. Lu, X.-Q. Li, Q. Li, and L. Zhu, "Generalized design approach to compact wideband multi resonant patch antennas," *Int. J. RF Microw. Comput.- Aided Eng.*, 2018.

[7]   W. F. Richards, J. D. Ou, and S. A. Long, "A theoretical and experimental investigation of annular sector, and circular sector microstrip antennas," *IEEE Transaction Antennas Propagation*, vol. 32, no. 8, pp. 864–867, 1984.

[8]   A. K. Bhattacharya and R. Garg, "Analysis of annular sector and circular sector microstrip patch antennas," *Electromagnetics*, vol. 6, no. 3, pp. 229–242, 1986.

[9]   V. K. Tiwari, A. Kimothi, D. Bhatnagar, J. S. Saini, V. K. Saxsena, and P. Kumar, "Theoretical analysis on circular sector microstrip antennas," *Indian J.Radio Space Phys.*, vol. 35, no. 2, pp. 133–138, 2006.

[10]   V. K. Tiwari, A. Kimothi, D. Bhatnagar, J. S. Saini, and V. K. Saxsena, "Theoretical and experimental investigations of circular sector microstrip antennas," *Indian J. Radio Space Phys.*, vol. 35, no. 3, pp. 206–211, 2006.

[11]   S. K. Ghosh, S. Chakraborty, L. L. K. Singh, and S. Chattopadhyay, "Modal analysis of probe fed circular sector microstrip antenna with and without variable air gap: Investigations with modified cavity model," *Int. J. RF Microw.Comput.-Aided Eng.*, vol. 28, no. 1, pp. 1–14, 2018.

[12]   A. A. Kishk and L. Shafai, "The effect of various parameters of circular microstrip antennas on their radiation efficiency and mode excitation," *IEEE Transaction Antennas Propagation*, vol. 34, no. 8, pp. 969–976, 1986.

[13]   R. Garg, P. Bhatia, I. Bahl, and A. Ittipiboon, *Microstrip Antenna Design Handbook*. London: Artech House, 2001.

[14]   Ansoft Corp., Pittsburgh, PA, "HFSS: High frequency structure simulator," 2014.

CHAPTER

4

Compact Design Guidelines for the Choice of Sector Angle of Circular Sector Microstrip Antenna

4.1 Introduction

The modal analysis, excitation of modes as function of feed location and radiation characteristics of circular sector microstrip antenna (CSMA) having various types of sectoral angle has been discussed in previous chapters. The issues related to numerous sector angles of CSMA have been discussed thoroughly. As such, because of asymmetric geometry of CSMA, it has a special feature to excite numerous modes including fractional modes that depend on sector angle and feed probe location. Therefore, it is necessary to have a suitable CSMA structure which will be applicable in all perspective. A systematic study has been carried out in this chapter for exact choice of sector angle as a better alternative of a circular microstrip antenna. Therefore, comprehensive design guidelines are provided to estimate best possible configuration at any specific application.

Notably, there are much application e.g in mobile communication base terminal for microcellular system; antenna is mounted in same substrate for active microwave components [1]. In most of the cases, CSMA with large sector angle ($\phi_0 \geq 180^0$) has been investigated. However, CSMA with sector angle ($\phi_0 \leq 180^0$) is preferable to keep the other electronics circuits beside the antenna. Typically, the advanced wireless services (AWS-2), the broadband PCS, cable antenna relay service, uses the lower range of microwave band i.e., 1-2 GHz [2]. Further, modern sub-6 GHz 5G applications are also limited from 2-6 GHz. Therefore, any array or 5G MIMO

configuration, individual radiators should be small enough to mount on limited space. Notably, sub-6 GHz MIMO antennas are purely linearly polarized [3]. At this stage, CMA takes large space than CSMA. Moreover, the low frequency CMAs resonating specially below 3-4 GHz has high cross polar (XP) radiation which makes the co-polar (CP) radiation vulnerable. At this present scenario appropriate selection of CSMA is required to develop the miniaturized printed antenna as a suitable replacement of conventional CMA. Therefore, the critical design issues of CSMA definitely demands noteworthy attention to the scientific community to design such antennas.
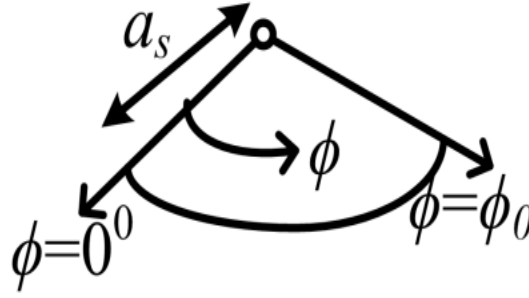
(a)

(b)

(c)

(d)

Fig. 4.1 (a) Schematic representation of CSMA of included angle ϕ_0, (b) top view fabricated prototype of 170^0 CSMA, (c) fabricated prototype of the equivalent circular patch, (d) bottom view of both prototypes.

At present, the investigation on CSMA geometry for widespread applications have been reported as it reveals extra compactness and conformality over bent

surfaces. Recently, proximity coupled CSMAs with large sector angle (ϕ_0) such as 270^0, 300^0, 320^0 & 340^0 etc have been reported [4], [5] for broad banding of patch. Novel dual mode dual stub loaded wideband 270^0 CSMA has been investigated in [6] where, higher order modes are utilized. Some more experimental investigations [7]-[8] have been reported for yielding circular polarization, Ku band applications. Employment of metamaterial in CSMA has been reported in [9] for obtaining quasi mono-polar pattern. However, all such investigations were based on simulation and the measurements were carried out to validate the proof of concept.

The resonance frequency formulation of CSMA using cavity model has been documented in chapter 2. The investigation into the influence of the feed-probe on the modes of CSMA has been discussed thoroughly in chapter 3. The radiation characteristics in CSMA and the employment of air substrate in CSMA to enhance the gain have been carried out in same chapter.

In this chapter it is aimed to develop comprehensive design guidelines for the selection of CSMA antenna geometry thoroughly, indicating the possibilities and limitations. Primarily, rigorous calculations are carried out and validated through measurements and simulation. Based on design guidelines, prototypes of 170^0 CSMA and conventional CMA have been fabricated for 1.86 GHz frequencies are fabricated, and their typical results are compared, which revealed that the 170˚ CSMA offers better radiation performance than the Conventional circular microstrip antenna (CCMA). The chapter has been organized in the following way. Section 4.2 has been described about the design consideration of CSMA in view of tininess. Selection of sector angle ϕ_0 in based on operating mode and frequency has been presented in section 4.2.1. Selection of sector angle ϕ_0 in based on miniaturization has been described and compared with respect to CMA in section 4.2.2. The discussion of experiential result has been verified in section 4.3. Finally, the best choice of sector angle ϕ_0 has been prescribed in section 4.4.

4.2   Design Consideration

In the present investigation, at first, the selection of lowest order frequency and operating mode of CSMA for any included angle ϕ_0 has been carried out in view of miniaturization. The close inspection of CSMA geometry depicts that, it demands a

special boundary condition which is not similar to conventional CMA. That is, the vanishing radial component of magnetic field boundary condition for vector potential wave equation at two truncated edges along ϕ *i.e*

$$H_\rho(\phi=0) = \frac{1}{\mu}\frac{1}{\rho}\frac{\partial A_z}{\partial \phi} = \frac{1}{\mu}\frac{1}{\rho}B_{mnp}J_m(k_\rho\rho)[-mA\sin m\phi + mB\cos m\phi][\cos(k_z z)] = 0 \quad (4.1)$$

Where, m is the mode number of CSMA of specific sector angle while, A and B are the constants and these can be determined from vanishing magnetic field boundary condition as is discussed in chapter 2. Following the theoretical formulation developed in chapter 2, it can be written as

$$m\phi_0 = q\pi \Rightarrow m = \frac{q\pi}{\phi_0} \quad (4.2)$$

where q = 0, 1, 2, 3, any positive integers.

It may be noted that, the determining factor of mode number m is dependent on the sector angle ϕ_0 and the number of circumferential field variation q. Although, this q is in integer form, the mode number m of CSMA of angle ϕ_0 is fractional. Therefore, CSMA can exhibit fractional modes depending on the chosen sector angle ϕ_0.

4.2.1 Selection of Sector Angle ϕ_0 in View of Operating Mode and Frequency

The dominant mode resonance frequency of CSMA can be written from chapter 2

$$f_r = \frac{\chi'_{mn}c}{2\pi a_s\sqrt{\varepsilon_{reff}}} \quad (4.3)$$

where, c is the free space velocity and a_s is the radial dimension of CSMA. The effective dielectric constant is ε_{reff} and χ'_{mn} is the nth root of derivative of Bessel function of order m (mode number). It is observed that, numerous values of mode numbers m are possible as there are plentiful numbers of possible sector angles ϕ_0 in between 0^0 to 360^0 in case of CSMA. Notably, the mode number m may also be fractional in many cases.

(a)

(b)
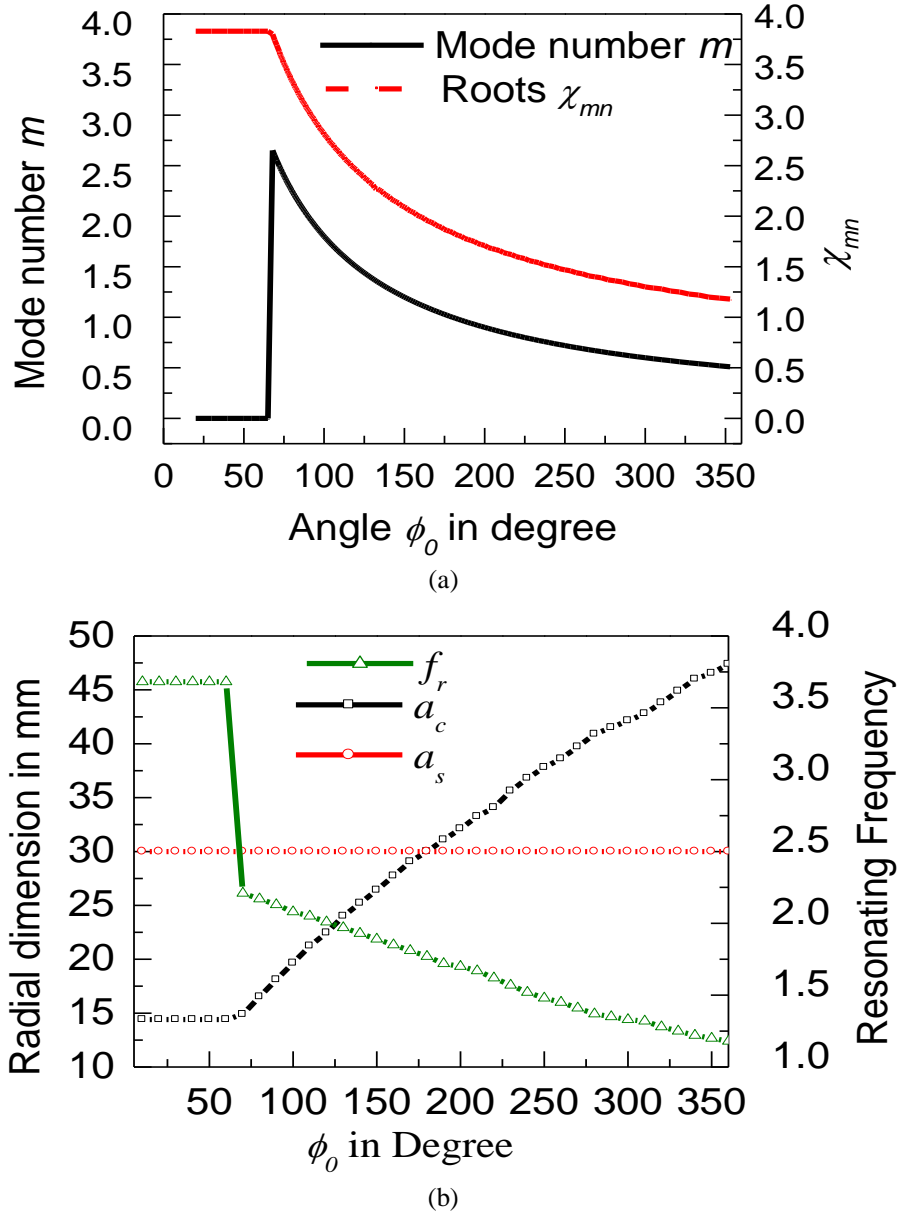
Fig. 4.2 (a) Possible mode number m and χ'_{mn} values for all possible sector angles of CSMA, (b) The resonant frequency of the CSMA ($a_s = 30$ mm) with different sector angles ϕ_0 and the corresponding radial dimension a_c for CCMA.

Also, the lowest χ'_{mn} value is responsible to excite the dominant mode frequency of CSMA. Therefore, mode number m is very crucial to determine the operating frequency of CSMA. The possible mode numbers m and the corresponding χ'_{mn} values are depicted in Fig. 4.2 (a) for the CSMA of any sector angle ϕ_0. In this figure, the proper dominant mode and its resonant Frequency may be obtained with the help of equation (4.3). From the Fig. 4.2 (a), it is observed that up to sector angle

$\phi_0 = 68^0$, the mode number m is independent of CSMA sector angle (ϕ_0) and it is zero.

Therefore, χ'_{mn} and the resonant frequency, are same for all sector angles from $\phi_0 \to 0^0$ to $\phi_0 \to 68^0$. In this range of sector angles, the radial dimension a_s is the main determining factor for the resonant frequency of CSMA at it's dominant TM_{01} mode. It also revels from the figure that any sector angle, beyond $\phi_0 = 68^0$, mode number (m) decreases and χ'_{mn} decreases. Therefore, resonant frequency shifts from one sector angle to another and may be determined from the modal chart (Fig. 4.2 (a)).

4.2.2   Selection of Sector Angle ϕ_0 in View of Miniaturization

The vital requirement of miniaturization comes in relation to the low frequency operations. Therefore, to excite the frequency below 5 GHz, the required patch dimensions in case of conventional CMA is large enough. Therefore, to excite lower frequency, the radial dimension of CSMA is chosen as $a_s = 30$ mm on standard PTFE substrate of permittivity $\varepsilon_r = 2.33$ and thickness $h = 1.575$ mm.

In order to excite same resonant frequency f_{rs} in CSMA (radial dimension a_s) and f_{rc} in CMA (radial dimension a_c),

$$f_{rs} = \frac{\chi'_{mn}c}{2\pi a_s \sqrt{\varepsilon_r}} = \frac{1.84c}{2\pi a_c \sqrt{\varepsilon_r}} = f_{rc} \Rightarrow a_c = \left(\frac{1.84}{\chi'_{mn}}\right) a_s \qquad (4.4)$$

equation (4.4) may be used to compare the required radial dimension of CMA and CSMA to excite a specific frequency. The resonant frequency of CSMA ($a_s = 30$ mm) of numerous sector angles ϕ_0 has been plotted in Fig. 4.2 (b). To excite the same frequency the corresponding radial dimension of circular patch (a_c) has also been given in same plot for comparison. The figure reveals that, if ϕ_0 varies from 5^0 to 359^0 in CSMA, with fixed a_s (= 30 mm) on traditional PTFE substrate, the operating frequency varies from 3.69 GHz to 1.18 GHz. It may be noted that, up to $\phi_0 = 68^0$, the operating frequency is independent of sector angle for CSMA and it always excites same mode ($m = 0$) with same frequency 3.69 GHz. Consequently, the radial dimension of CMA is fixed to 14.9 mm. Immediately after $\phi_0 > 68^0$, f_r of same CSMA suddenly decreases to 2.12 GHz and then continue to decrease up to 1.18 GHz gradually with the sector angle ϕ_0. Consequently, required radial dimension of

CMA (a_c) starts to increase from 14.9 to 47.3 mm. Fig.4.2(b) depicts that, up to 180^0, the required radial dimension of CMA is lesser than that of CSMA (i.e. $a_c < a_s$) and the situation gets reverse (i.e. $a_c > a_s$) when $\phi_0 > 180^0$.

The required areas for CCMA is denoted as A_c while the same for CSMA is A_s

$$A_c = \pi a_c^2 \tag{4.5}$$

$$A_s = \phi_0 \left. a_s^2 \middle/ 2 \right. = 0.15\phi_0 \left(\chi'_{mn} \right)^2 a_c^2 \tag{4.6}$$
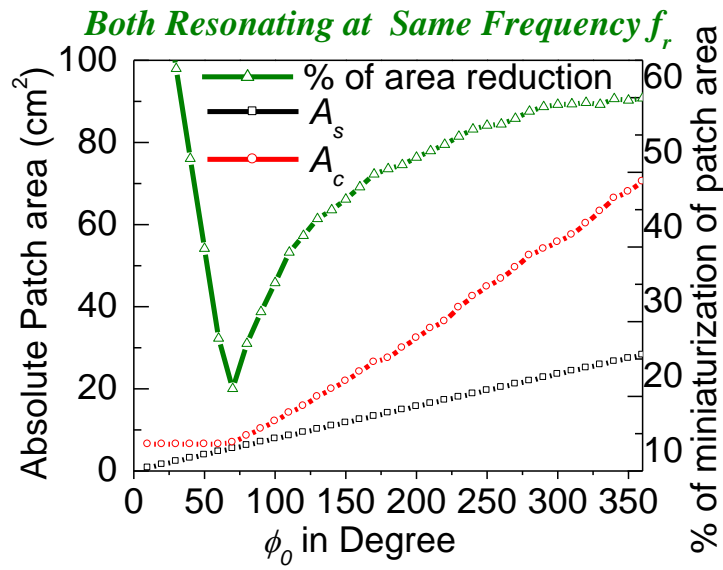
Fig. 4.3 Comparison of absolute patch area of CSMA and equivalent CCMA (both resonating at the same frequency) and the percentage of patch area reduction of CSMA in comparison to equivalent CCMA.

Therefore, the CSMA area is dependent on the sector angle ϕ_0, χ'_{mn} and obviously on mode number m. However, the rigorous investigation of χ'_{mn} values show that the smaller value of a_c than a_s (for $\phi_0 < 180^0$) does not help much in the reduction of patch radiating area (due to much smaller ϕ_0 value in respective CSMA) and as a result, the CMA radiating area is still greater than CSMA with specific ϕ_0 and obeys $A_c > A_s$.

The absolute patch radiating area for CMA and CSMA for above case is presented in Fig. 4.3. It shows that, the patch area is always greater for CMA in comparison to CSMA. The % area reduction of CSMA in comparison to CMA is also depicted in Fig. 4.3. It confirms that, the area of CSMA is always smaller than CMA except $\phi_0 = 68^0$. Therefore, 68^0 CSMA offers no apparent advantage over

90

CMA as both the radiators have similar radiating area. Notably, as $\phi_0 \neq 68^0$, the required patch area of CSMA become smaller than CMA. Although, the percent (%) area reduction of CSMA with very small ϕ_0 is high (around 65%) still, such small sector antenna may exhibit very poor radiation efficiency and hence avoidable to use in place of CMA.

Again, it is apparent that if $\phi_0 > 180^0$, patch area reduction is around 55-60%. However, for $\phi_0 > 180^0$, the physical geometry of CSMA becomes much border and it is difficult to keep associated circuitry beside the antenna structure in tiny electronic devices. Therefore, it is preferred to use CSMA with ϕ_0 either 180^0 or slightly lesser than 180^0 as it has equivalent radial dimension of CMA but with a patch are reduction of 50%. Therefore, $\phi_0 = 170^0$ CSMA has been chosen for experimental validation of radiation characteristics in the next section.

4.3   Experimental Result & Discussion

The fabricated prototypes of conventional CMA ($a_c = 29.5$ mm) and 170^0 CSMA ($a_s = 30$ mm) has been measured and compared. The detailed measured radiation parameters are presented in Table 4.1. The measured S_{11} profile for both the antennas is presented in Fig. 4.4 and it shows exactly similar performance in relation to the input impedance bandwidth. Both the antennas exhibit around 2% bandwidth and are resonation at 1.86 GHz (CMA) and 1.87 GHz (CSMA).

TABLE 4.1 Measured performance comparison of 170^0 CSMA and equivalent CCMA

Antenna Type	% Impedance bandwidth	Pattern Profile	Gain (dBi)	Beam Width (degree)		Efficiency (%)
				E plane	H plane	
Conventional CMA	2%	Broadside	5.27	82	84	88%
170^0 Sector CSMA	1.8%	Broadside	5.7	74	90	92%

Comparison of Fig. 4.5 and Fig. 4.6 revels the similarity in broadside side patterns at E plane for 170^0 CSMA and conventional CMA. The similar observation has been depicted in Fig. 4.5 and Fig. 4.6 for H plane. In both the cases, simulation results closely agree with the measured results
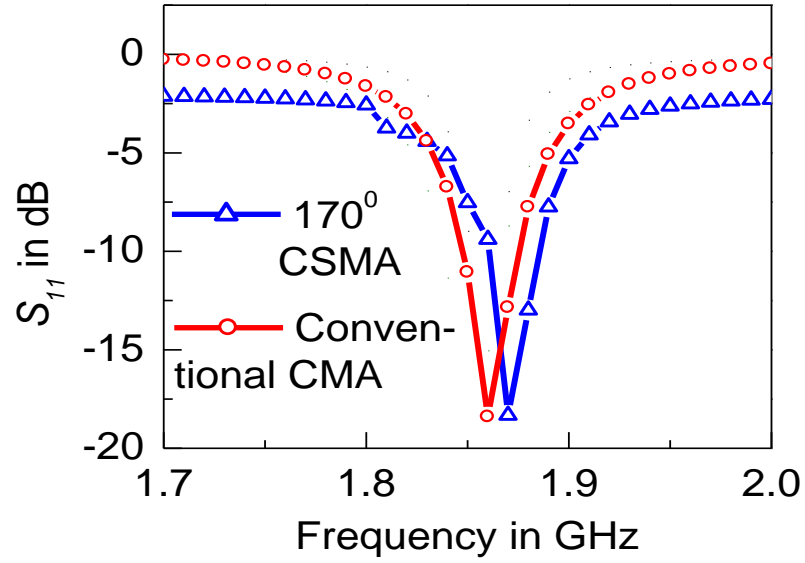
Fig. 4.4 The measured S_{11} profile of 170^0 CSMA is compare with CMA.

It seems that, the gains, patterns and beam widths of both the antennas are similar. It has seen that co-pole radiation pattern in both the plane is broadside. Therefore, judicious choice of CSMA parameters is very crucial and it is seen that, such 170^0 CSMA is well-competent to replace classical CMA. The simulated and measured co-pole radiation characteristics for both principal planes are depicted in Fig. 4.5 and Fig. 4.6.

(a)

(b)
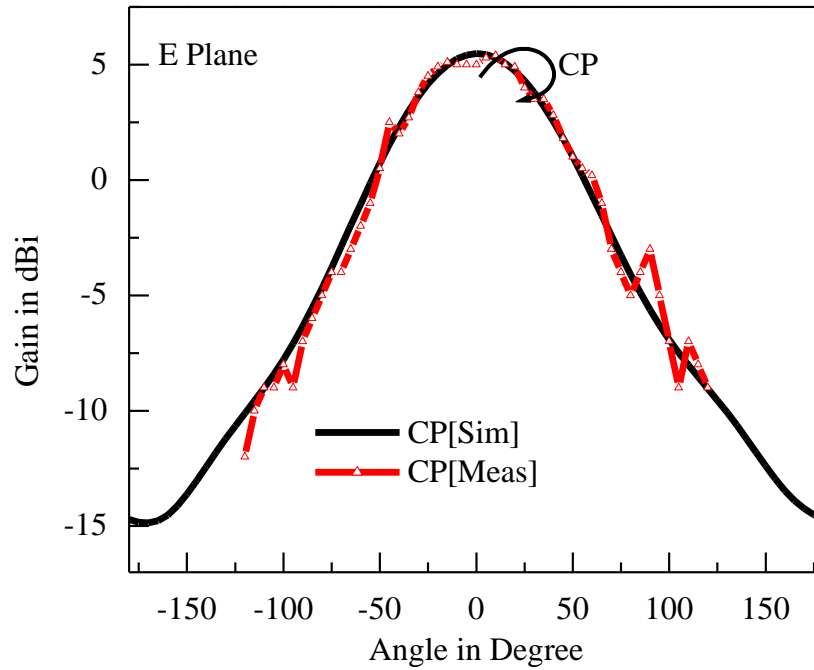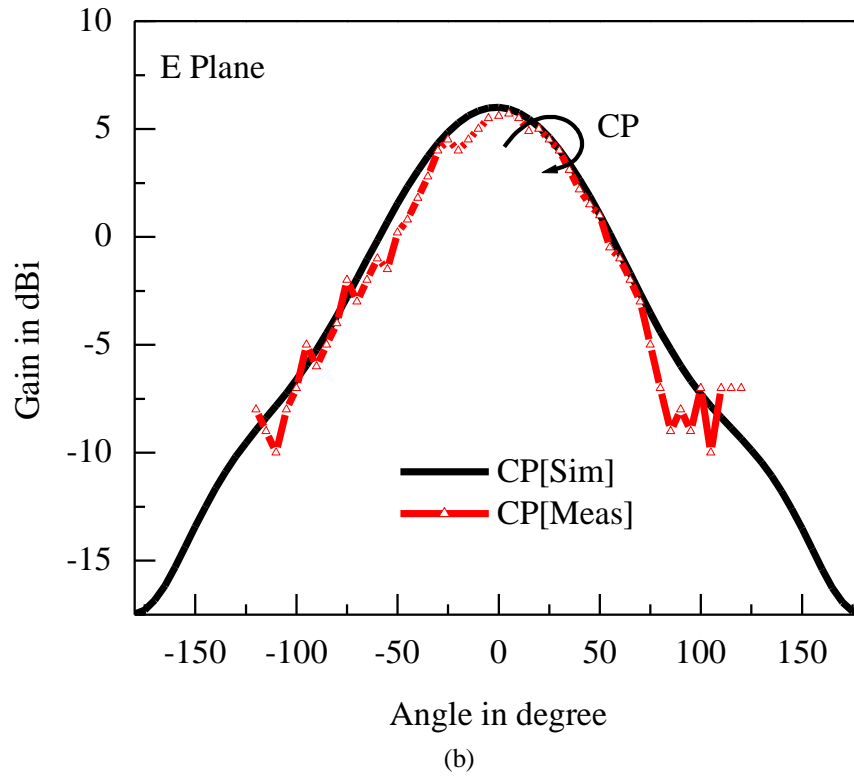
Fig. 4.5 The simulated and measured radiation of CP in (a) E plane CMA, (b) E plane CSMA.

(a)

(b)
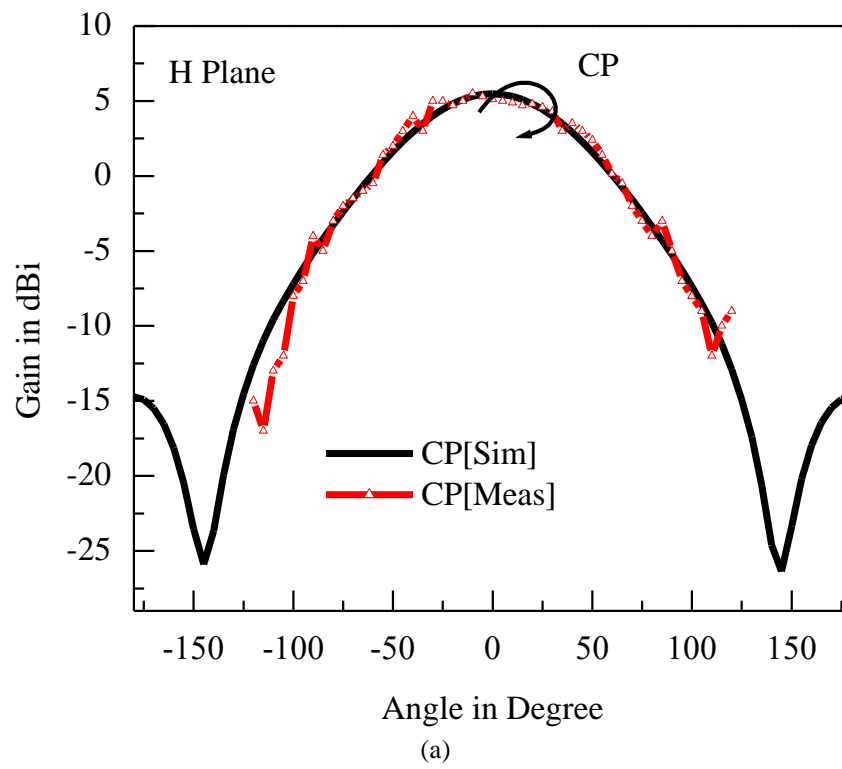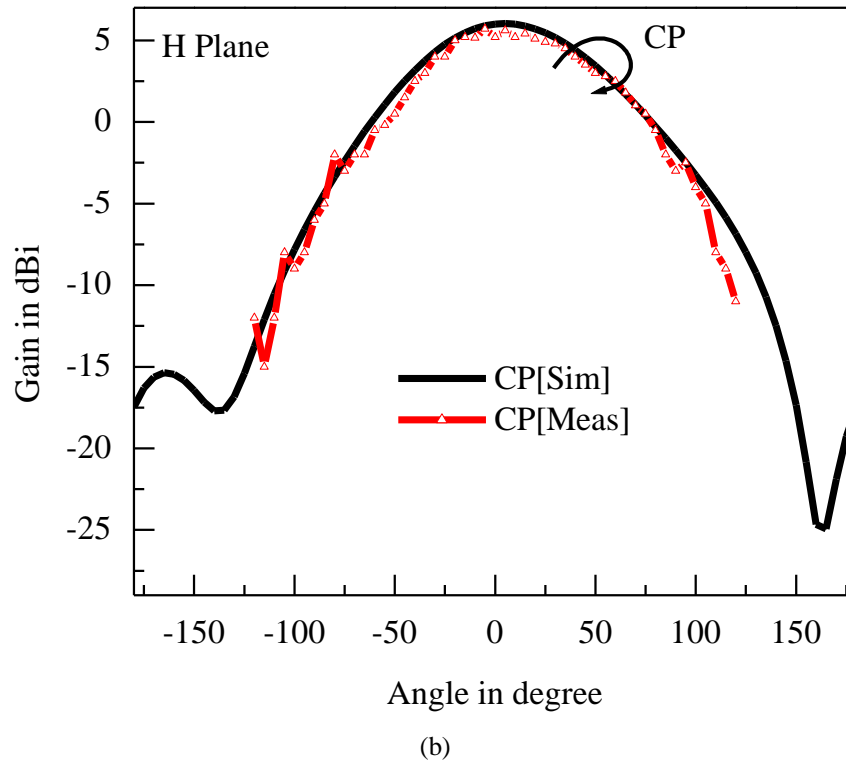
Fig. 4.6 The simulated and measured radiation of CP in (a) H plane CMA, (b) H plane CSMA.

4.4   Conclusion

The present study provides complete design guidelines without which it is really complicated to design an efficient CSMA for practical wireless applications. It is shown that, the judicious choice of sector angle is around 170^0 to 180^0 to miniaturization as well as better radiation performance. Further, efficient design of CSMA can offer better performance in comparison to classical circular patch and hence, relatively larger patch may be replaced with such CSMA.

References

[1]   R. B. Waterhouse, "Improving the Efficiency of Microstrip Patch Antennas. In: Microstrip Patch Antennas: A Designer's Guide," *Springer*, Boston, MA. 2003.

[2]   FCC White paper, www.fcc.gov/wireless/bureau-divisions/broadband-division/point-point-microwave.

[3]   Advanced Antenna Systems for 5G, 5G Americas (White paper).

[4]   A. Deshmukh, A. R. Jain, A. A. Joshi, T. A. Tirodkar, and K. P. Ray, "Broadband Proximity Fed Modified Circular Microstrip Antenna," *Proc.*

of Advances in Computing and Communications (ICACC), pp. 404-407, 2013.

[5] A. Deshmukh and N. V. Phatak, "Broadband Sectoral Microstrip Antennas," *IEEE Antennas Wireless Propagation Letter*, vol. 14, pp. 727-730, 2015.

[6] W. J. Lu, Q. Li, S. G. Wang, and L. Zhu, "Design approach to a Novel Dual Mode Wide Band Circular Sector Patch Antenna," *IEEE Transactions on Antennas and Propagations* , vol. 65, no. 10, pp. 4980-4990, 2017.

[7] W. H. Hsu and K. L. Wong, "Circularly-polarised disk-sector microstrip antenna," *Electron Letter*, vol. 34, pp.2188-2190, 1998.

[8] G. K. Oğuz and Ş. T. İmeci, "A compact size circular sector patch antenna for Ku-band applications," *International Applied Computational Electromagnetics Society Symposium- Italy (ACES)*, pp. 1-2, 2017.

[9] S. Yan and G. A. E. Vandenbosch, "Meta-Loaded Circular Sector Patch Antenna," *Progress In Electromagnetics Research*, vol. 156, pp. 37-46, 2016.

CHAPTER

5

A New Design Approach to Minimize the Cross Polarization of Circular Sector Microstrip Antenna

5.1 Introduction

The input characteristics of wide variety of sector angles of circular sector microstrip antenna (CSMA) and its comprehensive design guideline have been discussed in the earlier chapters. As per the discussions of chapter 4, CSMAs with 170^0 to 180^0 sector angle is the obvious choice in view of miniaturization of microstrip antenna. Further, to keep the associated circuitry beside the antenna, CSMAs with such sector angles are very much beneficial for antenna community looking for miniaturized antenna. 170^0 sector angle has been experimentally investigated in previous chapter. However, designing such 170^0 CSMA is still complex in comparison to 180^0 CSMA. 180^0 CSMA is also good in terms of miniaturization as is documented in chapter 4. Thus, in this chapter, 180^0 CSMA has been considered for through investigation with a view to germinate a specific CSMA as the replacement of circular microstrip antenna (CMA).

The semicircular patch (180^0) is very advantageous where the space is the key factor to organize a patch with conventional geometry. In fact, 50% of patch area reduction can be achieved using semicircular patch for a particular resonant frequency compared to conventional CMA. Hence, the accurate determination of mode as well as its radiation performance of a semicircular patch is very important in this scenario. The dominant mode of semicircular patch, its frequency and its radiation characteristic at its lowest order dominant mode have been investigated as thoroughly. The mathematical derivations to determine the accurate dominant mode

frequency are based on modified cavity model along with the accurate estimation of the fringing electric fields and resulting effective antenna dimension as is discussed in chapter 2.

The semicircular CSMA as an alternative of CMA has been presented in section 5.2. The radiation characteristic of 180^0 CSMA has been discussed in section 5.3. A new design approach has been proposed towards compact 180^0 circular sector microstrip antenna with low cross polarization in section 5.4. Evolution analysis of the proposed antenna has been presented in section 5.5. Proposed structure has been described in section 5.6. In section 5.7, the proposed design has been validated by simulation and experimental results. Section 5.8 contains the conclusions developed from the findings of the present work.

5.2　Semicircular CSMA as an alternative of CMA

A coaxially fed CSMA having radial dimension a, printed on a PTFE substrate (ε_r) with thickness h_1 is shown in Fig. 5.1 The antenna is fed at ρ_c from centre as shown in the figure using a coaxial probe.
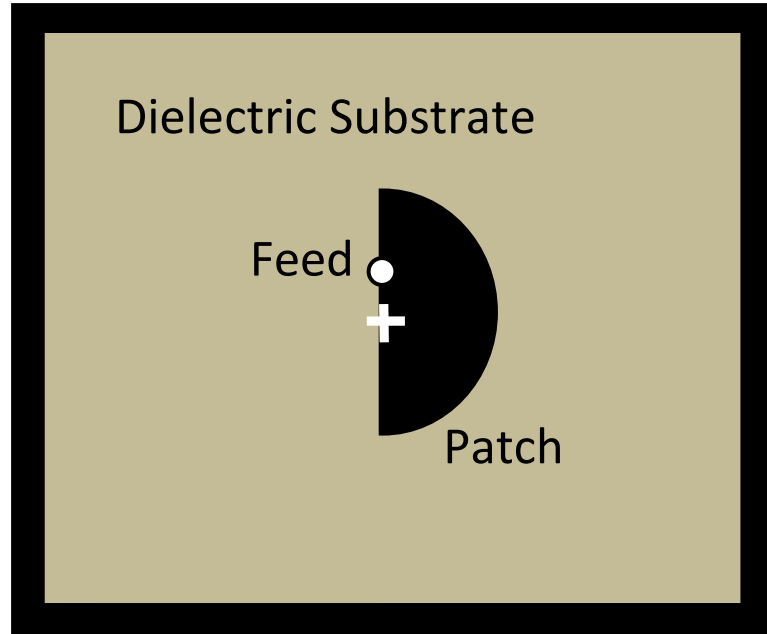
Fig. 5.1 Schematic representation of semicircular patch (Top View).

From the modal chart of chapter 4, it is found that for semicircular patch the dominant mode is TM_{mn} where $m = n = 1$. Therefore, the semicircular patch is having the same lowest order dominant mode (*i.e.* TM_{11}) like conventional circular patch.
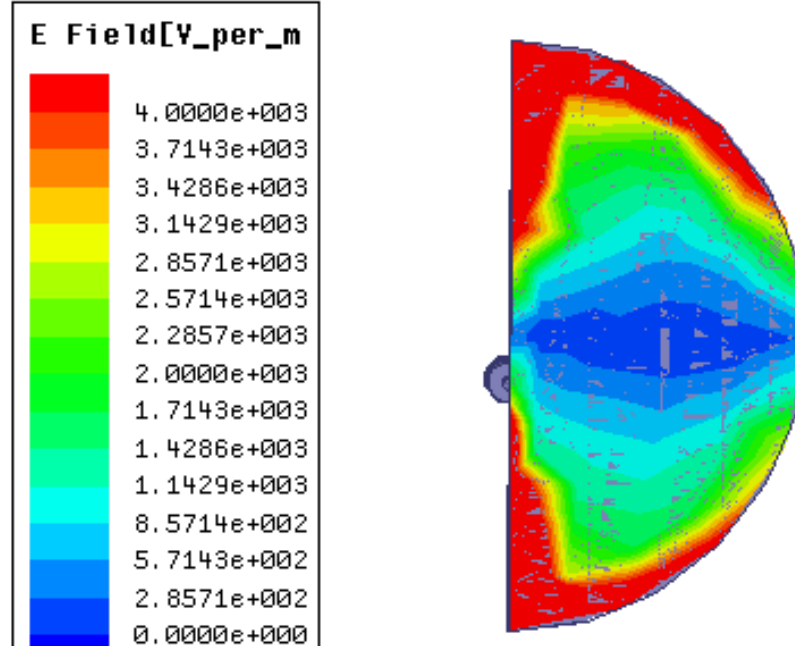
Fig. 5.2 Magnitude of electric field on patch surface to explain the number of field variation in radial and circumferential direction.

Thus, it is interesting to note that, though the geometry of the patch is different, dominant mode is similar for circular and semicircular patch. Therefore, for a particular operating frequency, one need not design the circular patch. Instead, a semicircular patch with 50% reduced patch area can be designed.

The magnitude of electric field over the patch is presented in Fig. 5.2. It is clear from the figure that, the number of field variation either in circumferential or in radial direction is 1. This confirms that the lowest order mode of semicircular patch is same as circular patch and it is TM_{11}.

5.3   Radiation characteristics of 180^0 CSMA

At first, the fundamental radiation characteristics of 180^0 CSMA has been studied. The radiation characteristics of corresponding CMA has also been investigated for comparison. The co-polar (CP) and cross polar (XP) radiation characteristics of both the CSMA (180^0) and equivalent CMA is portrayed in Fig.5.3. Both the antennas produce similar CP radiation beam at its broadside direction. It has been found from Fig. 5.3 that the gain of both the patches is around 6.4 dBi. However, there is significant degradation of XP radiation performance for 180^0 CSMA, in comparison

98

to equivalent CMA. Specifically, the profile of XP radiation beam is broadside in case of 180^0 CSMA while the same for conventional equivalent CMA is conical.
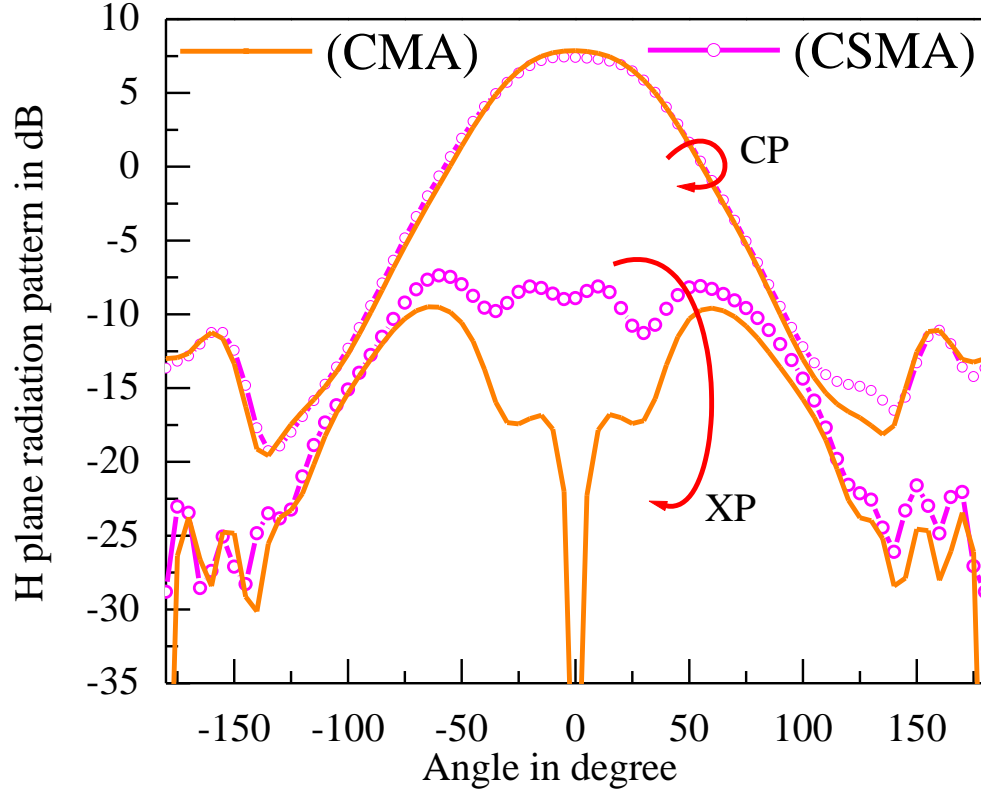
Fig. 5.3 The comparison between radiation properties of circular and semicircular patch in H planes.

It may be noted that, the conical XP profile is very much required than broadside XP profile for patch antennas. This is because, the conical XP profile doesn't have significant radiation of cross field at bore sight where main CP-beam maxima exists. Contrarily, the broadside XP profile produce significant cross field radiation at the bore sight and have the main CP beam gets affected. Therefore, the main challenge of the present investigation is to shape the XP beam profile of 180^0 CSMA from broadside to conical. The isolation between peak CP and peak XP gain is noted as cross polarization discrimination (XPD). The XPD of 180^0 CSMA at the bore sight direction is around 16 dB while the same for equivalent conventional CMA is around 23 dB. Therefore, the XPD is not at all satisfactory for 180^0 CSMA in comparison to conventional CMA.

Therefore, moderate radiation performance is revealed for semicircular patch compared to that of circular patch. Therefore, it is concluded that a patch of semicircular geometry with 50% reduced patch area may be an alternative to a patch

of conventional circular geometry. But polarisation purity of this sectoral antenna has to be high to make it as an efficient compact antenna.

In the next session a new design approach has been documented towards compact 180^0 circular sectormicrostrip antenna with low cross polarization.

5.4 Design Approach Towards Cross Pole Miniaturization by Defected Patch Surface (DPS).

Circular sector microstrip antenna (CSMA) with relatively smaller sector angle ($\phi_0 = 180^0$) is an excellent preference over circular microstrip antenna (CMA) [1]-[4]. Earlier, rectangular microstrip antenna (RMA) and CMA were widely investigated for patch area miniaturization in [5]-[15]. However, such miniaturized antennas suffer from very poor gain [11], bandwidth [9]-[11], and high cross-polar (XP) radiations [9]-[12], squinted E-plane dipole like profile and omnidirectional H-plane profile [13]. CSMA with very large sector angles i.e.$\phi_0 \sim 270^0, 340^0$ and350^0 have been investigated in [16]-[18] for broad banding or multi banding without any improvement in radiation performance or miniaturization. Further, [19] shows that 180^0 CSMA offers poor co-polar (CO) to cross polar radiation (XP) isolation (XPD) (around 8 dB) at the X band with a broadside XP pattern instead of a conical XP pattern which affects the main CO profile. Therefore, it is undeniably challenging to modulate the XP profile of 180^0 CSMA with improved XPD along with achieving miniaturization. It is well-known that linearly polarized CMA and RMA exhibit high XP radiations [1],[4], [20]-[27]. However, common XP radiation minimization techniques for instance, use of modified feed structures, defected ground structures (DGSs), and shorted patch and pins (SP); have not been investigated till date for minimizing XP radiations in CSMA with small sector angle ($\phi_0 \rightarrow 180^0$). Notably, a CSMA with sector angle $\phi_0 = 180^0$ has a thought-provoking feature of exciting similar dominant mode and resonant frequency in comparison with that of a conventional CMA with around 50% patch area reduction. Also, the ground plane dimension becomes a parameter of vital relevance to designing of miniaturized antenna [28].

100

(a)

(b)

Fig. 5.4 (a) Schematic representation of proposed antenna (top view), (b) fabricated prototypes over large and smaller ground planes.

Most of earlier reported structures could not show their efficacy as small antenna by circumscribing the patch radiator (including ground plane) within a sphere of radius ($\lambda/2\pi$) i.e., Wheeler limit. Therefore, a compact CSMA (with $\phi_0 = 180^0$) structure has been proposed, (Fig. 5.4) with improved radiation characteristics, low XP radiation along with miniaturization. Further, the proposed structure exhibits satisfactory performance on very small ground plane also.

5.5 Evolution analysis of the proposed antenna

First, a CMA with radius a was designed over the substrate (ε_r =2.33, thickness h =1.575 mm) at X band that acts as a reference CMA (Antenna#1) (Fig. 5.5 (a)). In step 2, the left half of the patch surface was removed which gave birth to a CSMA with $\phi_0=180^0$ (Antenna#2) as shown in Fig. 5.5(b).
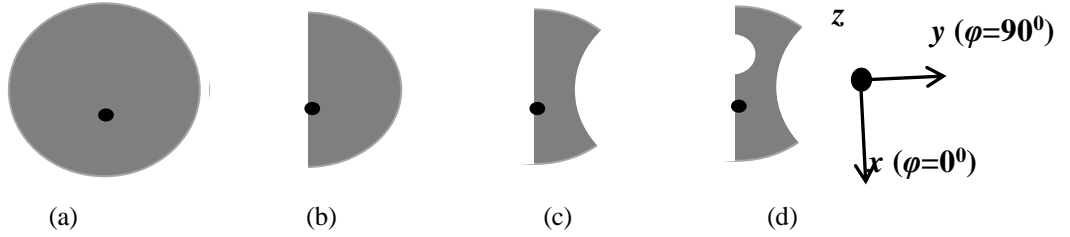
Fig. 5.5 Patch surface evolution (a) Antenna#1 (ref antenna), (b)Antenna#2, (c) Antenna#3, (d) Antenna#4 (final proposed antenna).

The parametric equation for the locus of Antenna#2 can be written as

$$x = a \cos \phi \tag{5.1}$$

$$y = a \sin \psi \tag{5.2}$$

where, $\phi \rightarrow 0$ to $\phi \rightarrow 180^0$ (ϕ_0) and $a = 6$ mm.

As observed from [2]-[3], both the antennas exhibit equivalence in modal characteristics when excited at the same dominant TM_{11} mode. Antenna#2 resonates at 8.67 GHz.

The modal electric fields beneath the patch (Antenna#2) corresponding to different modes can be written as [2], [3],

$$E_z/E_0 = \cos(m\phi)J_m(k_\rho\rho)\cos(k_z z) \tag{5.3}$$

where, k_ρ =1.84/a for TM_{11} mode (m=1) and k_ρ =3.05/a for higher order TM_{21} mode (m=2). Although, Antenna#2 may be thought of as an alternative of Antenna#1 with 50% patch area reduction (in the view of same excitation mode and frequency), there is a tendency of automatic excitation of higher order orthogonal TM_{21} mode in Antenna#2. This TM_{21} mode and the structural asymmetry in Antenna#2 cause massive degradation in XP radiation [20].
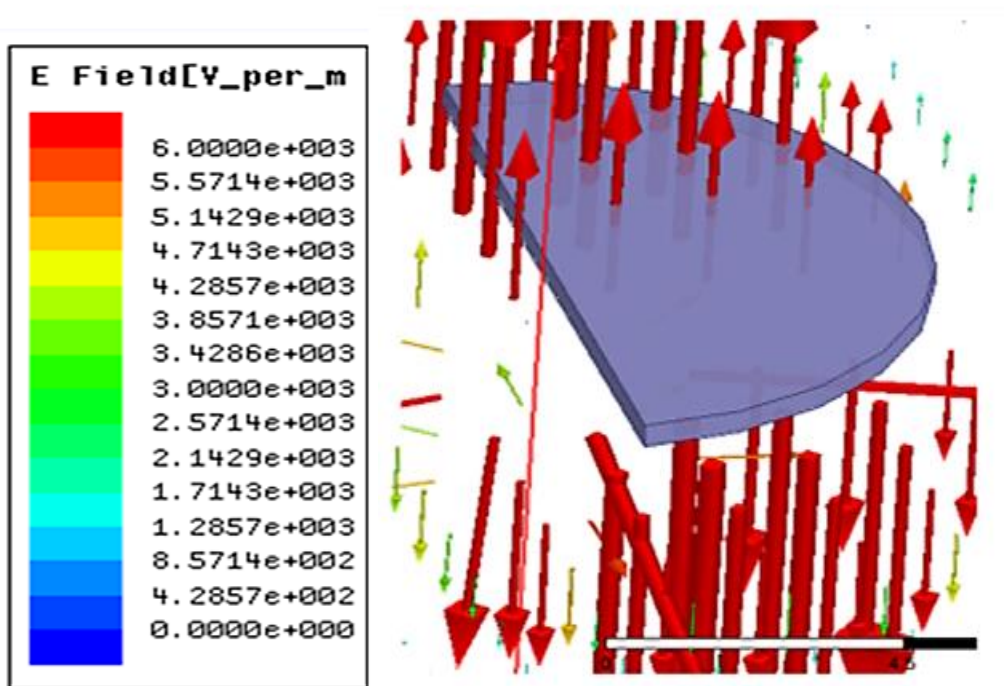
(a)
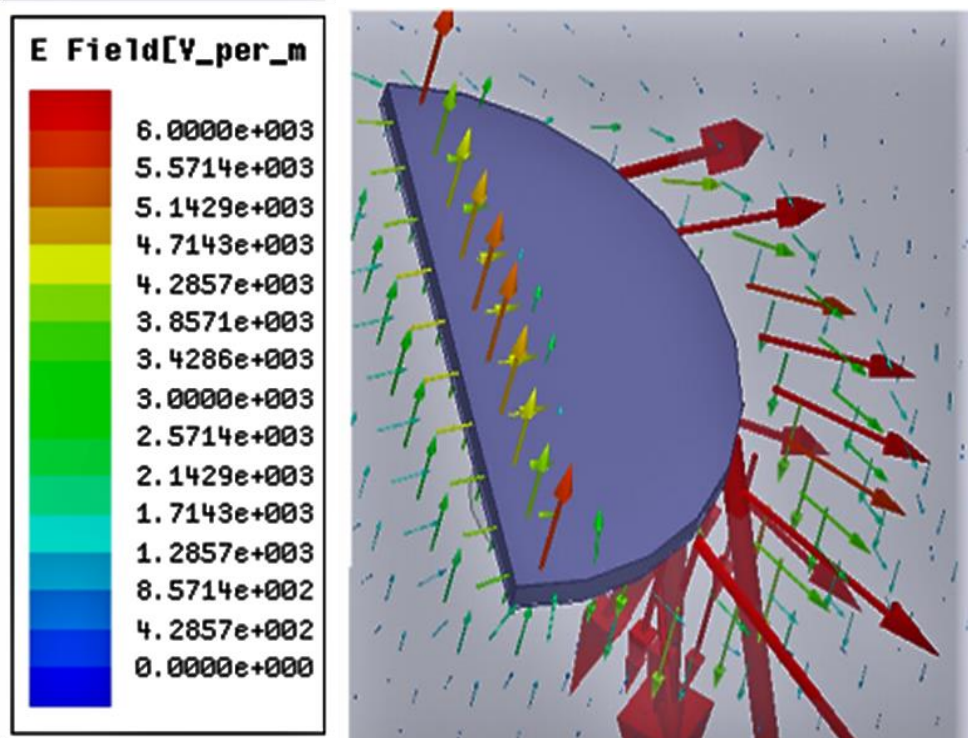
(b)
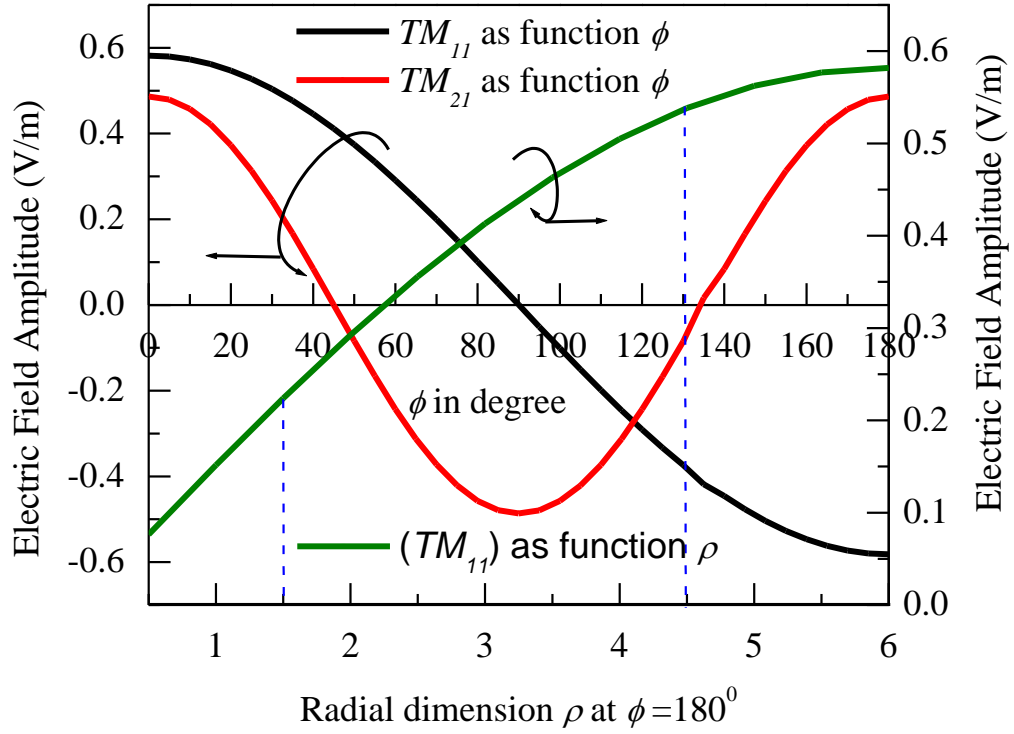
(c)

Fig. 5.6 The electric field vector distribution [29] in the substrate at (a) TM_{11} mode in Antenna#2, (b) TM_{21} mode in Antenna#2, (c) circumferential and radial variation of edge electric field magnitude for TM_{11} and TM_{21} mode.

The electric field vector distribution of TM_{11} and TM_{21} modes are depicted in Fig. 5.6 (a) and Fig. 5.6 (b) as a function of ϕ (patch circumferential angle). The E field magnitude distribution as a function of circumferential angle ϕ for TM_{11} (black) and TM_{21} (red) modes are presented in Fig. 5.6 (c). The close inspection of Fig. 5.6 (b) and Fig. 5.6 (c) proves that significant XP radiation arises due to the edge electric fields (for TM_{21} mode; Red curve) existing in the range of $\phi = 45^0$ to 138^0.

Further, in that specified range of ϕ, the fringing fields of dominant TM_{11} mode have significant cross field components which contribute to XP radiation rather than CO radiation. Therefore, with a view to perturb this TM_{21} mode significantly and TM_{11} mode partially, first notch is cut on the patch surface of Antenna#2 in the range of $\phi = 45^0$ to 138^0 which germinates Antenna#3 (Fig. 5.5 (c)). This in turn, suppresses the XP radiations from both the (i) higher order TM_{21} mode and (ii) orthogonal component of dominant TM_{11} mode.

To cut this first notch, a circle of radius $r = 6$ mm has been considered whose centre is at $(a + s)$ (centered at $x = 0$, $y = 8$ mm and $d_c = 4$ mm, $s = 2$ mm) from the

centre of the patch along 'y' axis as shown in Fig. 5.7. The locus of the circle which cuts the first notch is

$$\left. \begin{array}{l} x = r\ cos\ \psi \\ y = (a + s) + r\ sin\ \psi \end{array} \right\} \qquad (5.4)$$

where, $\psi \rightarrow 0$ to $\psi \rightarrow -180^0$

Locus of the circle which cuts the patch to develop second notch

Patch locus:
$x = a\ cos\ \psi$, $y = a\ sin\ \psi$
Where,
$\psi \rightarrow 0$ to $\psi \rightarrow 180^0$

Locus of circle which cuts the patch to develop first notch:
$x = r\ cos\ \psi$,
$y = (a + s) + r\ sin\ \psi$
Where,
$\psi \rightarrow 0$ to $\psi \rightarrow 180^0$
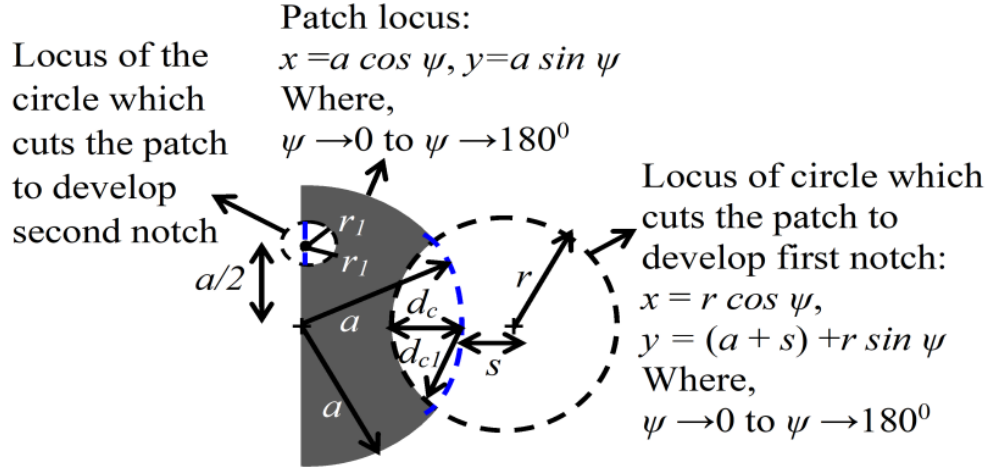
Fig. 5.7 Design topology of proposed CSMA surface

The H-plane radiation characteristics of Antenna#1, Antenna#2 and Antenna#3 have been depicted in Fig. 5.8(a) Antenna#2 exhibits broadside XP pattern with XPD of 13 dB at the bore sight whereas, the XPD in CMA (Antenna#1) is better (16 dB at $\pm 60^0$ elevation angle) with conical profile. However, with the introduction of first notch, the XPD starts to improve consistently in Antenna#3. The H-plane radiation profile of Antenna#3 has been depicted in Fig. 5.8(a) as the function of first notch depth d_c. It shows that, as r increases, d_c increases in Antenna#3 and the XPD becomes improved. The maximum XPD is 20-21 dB at $\pm 60^0$ elevation angle with d_c = 4 mm. Around 62% and 40% of improvement in XPD is exposed with Antenna#3 (d_c = 4 mm) compared to Antenna#2 and Antenna#1, respectively. The CO radiation patterns of all three antennas are exactly similar. The simulated gain for Antenna#1, Antenna#2 and Antenna#3 (d_c= 4 mm) are 7.84 dBi, 7.6 dBi and 7.35 dBi respectively.   It is observed from Fig. 5.8 (b) that, as d_c increases from 1 mm to 4 mm, the resonant frequency is decreased by 16% from 8.67 GHz (Antenna#1 and Antenna#2) to 7.43 GHz (Antenna#3 with d_c = 4 mm). Therefore, without much sacrificing it's gain performance, the miniaturization as well as improved XP
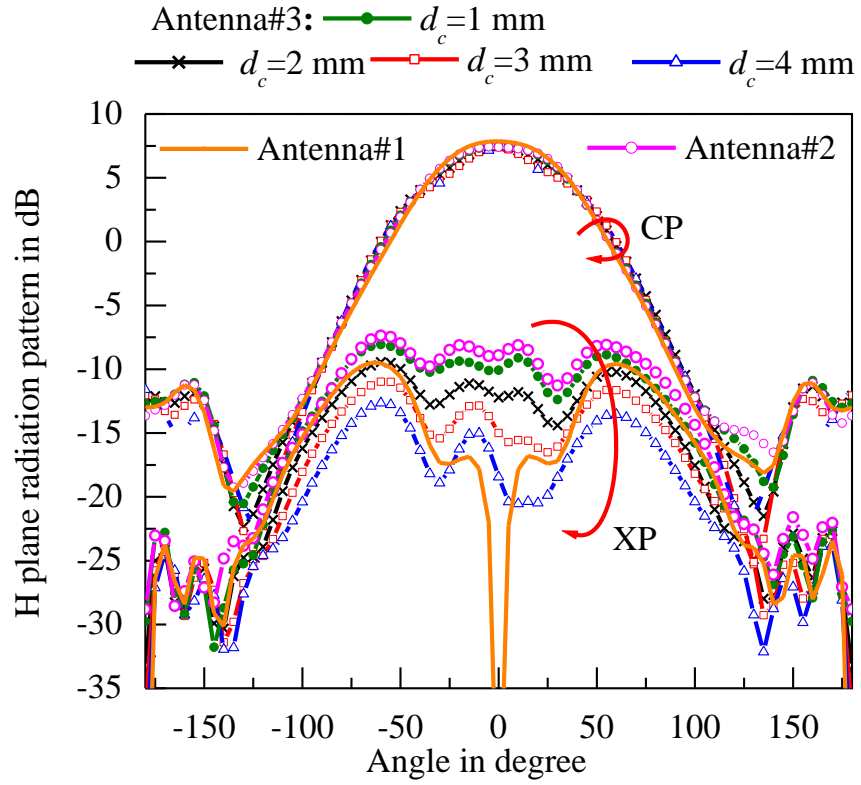
(a)
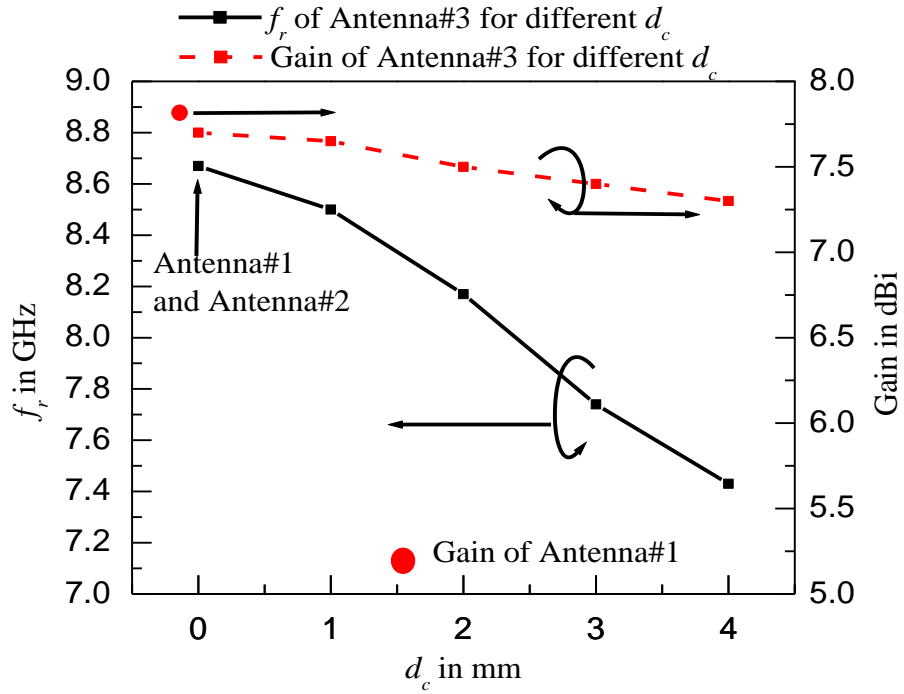
(b)

Fig. 5.8 (a) The effect of the depth d_c of first notch on simulated H plane radiation patterns of Antenna#1, Antenna#2, Antenna#3, (b) Simulated resonant frequencies and gain variation as function of d_c.

suppression can be achieved in Antenna#3. However, no apparent change is noted in E-plane CO and XP radiation and hence we refrain from giving the polarization performance in E-plane. Even though, Antenna#3 exhibits better performances in comparison to Antenna#1, Antenna#2 with respect to miniaturization and XPD, it may be noted that, the XPD at -15^0 (i.e., at bore sight and definitely within 3 dB beam width of CO main beam) is 23 dB while the same for Antenna#1 is 24 dB (Fig. 5.8 (a)). In fact, the horizontal component of the fringing field (Fig. 5.9 (a)) along the left truncated edge of Antenna#3 is mainly responsible for the increase in XP radiation near the bore sight (at -15^0). Recalling Fig. 5.6 (c), the electric field variation of TM_{11} mode along the radial dimension (Fig. 5.6 (c); green curve) reveals that, the significant amount of field i.e. (40% to 90% of maximum electric field at $\rho=a$) offering cross electric field components of own dominant TM_{11} mode exist in the range of $\rho=$ 1.5 mm to 4.5 mm in 180^0 CSMA ($a=$6 mm, along $\phi=180^0$). The electric field vector distribution in the substrate for Antenna#3 (Fig. 5.9 (a)) confirms the observation. Therefore, the second notch is cut on Antenna#3 in this specified region (i.e.,$\rho=$ 1.5 mm to 4.5 mm) to further reduce the XP radiation at bore sight direction.

(a)

(b)
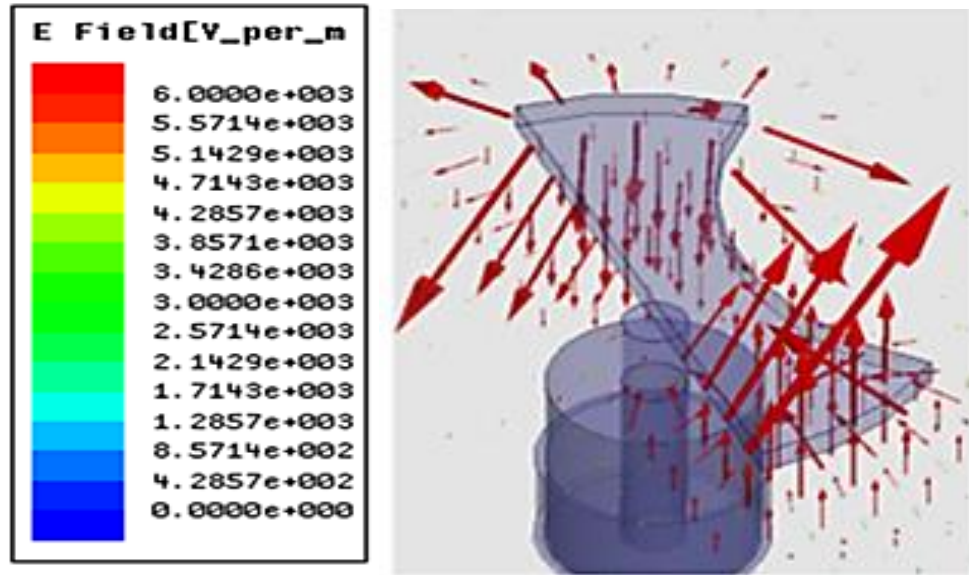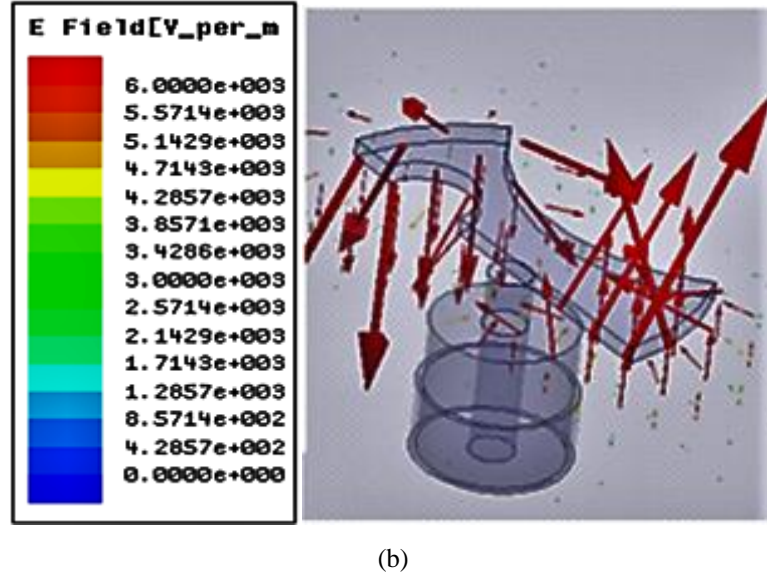
Fig. 5.9 Simulated electric field vector distribution in the substrate at excited dominant TM_{11} mode (a) Antenna#3, (b) Antenna#4 (proposed).

Notably, the second notch is cut at the upper left edge (opposite side of feed probe) of the patch in Antenna#3 to avoid the spurious radiation from feed probe. To cut this second notch, another circle of radius $r_1 = 1.5$ mm has been considered whose centre is at $-a/2$ (centered at $x = -a/2$, $y = 0$ mm) from the centre of the patch along 'x' axis as shown in Fig. 5.7. The locus of the second notch can be written as $x = a/2 + r_1 \cos\psi_1$ and $y = r_1 \sin \psi_1$ where, $\psi_1 \to 0$ to $\psi_1 \to 180^0$

Consequently, the electric field follows the curvature of the notch periphery as is shown in Fig. 5.9 (b). The close inspection of Figs. 5.9 (a) and (b) reveals that, the presence of 2nd notch converts some of the cross fields (E_y) from the left upper truncated edge of the patch to co-polar fields (E_x). This effectively reduces the orthogonal electric field component (from upper left edge of the patch) offering XP radiation near the bore sight direction. In Antenna#4, the XPD is improved significantly and it becomes 28-40 dB (Fig. 5.10 (a) and 5.10 (b)). However, CO gain and radiation profile (7.35 dBi) are exactly similar for all values of r_1. Also, as r_1 increases, the resonant frequency decreases further from 7.43 GHz (Antenna#3) to 7.22 GHz (Antenna#4). The resonant frequencies and XPD at -60^0 and -15^0 elevation angle is portrayed in Fig. 5.10 (b) establishes the superiority of the Antenna#4 (with $d_c = 4$ mm and $r_1 = 1.5$ mm) over Antenna#1, #2 and #3 in relation to the miniaturization and improvement in XPD.

108
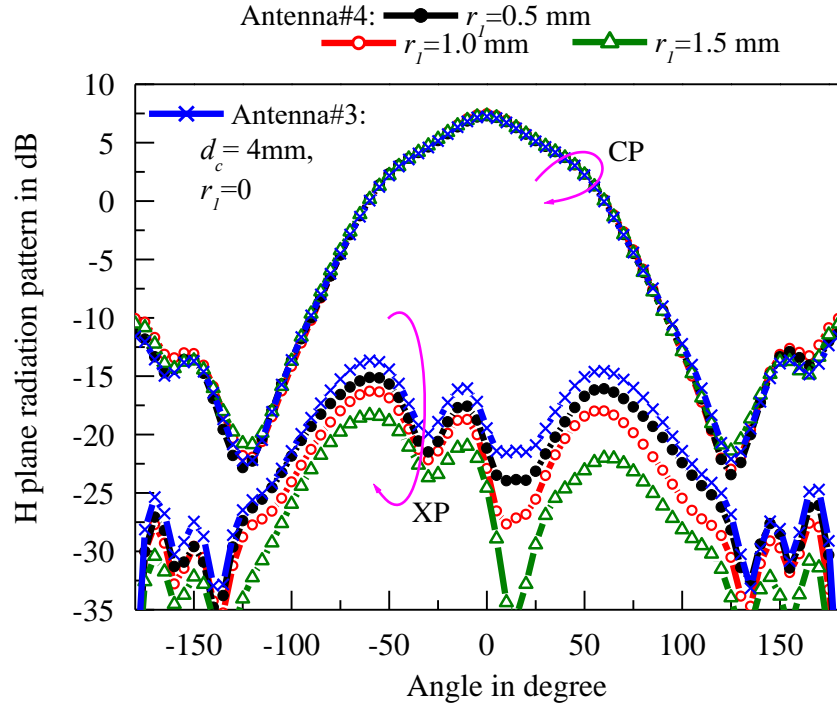
(a)
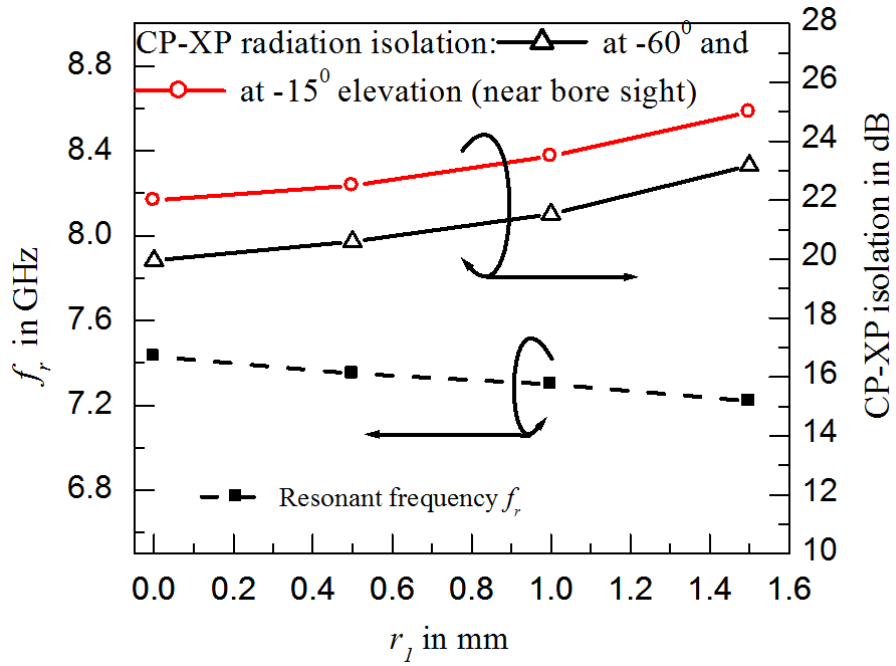
(b)

Fig. 5.10 The effect of the depth r_1 of second notch on (a) H plane radiation patterns of Antenna#3, (b) resonant frequencies and XPD as function of r_1.

It may be noted that, two notches at the patch surface effectively modulates the locus of surface current paths in such a way that, the orthogonal current component

reduces. The electric surface current on patch surface of Antenna#2 at TM_{11} mode follows the longitudinal path with a curvature (current lines are tilted; Fig. 5.11(a) and Fig. 5.11 (b) while flowing from lower to upper section of the patch. Therefore, the horizontal current components (red) due to tilted current lines (Fig. 5.11(b)) contribute in XP radiation.

(a)

Co polar field

Responsible for cross polar field
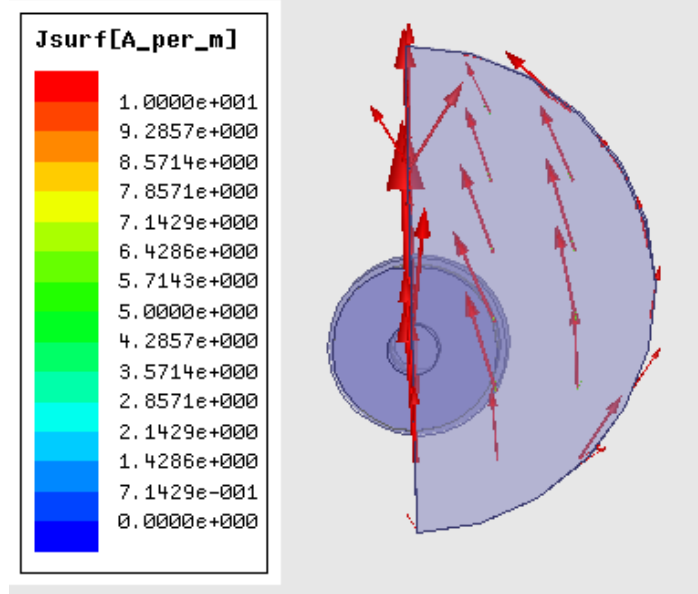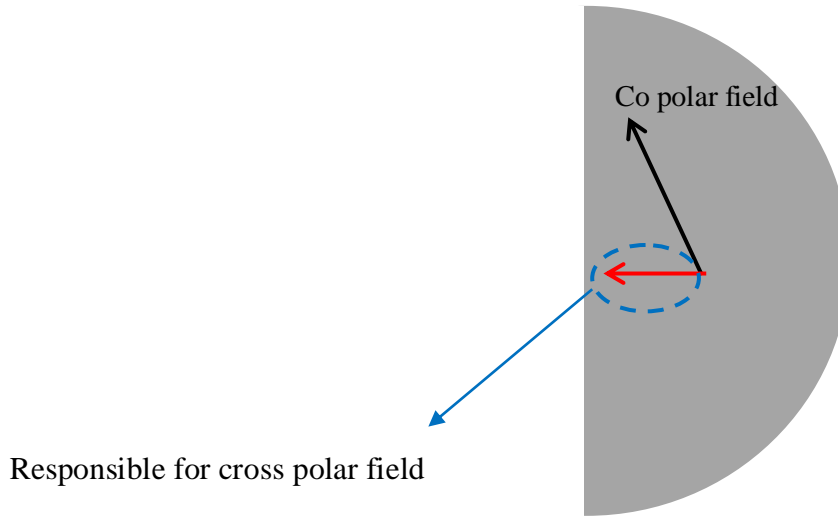
(b)

Fig. 5.11 The electric surface current over the patch surface (a) simulated (Antenna#2), (b) schematic (Antenna#2).

(a)

Co polar field

Cancels each other

Still radiates cross polar field
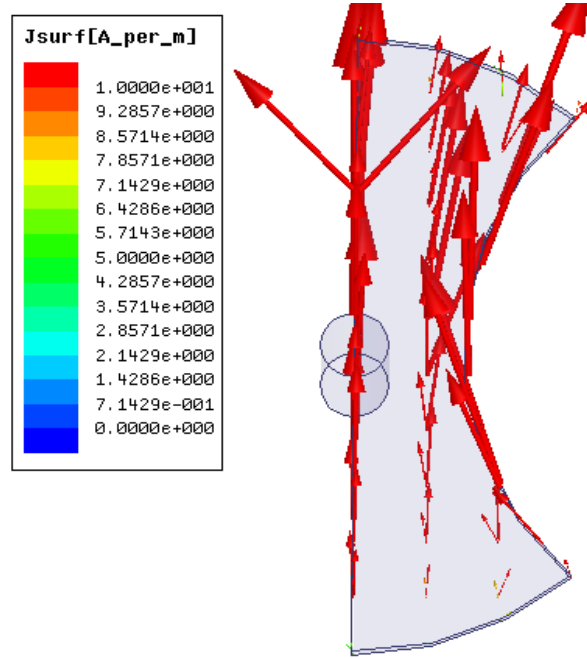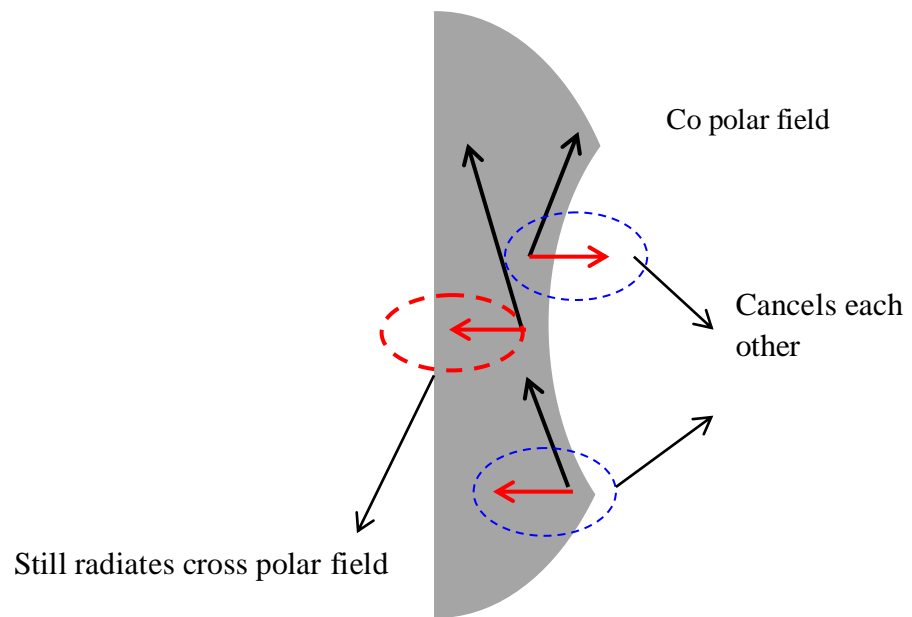
(b)

Fig. 5.12 The electric surface current over the patch surface(a) simulated (Antenna#3), (b) schematic (Antenna#3).

(a)

Cancels each other

(b)
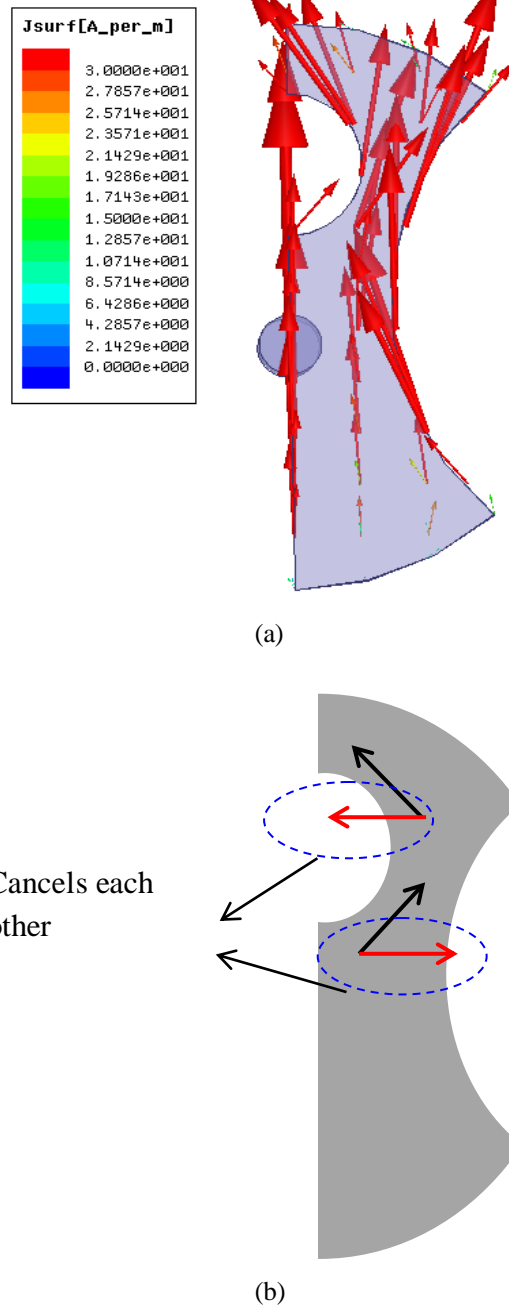
Fig. 5.13 The electric surface current over the patch surface (a) simulated (Antenna#4), (b) schematic (Antenna#4).

Contrarily, due to the presence of first notch in Antenna#3, the horizontal current components in lower and upper half sections of the patch cancel each other as is explained in Fig. 5.12 (a) and Fig. 5.12 (b). Therefore, the effects of horizontal current component near patch periphery can be controlled to reduce the XP radiation and also to achieve nearly conical pattern instead of broadside. Notably, some electric surface currents near the central region of the patch still exist that leaves

some horizontal current component. Hence, in Antenna#4, a second small notch is cut at the upper side of the patch along $\phi = 180^0$ as shown in Fig. 5.13. This effectively reduces the horizontal electric current components more on the patch surface of Antenna#4, as is explained in Fig. 5.13 (a) and Fig. 5.11 (b).

5.6   Proposed Structure

First, a semicircular CSMA (with $\phi_0 = 180^0$) having radius $a = 6$ mm has been fabricated with copper strip (0.5 mm thickness) on RT-5870 ($\varepsilon_r = 2.33$ and thickness $h = 1.575$ mm) substrate. First, the dimensions of substrate and ground plane are chosen to be 60 mm $\times$ 60 mm ($\sim 1.4\lambda_0 \times 1.4\lambda_0$). First notch is cut on the patch with $d_c = 4$mm (i.e.$r = 6$ mm, $s = 2$ mm) (Fig. 5.7). The second notch is cut on the patch at the opposite side with a circular locus (centered at $a/2 = 3$ mm) of $r_1 = 1.5$ mm, as described in Fig. 5.7. The patch is fed at 0.8 mm from the centre point (Fig. 5.4). Further, the same structure is fabricated on small ground plane (28 mm $\times$ 28 mm or $\sim 0.66\lambda_0 \times 0.66\lambda_0$). Moreover, the structure has been fabricated on very small ground plane (14 mm $\times$ 14 mm or $\sim 0.33\lambda_0 \times 0.33\lambda_0$) to be considered as small antenna as this whole antenna (including ground plane) can be enclosed within a sphere where $k.R < 1$.

5.7   Results and Discussions

The reference Antenna#1 of 7 mm radius has also been fabricated on same substrate with 60 mm $\times$ 60 mm ground plane. In Fig. 5.14 (a), the measured reflection coefficient profiles for the proposed Antenna#4 and the reference CMA (Antenna#1) are presented. Both the antennas resonate near 7.22 GHz with almost similar impedance bandwidth. In the E-plane, the XPD is more than 30 dB for both Antenna#1 and Antenna#4 (Fig. 5.14 (b)). The measured CO gain of Antenna#1 and Antenna#4 are 7.4 dBi and 7.1 dBi, respectively. The Fig. 5.13 (a) reveals that the XPD of the Antenan#4 (designed over large ground plane) is around 25 dB over entire elevation angle near the bore sight in H-plane whereas; the same for Antenna#1 is only 15 dB. For further corroboration of the validity of the results for the Antenna#4, the complete radiation pattern has been examined on smaller (28 mm $\times$ 28 mm) (resonating at 7.17 GHz) and very small (14 mm $\times$ 14 mm) (resonating at

7.21 GHz) ground planes (Fig. 5.15 (b), Fig. 5.16(a)). Both the structuresreveal symmetry in E and H-plane CO radiation patterns with consistent and more than

(a)

(b)
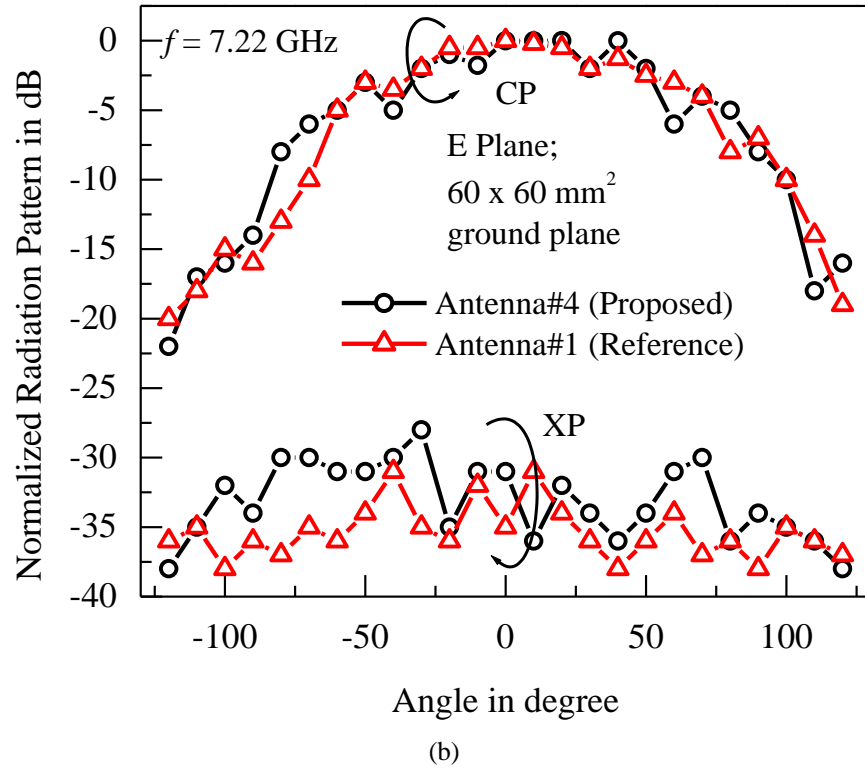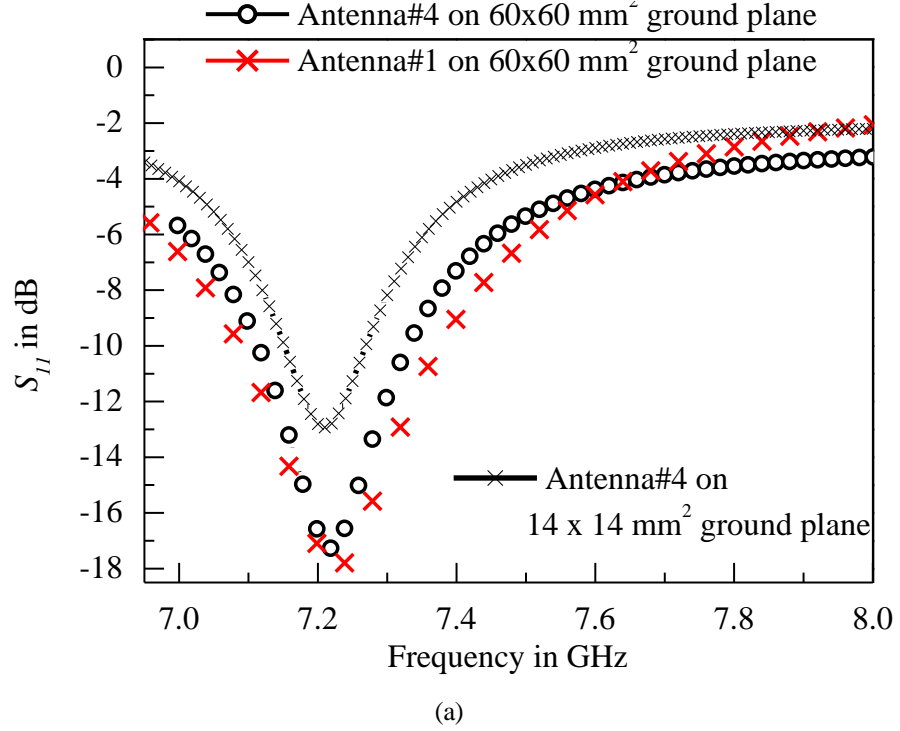
Fig. 5.14 Measured results for (a) reflection coefficient profiles, (b) comparison of E plane radiation patterns for reference CMA and proposed antenna over large (60 mm × 60 mm) ground plane.
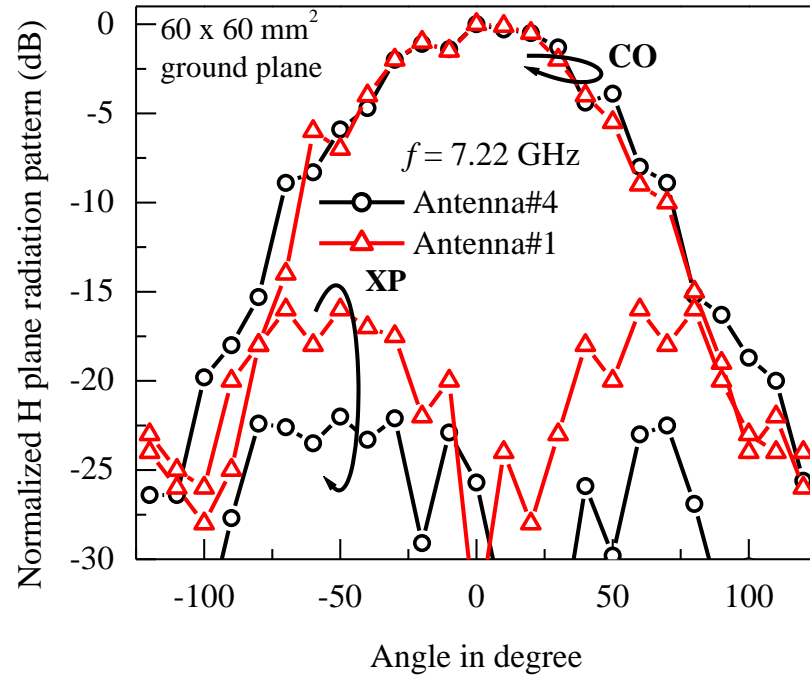
(a)
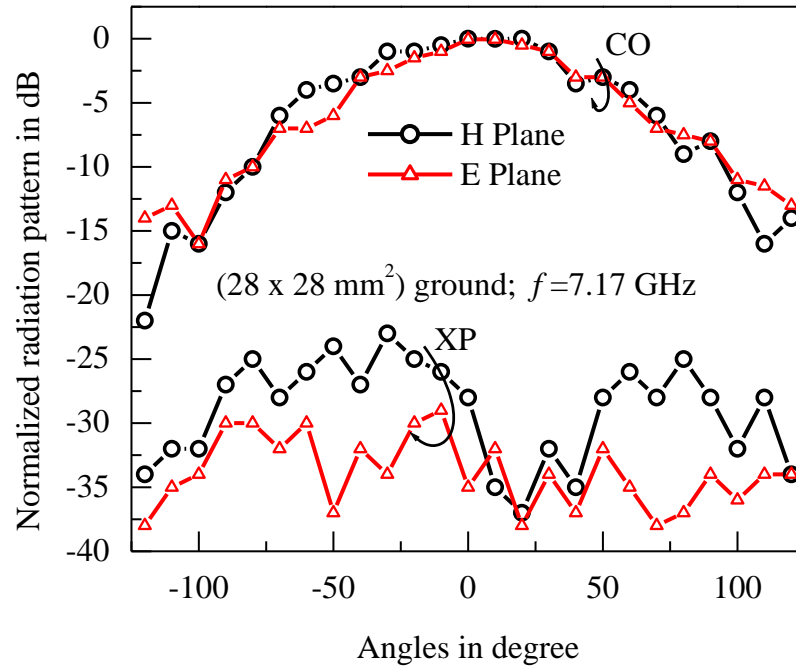
(b)

Fig. 5.15 (a) Comparison of H plane radiation patterns for reference CMA and proposed antenna over large (60 mm × 60 mm) ground plane, (b) measured E and H plane radiation patterns for proposed antenna over medium/small (28 mm × 28 mm) ground.
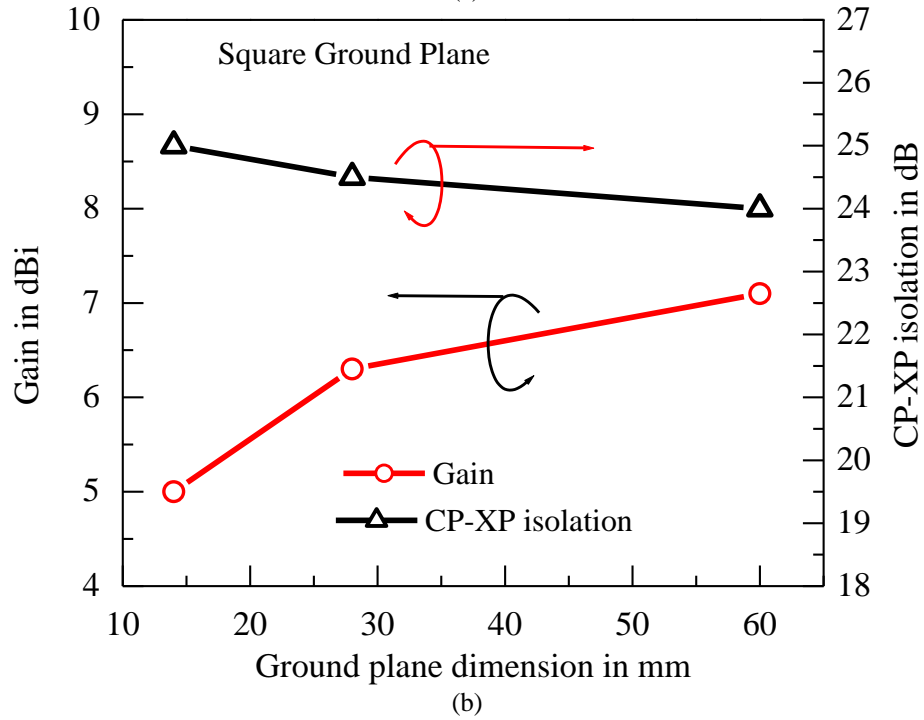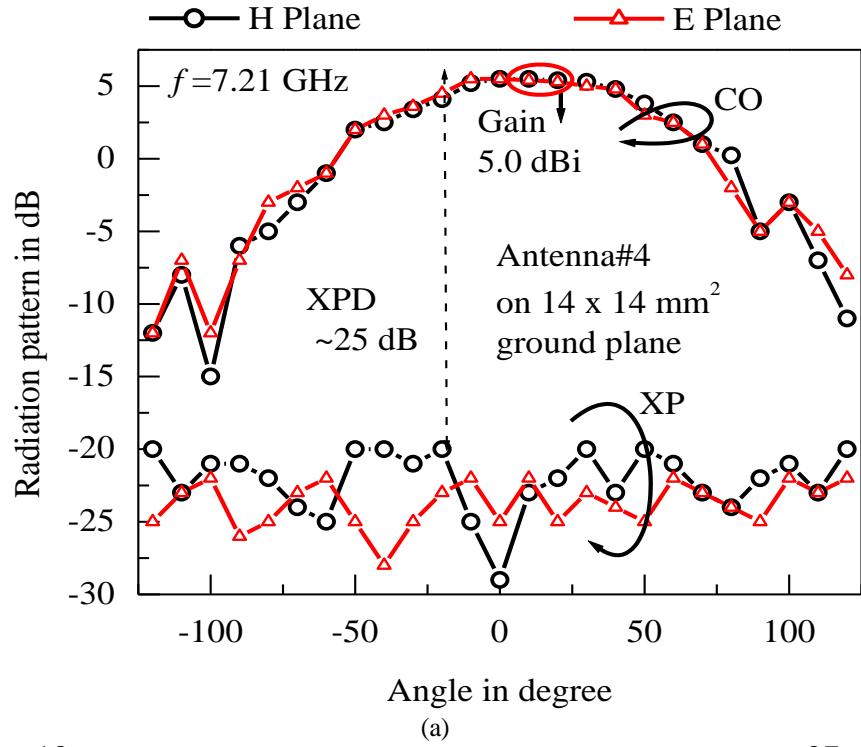
Fig. 5.16 (a) Measured E and H plane radiation patterns for proposed antenna over very small (14 mmx14 mm) ground plane, (b) variation of CO gain and XPD as a function of ground plane dimension of proposed antenna.

25 dB of XPD in H-plane with around 5 dBi gain. The measured efficiencies of the proposed antenna over large and very small ground planes are 82% and 68%, respectively.

Notably, the reference antenna (Antenna#1) with larger radius has the efficiency of 86%. The measured gain and XPD variation of the proposed antenna as function of ground plane size is depicted in Fig. 5.16 (b). As the ground plane size reduces, the gain reduces, and E plane beamwidth becomes narrow while H plane beamwidth becomes broad [30]. Therefore, smaller ground plane bringssymmetry in E and H plane radiation patterns and hence, XPD improves [30], However, gain to directivity ratio decreases and hence efficiency decreases. The performance of the Antenna#4 has been compared with the available relevant literatures in Table 5.1. This confirms the consistency and superiority of the present structure over others.

Table 5.1 Performance comparison of Antenna#4 with other works

Ref.	Gain (dBi)	Fractional bandwidth (%)	Minimum CO-XP radiation isolation (dB)	Miniaturization of patch area w. r. t reference antenna
[8]	4.4	2	17.5	74%
[10]	-	1.8	XP radiation > CO radiation	74%
[12]	6.2	4.5	Very Poor	21.12%
[11]	2.9	1.8	XP radiation > CO radiationby 14 dB	85%
[13]	4.13	3.8	15	74%
[14]	2-7	140	0	0%
Antenna#4 $(60 \times 60 \text{ mm}^2)$	7.1	4.0	24	82%
Antenna#4 $(14 \times 14 \text{ mm}^2)$	5.0	2	25	82%

5.8   Conclusion

A compact semicircular CSMA has been investigated thoroughly and is found to be a better alternative of conventional CMA. Although small, the radiation characteristic of the present antenna is even far better than the conventional CMA geometry which find potential applications. The present antenna works very well on very small ground plane and may be treated as small antenna.

References

[1]   R. Garg, P. Bhartia, I. Bahl, and A. Ittipiboon, "Microstrip Antenna Design Handbook", Artech House, Norwood, 2001.

[2]   S. K. Ghosh, A. Ghosh, S. Chakraborty, L. L. K. Singh, and S. Chattopadhyay, "The influence of feed probes on the modes of circular sector microstrip antennas: An Investigation", *IEEE Antennas and Propagation Magazine*, vol. 63, no. 4, pp. 33-42, 2021.

[3]   S. K. Ghosh, S. Chakraborty, L. L. K. Singh, and S. Chattopadhyay, "Modal Analysis of Probe-fed Circular Sector Microstrip Antenna with and without Variable Air Gap: Investigation with Modified Cavity Model," *International Journal of RF and Microwave Computer Aided Engineering*, Wiley, vol. 28, no. 1, 2018.

[4]   D.M. Pozar, D. H. Schaubert, "Microstrip Antennas: The Analysis and Design of Microstrip Antennas and Arrays," *IEEE and Wiley-Interscience*, 1995.

[5]   T. Cai, G-M. Wang, X-F. Zhang, Y-W. Wang, B-F.Zong, and H-X. Xu, "Compact Microstrip Antenna With Enhanced Bandwidth by Loading Magneto-Electro-Dielectric Planar Waveguided Metamaterials," *IEEE Transactions on Antennas and Propagation*, vol. 63, no.5, pp. 2306-2311, 2015.

[6]   J-D. Zhang, L. Zhu, Q-S. Wu, N-W. Liu, and W. Wu, "A Compact Microstrip-Fed Patch Antenna With Enhanced Bandwidth and Harmonic Suppression," *IEEE Transactions on Antennas and Propagation*, vol. 64, no.12 , pp. 5030-5037, 2016.

[7]   H. Y. Zang, H. Zhai, L. Xi, and Long Li, "A Compact Microstrip Antenna with Enhanced Bandwidth and Ultra-Wideband Harmonic Suppression," *IEEE Transactions on Antennas and Propagation*, vol. 60, no.8 , pp. 3559-3567, 2019.

[8]   M. Yang, Z. N. Chen, P. Y. Lau, X. Qing, and X. Yin, "Miniaturized Patch Antenna With Grounded Strips," *IEEE Transactions on Antennas and Propagation*, vol. 63, no. 2, pp. 843-848, 2015.

[9]   A. Motevasselian, and W. G. Whittow, "Miniaturization of a Circular Patch Microstrip Antenna Using an Arc Projection," *IEEE Antennas and WirelessPropagation Letters*, vol. 16, pp. 517-520, 2017.

[10]   N. Kuga and H. Arai,"Circular Patch Antennas Miniaturized by Shorting Posts," *Electronics and Communications in Japan*, vol. 79, no.6, pp. 51-58, 1996.

[11]   R. Waterhouse, "Small microstrip patch antenna," *Electronics Letters*, vol. 31, no. 8, pp. 604-605, 1995.

[12]   S. Lee, J. Woo, M. Ryu, and H. Shin, "Corrugated circular microstrip patch antennas for miniaturization," *Electronics Letters*, vol. 38, no. 6, pp.262-263, 2002.

[13]   S. Painam and C. Bhuma, "Miniaturizing a Microstrip Antenna Using Metamaterials and Metasurfaces [Antenna Applications Corner]," *IEEE Antennas and Propagation Magazine*, vol. 61, no. 1, pp. 91-135, 2019.

[14]   L. Guo, M. Min, W. Che, and W. Yang, "A Novel Miniaturized Planar Ultra-Wideband Antenna," *IEEE Access*, vol. 7, pp. 2769-2773, 2019.

[15]   H. Shi, J. Shi, J. Li, J. Chen, Z. Li, S. Zhu, T. Ali Khan, A. Zhang, "Miniaturized Circularly Polarized Patch Antenna Using Coupled Shorting Strip and Capacitive Probe Feed," *International Journal of Electronics and Communications,* vol. 98, pp. 235-240, 2019,

[16]   A. A. Deshmukh and N. V. Phatak, "Broadband Sectoral Microstrip Antennas," *IEEE Antennas Wireless Propagation Letter*, vol. 14, pp. 727-730, 2015.

[17]   W. J. Lu, Q. Li, S. G. Wang, and L. Zhu, "Design approach to a novel dual-mode wideband circular sector patch antenna*," IEEE Transactions on Antennas and Propagation*, vol. 65, no. 10, pp. 4980-4990, 2017.

[18]   Q. Li, W. J. Lu, S. G. Wang, and L. Zhu, "Planar quasi-isotropic magnetic dipole antenna using fractional-order circular sector cavity resonant mode," *IEEE Access*, vol. 5, pp. 8515-8525, 2017.

[19]   S. K. Ghosh, S. K. Varshney, S. Chakraborty, L. L. K. Singh, and S. Chattopadhyay, "Probe-fed semi circular microstrip antenna vis-à-vis circular microstrip antenna: a necessary revisit," *IOP Conf. Series: Materials Science and Engineering*, vol. 331, pp.1-7, 2018.

[20]   C. Kumar, D. Guha, "Asymmetric and Compact DGS Configuration for Circular Patch with Improved Radiations," *IEEE Antennas & Wireless Propagation Letters*, vol.19, no.2, pp.355-357, 2020.

[21]   A. Ghosh, D. Ghosh, S. Chattopadhyay, and L. L. K. Singh, "Rectangular microstrip antenna on slot type defected ground for reduced cross polarized radiation," *IEEE Antennas Wireless Propagation Letter*, vol. 14, pp. 321–324, 2015.

[22]   D. Ghosh, S. K. Ghosh, S. Chattopadhyay, S. Nandi, D. Chakraborty, R. Anand, R. Raj, and A. Ghosh, "Physical and quantitative analysis of compact rectangular microstrip antenna with shorted non-radiating edges for reduced cross-polarized radiation using modified cavity model," *IEEE Antennas Propagation Magazine*, vol. 56, no. 4, pp. 61–72, 2014.

[23]   C. Kumar, M. I. Pasha, and D. Guha, "Microstrip Patch With Nonproximal Symmetric Defected Ground Structure (DGS) for Improved Cross-Polarization Properties over Principal Radiation Planes," *IEEE Antennas Wireless Propagation Letter*, vol. 14, 2015.

[24] T. Sarkar, A. Ghosh, L. L. K. Singh, S. Chattopadhyay, and C-Y-D. Sim, "DGS-Integrated Air-Loaded Wideband Microstrip Antenna for X- and Ku-Band," *IEEE Antennas Wireless Propagation Letter*, vol. 19, pp. 114–118, 2020.

[25] S. Sharma, S. A. Imam, B. K. Kanujia, M.K. Khandelwal, "Bandwidth Enhancement of Multiple Notch Bands and Cross polarization Suppression of Microstrip patch Antenna for Modern Wireless Applications," *Wireless Personal communication*, vol. 98, pp. 2553-2568, 2018.

[26] S. Chattopadhyay and S. Chakraborty, "A Physical Insight Into the Influence of Dominant Mode of Rectangular Microstrip Antenna on Its Cross-Polarization Characteristics and Its Improvement With T-Shaped Microstrip Antenna," *IEEE Access*, vol. 6, pp. 3594-3602, 2018.

[27] S. Chakraborty, A. Ghosh, S. Chattopadhyay, and L. L. K. Singh, "Improved cross-polarized radiation and wide impedance bandwidth from rectangular microstrip antenna with dumbbell-shaped defected patch surface," *IEEE Antennas Wireless Propagation Letter*, vol. 15, pp. 84-88, 2016.

[28] S.R. Best, "The Significance of Ground-Plane Size and Antenna Location in Establishing the Performance of Ground-Plane-Dependent Antennas," *IEEE Antennas and Propagation Magazine*, vol. 51, no. 6, pp. 29-43, 2009.

[29] HFSS, High frequency structure simulator, Ver. 14, Ansoft Corp, USA.

[30] A. A. Kishk, and L. Shafai, "The effect of various parameters of circular microstrip antennas on their radiation efficiency and the mode excitation," *IEEE Transactions on Antennas and Propagation*, vol.34, no.8, pp. 969-976,1986.

CHAPTER

6

Conclusion and Scope for Future Studies

In the dissertation, the various issues of circular sector microstrip antenna (CSMA) has been investigated thoroughly in the light of clear physical insight as well as experiments. Some very critical and important issues of CSMA has been studied and documented which will be helpful for scientific and research community. CSMA is advantageous and most useful as it requires less space compare to all other conventional structure like rectangular & circular as is discussed in chapter 1. These CSMAs with individual sector angle has different unique input and radiation features. In fact, different sector angle of CSMA excites different fundamental and higher order modes. Therefore, CSMA has unique feature to excite numerous numbers of fundamental modes based on it's sector angle. Therefore, scientific and research community is in urgent need of through and methodological study on the determination of fundamental mode and its frequency.

To alleviate the lacuna of earlier studies, a modified cavity model has been developed to determine the fundamental mode and its resonant frequency in chapter 2. The modal fields of the dominant as well as higher order modes of numerous CSMAs with different sector angles have been thoroughly studied. In this chapter 2, an improved, accurate and comprehensive computer-aided design formulation for accurately determining the resonant frequency of a CSMA has been proposed. The proposed formulation accurately estimates the dominant and higher mode resonances in a CSMA with and without an air gap between the substrate and the ground plane. No published work that presents the variation of the resonant frequency of a CSMA with substrate thickness, air gap height, substrate permittivity, and the radial

dimension of the antenna is available till date. Considering all the above-mentioned factors, the resulting variations of resonant frequencies as a function of the aforementioned parameters, have been included in the present study. An improved formulation of Computer aided design (CAD) has been proposed for easy prediction of exact resonance frequency of CSMA without much effort to the rigorous simulation. The propose CAD formulation exhibits much improved and provides more accurate result in relation to simulated and measured result.

Chapter 3 deals with the excitation of desired modes in a circular sector microstrip antenna (CSMA) as a function of feed location. The key influence of the feed-probe position in exciting particular mode has been thoroughly studied. Also, the investigation has been done for wide range of sector angles. The proposed theory has been validated through simulation as well as experiments. Excellent agreement is reveled amongst theoretical prediction, simulation and measurements. An accurate but quick hand approximate theoretical technique has been developed to determine the feed location of a CSMA which can excite a specific mode based on *E/H* ratio. The gain of the antenna has also been analyzed and enhanced by incorporations the air instead of conventional substrate. The comparative study using air and PTFE substrate for identical patch has been investigated to estimate the gain enhancement of a particular sector angle. An easy and a quick hand formulation is developed to determine the gain enhancement of CSMA with air substrate in comparison to conventional PTFE substrate. This easy technique will be surely be helpful for scientist and practicing engineers looking for designing CSMAs.

As such, CSMA of different sector angles have entirely different characteristics and hence, suitable choice of sector angle is very critical to design CSMA with optimum performance. Therefore, a compact design guideline of CSMA has been documented in chapter 4. Thorough design opportunities and limitations are presented in this chapter. In fact, the comprehensive design guidelines provided in chapter 4 will be very much beneficial for future designers to estimate best possible configuration for any specified application. Based on design guidelines, prototypes are fabricated, measured and compared with conventional circular patch. This reveals that 170^0 to 180^0 CSMA has better performance in comparison to classical circular patch.

Based on theories developed in chapter 2 to 4, a semicircular patch with defected patch surface approach has been developed for much improved radiation characteristics in comparison to conventional CMA in chapter 5. However, in course of investigation, it is observed that the cross polarization of such antennas with 170^0 to 180^0 sector angles are comparatively high with respect to CMA. Therefore, in chapter 5, the cross polarization of 180^0 CSMA has been minimized a new technique called defected the patch surface approach. This can be done by judiciously cutting the notch on the patch surface. In addition with that, the ground plane dimension has also been investigated to see the effect on ground plane dimension on new antenna characteristics. Notably, the designed antenna worked well as very small ground plane and can be designated as small antenna.

The investigation on theoretical and experimental study has been presented in this dissertation which is important for commercial and engineering applications, along with research and future application.

The investigation documented in this dissertation germinates a plentiful opportunity of CSMA over other geometries. CSMAs with different sector angles have different excitation mode and hence they have different radiation performance. Therefore, some other investigation may also be carried out individually for individual sector angles. Improved radiation performance in comparison to CMA has been established with DPS loaded 180^0 CSMA. Hence, other CSMA angles may also be explored to yield more improved radiation characteristics of CSMA in comparison to CMA. Broad banding or dual banding of CSMA may also be explored based on theory developed in chapter 2 to chapter 4.

List of Publications

Journals (SCI):

[1] S. K. Ghosh, A. Ghosh, S. Chakraborty, L. L. K. Singh, and S. Chattopadhyay, "Design Approach Toward Compact Circular Sector Microstrip Antenna With Low Cross Polarization," *IEEE Antennas and Wireless Propagation Letters*, vol. 20, no. 3, pp. 376-380, 2021.

[2] S. K. Ghosh, A. Ghosh, S. Chakraborty, L. L. K. Singh, and S. Chattopadhyay, "The Influence of Feed Probes on the Modes of Circular Sector Microstrip Antennas: An Investigation," *IEEE Antennas and Propagation Magazine*, vol. 63, no. 4, pp. 33-42, 2021.

[3] Sudip Kumar Ghosh**,** Subhradeep Chakraborty L. Lolit Kumar Singh, and Sudipta Chattopadhyay, "Modal analysis of probe-fed circular sector microstrip antenna with and without variable air gap: Investigation with modified cavity model", *International journal RF Microwave Computer Aided Engineering***,** vol.28, no. 1, pp.1-14, 2018.

[4] S. K. Ghosh, A. Ghosh, L. L. K. Singh, and S. Chattopadhyay, "Design Challenges of Circular Sector Microstrip Antenna: 170°Circular Sector is a better Alternative of Circular Microstrip Antenna" Advanced theory and Simulations (communicated).

Conferences:

[1] Sudip Kumar Ghosh, Abhijyoti Ghosh, Subhradeep Chakraborty, L. Lolit Kumar Singh, and Sudipta Chattopadhyay, "Estimation of Gain Enhancement of Circular Sector Microstrip Antenna with Air Substrate". *3rd International Conference on Communication, Device and Networking (ICCDN-2019)*, Sikkim, 9th -10th December, 2019. doi: 10.1007/978-981-15-4932-8_57. **(Presented)**

[2] Sudip Kumar Ghosh, Subhradeep Chakraborty, Abhijyoti Ghosh, Sudipta Chattopadhyay, L. L. K. Singh, "An Investigation into the Equivalnce of Radiation Characteristics of 90° Circular Sector Microstrip Antenna vis-à-vis Circular Microstrip Antenna", *IEEE Indian Conference on Antennas and Propogation (InCAP),* hydrabad, 2018. doi: 10.1109/INCAP.2018.8770757.

[3] S. K. Ghosh, S K Varshney, S. Chakraborty, L. L. K. Singh, and S. Chattopadhyay, "Probe-fed Semi Circular Microstrip Antenna vis-a-vis Circular Microstrip Antenna", *Proceedings of 3rd International Conference on Communication Systems (ICCS-2017),* 14th -16th October, 2017, published in IOP Conf. Series: Materials Science and Engineering, vol. 331, no. 012026 2018. doi:10.1088/1757-899X/331/1/012026. **(Presented)**

Design Approach Toward Compact Circular Sector Microstrip Antenna With Low Cross Polarization

Sudip K. Ghosh [ID], Abhijyoti Ghosh [ID], Subhradeep Chakraborty, *Member, IEEE*, L. Lolit K. Singh, and Sudipta Chattopadhyay [ID], *Member, IEEE*

Abstract—In this letter, a novel and compact 180° circular sector microstrip antenna has been proposed. The patch surface has been designed with a proper design insight to perturb and control the orthogonal surface current paths and orthogonal field components at the truncated edges for suppression of cross-polar (XP) radiations over the whole elevation without hampering its radiation pattern and bandwidth. The proposed antenna gives consistently better performance with different (large, medium, and small) ground plane sizes in spite of massive miniaturization (of 82%) with reference to conventional circular microstrip antenna at the same frequency. The proposed antenna can also be circumscribed completely within a sphere of radius ($\lambda/2\pi$), i.e., wheeler limit and hence can stand well as a small antenna.

Index Terms—Circular sector microstrip antenna, cross-polarized radiation, radiation characteristics.

I. INTRODUCTION

IN RECENT years, there is an increased surge in exploring and enhancing the characteristics of tiny antennas, which can be implemented in the limited available spaces in miniaturized compact wireless communication device without hampering the antenna performance. In this perspective, circular sector microstrip antenna (CSMA) with relatively smaller sector angle ($\phi_0 = 180°$) is an excellent preference over circular microstrip antenna (CMA) [1]–[4]. Earlier, rectangular microstrip antenna (RMA) and CMA were widely investigated for patch area miniaturization in [5]–[15]. However, such miniaturized antennas suffer from very poor gain [11], bandwidth [9]–[11], and high cross-polar (XP) radiations [9]–[12], squinted E-plane dipole like profile and omnidirectional H-plane profile [13]. CSMA with very large sector angles, i.e., $\phi_0 \sim 270°$, 340°, and 350° have been investigated in [16]–[18] for broad banding or multibanding without any improvement in radiation performance or miniaturization. Further, Ghosh *et al.* [19] shows that 180° CSMA offers poor copolar (CO) to cross-polar radiation (XP) isolation (XPD) (around 8 dB) at the X-band with a broadside XP pattern instead of a conical XP pattern which affects the
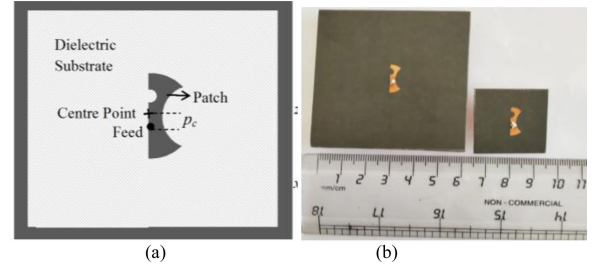
Fig. 1. (a) Schematic representation of proposed antenna (top view) and (b) fabricated prototypes over large and smaller ground planes.

main CO profile. Therefore, it is undeniably challenging to modulate the XP profile of 180° CSMA with improved XPD along with achieving miniaturization. It is well-known that linearly polarized CMA and RMA exhibit high XP radiations [1], [4], [20]–[27]. However, common XP radiation minimization techniques for instance, use of modified feed structures, defected ground structures (DGSs), and shorted patch and pins (SP); have not been investigated till date for minimizing XP radiations in CSMA with small sector angle ($\phi_0 \rightarrow 180°$). Notably, a CSMA with sector angle $\phi_0 = 180°$ has a thought-provoking feature of exciting similar dominant mode and resonant frequency in comparison with that of a conventional CMA with around 50% patch area reduction. Also, the ground plane dimension becomes a parameter of vital relevance to designing of miniaturized antenna [28]. Most of earlier reported structures could not show their efficacy as small antenna by circumscribing the patch radiator (including ground plane) within a sphere of radius ($\lambda/2\pi$), i.e., Wheeler limit.

Therefore, in this letter, a compact CSMA (with $\phi_0 = 180°$) structure has been proposed, (see Fig. 1) with improved radiation characteristics, low XP radiation along with miniaturization. Further, the proposed structure exhibits satisfactory performance on very small ground plane also.

II. EVOLUTION ANALYSIS OF THE PROPOSED ANTENNA

First, a CMA with radius a was designed over the substrate ($\varepsilon_r = 2.33$, thickness $h = 1.575$ mm) at X-band that acts as a reference CMA (Antenna#1) [see Fig. 2(a)]. In step 2, the left half of the patch surface was removed which gave birth to a CSMA with $\phi_0 = 180°$(Antenna#2) as shown in Fig. 2(b). The parametric equation for the locus of Antenna#2 can be written as

$$x = a \cos\phi \text{ and } y = a \sin\psi \tag{1}$$

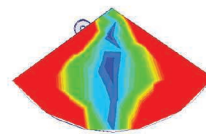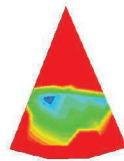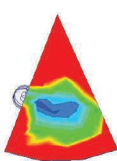where $\phi \rightarrow 0$ to $\phi \rightarrow 180°$ (ϕ_0) and $a = 6$ mm

Sudip Kumar Ghosh, Abhijyoti Ghosh, Subhradeep Chakraborty,
Lourembam Lolit Kumar Singh, and Sudipta Chattopadhyay

The Influence of Feed Probes on the Modes of Circular Sector Microstrip Antennas

An investigation.

In this article, the key influence of the feed-probe position for the excitation of desired modes in a circular sector microstrip antenna (CSMA) is thoroughly investigated via physical analysis comprising simulations and measurements. The approximate feed location used to excite a particular mode is also empirically determined to facilitate further exploration of CSMAs. Based on the proposed analysis and simulations, CSMAs with a wide range of sector angles are studied, and good agreements are revealed when compare with the measurements.

INTRODUCTION

In recent years, there has been increased attention toward exploring and enhancing the radiation and input characteristics of circular sector microstrip antenna (CSMAs) for modern applications due to its conformality over curved surfaces and better compactness compared to other regularly shaped patch geometries, i.e., rectangular and circular. Aside from applying a circularly polarized CSMA (see [1]), recently, other significant works on wideband and multiband CSMAs have been reported in [2]–[6]. Notably, all of these investigations were initiated by applying appropriate

RESEARCH ARTICLE
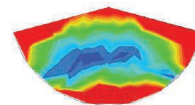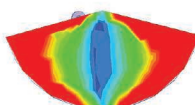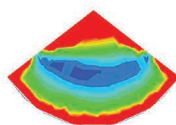
Modal analysis of probe-fed circular sector microstrip antenna with and without variable air gap: Investigation with modified cavity model

Sudip Kumar Ghosh[1] | Subhradeep Chakraborty[2] | L. Lolit Kumar Singh[3] | Sudipta Chattopadhyay[3] (ORCID)

[1] Siliguri Institute of Technology, Siliguri, West Bengal, India

[2] CSIR-Central Electronics Engineering Research Institute, Pilani, Rajasthan, India

[3] Department of Electronics and Communication Engineering, Mizoram University, Aizawl, Mizoram, India

Correspondence
Sudipta Chattopadhyay, Department of Electronics and Communication Engineering, Mizoram University, Aizawl, Mizoram, India.
Email: sudipta_tutun@yahoo.co.in

Abstract

Determination of accurate modal fields is one of the most crucial issues to understand the proper behavior of circular sector microstrip antennas (CSMAs) to achieve the best performance. In this article, dominant and higher order modal characteristics have been rigorously studied which germinate an improved, accurate, and efficient computer-aided design (CAD) formulation to estimate the resonant frequency of CSMA with and without air gap between substrate and ground plane. The proposed formulation can address the wide variety of issues (such as substrate height, substrate permittivity, air gap height, higher order modes, etc.). The computed results were validated against the results obtained from high-frequency structure simulator (HFSS) and our own experiments, while they have been also justified through the results obtained from the available literature.

KEYWORDS
antenna parameters, circular sector, microstrip antenna, resonant frequency

1 | INTRODUCTION

IN the modern era of microwave communications, the design and analysis of miniaturized and multifunctional antennas of different geometries continue to be the focus of state-of-the-art research. In this scenario, microstrip patch antennas (MPAs) are extremely useful and are the obvious choice of the designers because of their light weight, small size, and excellent compatibility with monolithic microwave integrated circuits. The most common geometries of MPAs, such as rectangular and circular, have been extensively studied, analyzed, and implemented for at least the last three decades. In fact, a significant number of analyses[1–6] and applications[7–12] of common MPA geometries have been reported during the last two decades. However, in various practical wireless applications, radiators should be conformally mounted onto the previously existing structures, where space limitation is a crucial problem. In such applications, a circular sector microstrip antenna (CSMA) is highly advantageous because it requires less space than a conventional patch antenna of common geometries. Approximately 30% and 35% patch area reductions can be achieved with a CSMA using 60° and 90° sector angles, respectively, compared with a conventional circular MPA. Therefore, an accurate analysis of CSMA is a priority in the present scenario of printed antenna research. In this context, we have found a limited number of analyses,[13–17] in which the computation of the accurate resonant frequency of CSMA with arbitrary sector angles has been dealt with.

The formulation of the resonant frequency of a CSMA based on the cavity model was first reported in ref. 13. The electric field beneath the patch and the eigen functions of those antennas were also presented in ref. 13. In ref. 14, a generalized transmission line modeling was used for computing the resonant frequency of a CSMA. However, the effect of fringing fields, which should be considered for the accurate estimation of the resonant frequency of a CSMA, was not included in refs. 13 and 14.

PARTICULARS OF THE CANDIDATE

NAME OF CANDIDATE : SUDIP KUMAR GHOSH

DEGREE : PH. D

DEPARTMENT : ELECTRONICS AND COMMUNICATION ENGINEERING

TITLE OF THESIS : QUALITATIVE AND QUANTITATIVE ANALYSIS ON SOME CHARACTERISTICS OF   CIRCULAR SECTOR MICROSTRIP ANTENNAS

DATE OF ADMISSION : 01 AUG 2017

APPROVAL OF RESEARCH PROPOSAL:

    1. DRC : 10 Apr 2018

    2. BOS : 17 APR 2018

    2. SCHOOL BOARD : 23 APR 2018

MZU REGISTRATION NO. : 1702110

PH. D REGISTRATION NO. : MZU/PH.D./1179 OF 23 APR 2018

EXTENSION : NO

_____

Head

Department of   Electronics and Communication Engineering

BIO-DATA OF THE CANDIDATE

Name of Candidate	:	Sudip Kumar Ghosh
Date of Birth	:	22/04/1981
Contact	:	6297309721
		sdpghsh@gmail.com
Permanent Address	:	S/O: Panchanan Ghosh
		Vill: Sultannagar
		PO: Radhakantapur
		Dist: Paschim Medinipur
		Pin: 721211
		State: West Bengal
Married	:	Yes

Educational Details

(a) M.Tech MAKAUT,	:	Mobile Communication and Networking, West Bengal
(b) Ph.D Course work	:	SGPA of 9.00.
Present Occupation Details	:	Assistant Professor, department of Electronics & Communication Engineering
Organization	:	Siliguri Institute of Technology

ABSTRACT

QUALITATIVE AND QUANTITATIVE ANALYSIS ON SOME CHARACTERISTICS OF CIRCULAR SECTOR MICROSTRIP ANTENNAS

SUDIP KUMAR GHOSH

PH. D REGN NO: MZU/PH.D./1179 OF 23.04.2018

MZU REGN NO: 1702110

DEPARTMENT OF ELECTRONICS AND COMMUNICATION

ENGINEERING

SCHOOL OF ENGINEERING AND TECHNOLOGY

SEPTEMBER 2021

QUALITATIVE AND QUANTITATIVE ANALYSIS ON SOME CHARACTERISTICS OF CIRCULAR SECTOR MICROSTRIP ANTENNAS

BY

SUDIP KUMAR GHOSH

Department of Electronics and Communication Engineering

Name of Supervisor : Prof. Sudipta Chattopadhyay

Name of Joint Supervisor : Prof. L. Lolit Kumar Singh

Submitted

In partial fulfillment of the requirement of the Degree of Doctor of Philosophy in Electronics and Communication Engineering of Mizoram University, Aizawl

In this modern era, the scientific and research community looking for a miniaturized antenna structure other than conventional circular microstrip antenna geometry. This is very much helpful for modern wireless industries to develop miniaturized hand-held wireless communication equipments. In this stage, circular sector microstrip antenna is highly applicable as it requires less patch size compare to other conventional geometry. In this dissertation, one of the miniaturized and versatile antenna structures, named circular sector microstrip antenna (CSMA) has been broadly investigated. Which can be derived from circular microstrip antenna (CMA) structure by cutting a sector angle. In comparison to the conventional circular patch geometries, the CSMA is hardly explored by researchers till date. Therefore, to implement such CSMA in different applications, it is imperative to investigate its basic input, radiation characteristics and the modal behavior along with miniaturization.

So, the determination of the lowest order dominant mode of CSMA is the most vital and primary focus to explore CSMA characteristics. In this context, the modal behavior of such antenna is not analyzed elaborately in available literatures and reported design formulations also fail to predict accurate resonant frequencies of CSMA with different sector angle. Accurate dominant mode for CSMA with arbitrary sector angle is not clear and based on simulation only. Simple theoretical design formulas are still important to estimate the operating frequency before run any simulator. Accurate theoretical formulas are very much required from application point of view. Therefore, the structure has not been studied methodically till date.

The modal analysis of dominant and higher order mode of different sector angles has been thoroughly studied using modified cavity model. Computer aided theoretical formulation (CAD) has been developed for accurate determination of dominant mode and higher order mode (HOM) in chapter 2. The modal fields of the dominant as well as higher order modes of numerous CSMAs with different sector angles have been thoroughly studied. In this chapter 2, an improved, accurate and comprehensive computer-aided design formulation for accurately determining the resonant frequency of a CSMA has been proposed. The proposed formulation accurately estimates the dominant and higher mode resonances in a CSMA with and without an air gap between the substrate and the ground plane. No published work

that presents the variation of the resonant frequency of a CSMA with substrate thickness, air gap height, substrate permittivity, and the radial dimension of the antenna is available till date. Considering all the above-mentioned factors, the resulting variations of resonant frequencies as a function of the aforementioned parameters, have been included in the present study.

The accurate estimation of the feed-probe position for the excitation of desired modes in a circular sector microstrip antenna (CSMA) is also another basic design requirement. Moreover, optimization of feed positions for the excitation of dominant modes is very essential to obtain the optimum performance of CSMA. Therefore, effect of feed probe location on the excitation of a particular mode (lowest order dominant and HOMs) has been thoroughly studied in chapter 3. Infact, different modes can be excited with CSMA of different angles based on different feed locations. Correspondingly, radiation characteristics changes for a particular CSMA. Even polarization of radiation fields also changes due to feed probe location. Modal behavior of different excited electromagnetic modes in CSMA as a function of feed-probe position is not analyzed elaborately in available literatures. Therefore, to identify the feed location for excitation of particular mode in CSMA for a wide variety of sector angles a simple, quick hand & accurate technique has been carried out. The estimation of the suitable range of feeding position has been thoroughly investigated and quick hand and accurate technique is proposed in chapter 3. The modal fields of the dominant as well as higher order modes of numerous CSMAs with different sector angles have been thoroughly studied in chapter 3. The new theoretical approximation technique has been derived based on E/H ratio beneath the patch to excite a specific mode. Indeed, CSMAs with different range of sector angles has been classified and discussed scientifically by the relation of E/H ratio. A particular range of $|E/H|$ has been recommended on which a particular mode can be excited. Moreover, a range of feed location has been approximated across which a particular mode can be excited if probe is placed. Hence, the present investigation will be surely helpful to the scientific community to germinate new ideas related to the excitation of modes with desirable polarizations as a function of feed-probe location for practical applications. Previous two chapters, the investigation has been carried out only of input characteristics. So, the radiation characteristics and gain of

this antenna have been given equal importance to explore the performance of the antenna in large extent. The Gain of this antenna is generally 7.1 dBi that has been improved to 9.9 dBi by introduction an air substrate. The quick hand formula has been developed for calculating the enhancement of gain of CSMA with air substrate in comparison to conventional substrate.

In chapter 4, the complete design guideline has been prescribed for the specific application. The behavior of CSMA is generally varied with sector angles due to its different type of geometry. Thus, selection of sector angles in terms of operating mode, frequency and miniaturization has been thoroughly studied for better selection of CSMA angles. A compact and comprehensive guideline has been prescribed documented in chapter 4.

In chapter 5, CSMA of 180^0 sector angle has been considered based on an earlier investigation documented in chapter 3 to chapter 4. An investigation in view of the replacement of CMA with 180^0 CSMA has been successfully proposed. The minimization of patch area is always advantageous and around 82% miniaturization has been achieved in comparison to conventional CMA exciting the particular dominant mode. In order to improve the polarization purity, the patch area has been defected judiciously. The proposed antenna in chapter 5, works on very small ground plane and satisfactory radiation performance is revealed.

The thorough investigation presented in this dissertation is most up to date with cutting edge technologies and complete in all aspects and hence should be very much helpful for efficient CSMA design.